Phylogenetics and phylogeography of the *Hipposideros commersoni* (Chiroptera) species complex with special reference to Malagasy populations

by

Andrinajoro Rianarivola RAKOTOARIVELO
212561514

Submitted in fulfilment of the academic requirements for the degree of

Doctor of Philosophy

in the

School of Life Sciences

College of Agriculture, Engineering and Science

University of KwaZulu-Natal

Westville

South Africa

December 2015

As the candidate's supervisor, I have approved this thesis for submission

Prof. J. M. Lamb ----------

Dr. S. Willows-Munro ----------

Dr. M. C. Schoeman ----------

ABSTRACT

Hipposideros commersoni is endemic to Madagascar and is relatively common in the western portion of the island, where it is found in different habitats from sea level to 1325 m. A previous study on patterns of morphological variation within the species highlighted the presence of two distinct morphotypes larger individuals in the north of Madagascar and smaller individuals in the south. Molecular techniques using DNA sequence data in combination with morphology have been previously used to identify cryptic hipposiderid species. This thesis presents the results of analyses based on molecular data and craniodental measurements in *H. commersoni* occurring on Madagascar, and related African forms. The molecular analyses suggest that *H. commersoni* with respect to Madagascar is paraphyletic, with strong support for the presence of independently evolving lineages. Two individuals amongst those sequenced from areas in the south of Madagascar represent a unique evolutionary lineage (Clade A), distinct from other *H. commersoni*, and has been recently named as a new species, *H. cryptovalorona*. This species is sister to *H. gigas* and *H. vittatus*, both restricted to Africa. Within *H. commersoni*, the molecular data support two geographically distributed clades -- one in the south (Clade B) and the other in the north (Clade C). Morphometric data were consistent with the molecular analyses, suggesting a north–south break within *H. commersoni*. Bayesian clustering analysis showed that *H. commersoni* comprised four main lineages: B1, B2, B3 and C. The most recent common ancestor of *H. commersoni* was dated to 3.33 million years ago or the mid-Pliocene. Population expansion events were inferred for groups B1, B2 and B3 from approximately 127,600 (group B1) to 6,870 years BP (group B2). Conflicting results were obtained from Bayesian clustering and AMOVA analyses; strong population genetic structure was obtained from the former but not the latter. Sequence data indicated that genetic subdivisions failed to support an isolation-by-distance model. Lineage dispersal, genetic divergence and expansion events of *H. commersoni* are likely to be associated with Plio-Pleistocene climate fluctuations. Our data indicate the northern and the central western regions of Madagascar may have acted as refugia for this species during the Plio-Pleistocene.

PREFACE

The research contained in this thesis was completed by the candidate while based in the Discipline of Biology, School of Life Sciences of the College of Agriculture, Engineering and Science, University of KwaZulu-Natal, Westville, South Africa. The research was financially supported by the College of Agriculture, Engineering and Science, School of Life Sciences, University of KwaZulu-Natal, as well as the IDP Foundation Inc. associated with the Field Museum of Natural History African Training Fund.

The contents of this work have not been submitted in any form to another university and, except where the work of others is acknowledged in the text, the results reported are due to investigations by the candidate.

_____

Signed: Prof. J. M. Lamb ----------

Dr. S. Willows-Munro ----------

Dr. M. C. Schoeman ----------

Date:

DECLARATION 1: PLAGIARISM

I, Andrinajoro Rianarivola Rakotoarivelo, declare that:

(i) the research reported in this dissertation, except where otherwise indicated or acknowledged, is my original work;

(ii) this dissertation has not been submitted in full or in part for any degree or examination to any other university;

(iii) this dissertation does not contain other persons' data, pictures, graphs or other information, unless specifically acknowledged as being sourced from other persons;

(iv) this dissertation does not contain other persons' writing, unless specifically acknowledged as being sourced from other researchers. Where other written sources have been quoted, then:

a) their words have been re-written but the general information attributed to them has been referenced;

b) where their exact words have been used, their writing has been placed inside quotation marks, and referenced;

(v) where I have used material for which publications followed, I have indicated in detail my role in the work;

(vi) this dissertation is primarily a collection of material, prepared by myself, published as journal articles or presented as a poster and oral presentations at conferences. In some cases, additional material has been included;

(vii) this dissertation does not contain text, graphics or tables copied and pasted from the Internet, unless specifically acknowledged, and the source being detailed in the dissertation and in the References sections.

DECLARATION 2: PUBLICATIONS

My role in each paper, listed below, is indicated. The * indicates corresponding author.

Publication 1 (Chapter 1)

Rakotoarivelo AR*, Willows-Munro S, Schoeman MC, Lamb JM, Goodman SM. 2015. Cryptic diversity in *Hipposideros commersoni* sensu stricto (Chiroptera: Hipposideridae) in western portion of Madagascar. *BMC Evolutionary Biology* **15:** 235–253.

I co-conceived the original idea of the paper, processed tissue samples from the stages of DNA isolation to completion of sequencing, completed molecular phylogenetic analysis, performed statistical analyses on morphological and craniodental data, and led the writing of the first version of manuscript, as well as preparing the final version.

Publication 2 (Chapter 2)

Goodman SM*, Schoeman, MC, Rakotoarivelo, AR, Willows-Munro, S. 2016. How many species of *Hipposideros* have occurred on Madagascar since the Late Pleistocene? *Zoological Journal of the Linnean Society*.

The research reported on is based on data processed from voucher specimens held in different natural history museums. The morphological work was carried out by S. M. Goodman and M. C. Schoeman, the molecular work was carried out by A. R. Rakotoarivelo and S. Willows-Munro. I contributed to the writing the molecular phylogenetic portions of manuscript and contributed to the final version. This paper is scheduled to be published in April 2016.

Publication 3 (Chapter 3)

Rakotoarivelo AR*,Goodman SM, Schoeman MC, Lamb J, Willows-Munro S. Manuscript. Phylogeography and population genetics of *Hipposideros commersoni* s.s. (Chiroptera: Hipposideridae), an endemic Malagasy bat. To be submitted in the near future to *Molecular Phylogenetics and Evolution.*

I co-conceived the original idea of the paper, processed tissue samples from the stages of DNA isolation to completion of sequencing, completed data analyses, led the writing of the first version of manuscript, and I am taking the lead role in preparing the manuscript for publication..

Signed:

Date:

TABLE OF CONTENTS

Page

ACKNOWLEDGMENTS

I cordially thank Dr. Sandi Willows-Munro for introducing me into the world of molecular techniques and phylogenetic analysis. I am grateful for her endless support and guidance.

I would like thank Pr. Jennifer Lamb for supervising my PhD study, without whom this study would not have been possible.

Further, I would like to thank Dr M Corrie Schoeman and for tutoring my journey into the world of bats.

I wish to thank Pr. Steven M Goodman for providing me with the opportunity to research this theme and for providing constant guidance, support and assistance throughout the duration of this project. Thanks for being an inspiration to my peers and me.

My further thanks go to the postgraduate students in the Conservation Genetics lab (Pietermaritzburg) for their friendship and support over the last two stressful years.

A special mention to Pr. Achille Raselimanana and all the Association Vahatra staff members in Madagascar for their support.

I am grateful to the Département de Biologie Animale, Université d'Antananarivo; Madagascar National Parks (MNP) and the Ministère des Forêts et de l'Environnement, Direction générale des Forêts, Direction de la Conservation de la Biodiversité et du Système des Aires Protégées for their administrative support and for providing research permits to conduct this work.

I am grateful to Karen Samonds for access to subfossil material of *Hipposideros besaoka*. For providing tissues of *Hipposideros* from Tanzania, we are grateful to the late William Stanley and for access to tissue samples, we acknowledge John Phelps (FMNH) and Julie Feinstein (AMNH). For access to specimens, I acknowledge Jean-Marc Pons and Cécile Callou (MNHN), Voahangy Soarimalala (UADBA), and Kristofer Helgen (USNM).

For their valuable comments on previous versions of different portions of this thesis, I acknowledge the help of Andrey Puzachenko, Miguel Vences, Ara Monadjem and an anonymous reviewer.

Dissertation research and laboratory work was done at the Conservation Genetics Laboratory of the University of KwaZulu-Natal, Pietermaritzburg Campus. My dissertation related work activities were funded by the College of Agriculture, Engineering and Science, School of Life Sciences, University of KwaZulu-Natal, as well as the IDP Foundation Inc. associated with the Field Museum of Natural History African Training Fund.

Finally, I would like to thank my wife, Nanou, my sons, Tendro and Vahy, for their unconditional love and support through this journey. Tiako loatra ianareo!

Thanks to God almighty.

GENERAL INTRODUCTION

Bats are known for being the only mammal group capable of self-powered flight, as well as the only mammal capable of sophisticated laryngeal echolocation (MacDonald, 2006). Bats belong to the Order Chiroptera and are one of the most diverse living groups of mammals, which include about 1200 species in 200 genera. They account for more than 20% of terrestrial mammals (Simmons, 2005). Over the past 20 years, considerable progress has been made to elucidate the chiropteran systematics at different taxonomic levels. Earlier studies based on morphological characters divided Chiroptera into two suborders: Megachiroptera and Microchiroptera (Simmons and Geiser, 1998). Recent molecular studies separated bats into two separate groups (Springer *et al.*, 2001): Yinpterochiroptera, containing the formerly recognized Megachiroptera and the Rhinolophoidea and 2) Yangochiroptera, including all remaining groups of bats.

The Hipposideridae, also known as Old World leaf-nosed bats, is one of the most widespread and abundant groups of insectivorous bats in the Old World tropics. They inhabit tropical and subtropical regions of Africa and the Middle East, through Asia and Australia (Simmons, 2005). There are 70 species currently recognized within the genus *Hipposideros* (Bates *et al.*, 2007; Guillén-Servent and Francis, 2006; Simmons, 2005), and aspects of their external and cranial morphology have been used as taxonomic characters. Tate (1941) described 11 species groups in his revision of the genus, whereas Hill (1963) recognized only seven distinct groups. Koopman (1994) and Simmons (2005) subsequently modified the classification and recognized nine species groups. Notably large members of the genus, classically considered geographical forms of *H. commersoni* and called Commerson's leaf-nosed bat, are distributed throughout sub-Saharan Africa and on Madagascar. The classification of these animals has differed through time. Taxonomists formerly divided the species into five subspecies with presumed non-overlapping geographical ranges: *H. c. commersoni* restricted to Madagascar; *H. c. thomensis* to the islands of Principe and São Tomé; *H. c. gigas* primarily in western equatorial Africa; *H. c. niangarae* in the Niangara Region of the Congo; and *H. c. marungensis* from eastern Africa to southern Africa and Namibia (Nowak, 1999).

In an even earlier classification, Hill (1963) recognized three subspecies of *H. commersoni* based on body size, particularly forearm length: the largest, *H. c. gigas*, being primarily located in western regions of equatorial Africa; *H. c. marungensis* in eastern Africa to southern Africa; and *H. c. thomensis* on the islands of Principe and São Tomé. According to

Hill's analysis, *H. c. commersoni* is much closer in size to *H. c. thomensis* than the other African taxa.

Subsequently, Koopman (1994) and Simmons (2005) classified members of the genus into morphological species groups. The *commersoni* group included *commersoni* on Madagascar and *thomensis*, *gigas*, and *vittatus* on continental Africa and offshore islands. Based on differences in morphology and echolocation calls (Pye, 1972; McWilliam, 1982), Simmons (2005) raised these different forms to the level of species. In a recent molecular phylogeny, it was found that *Hipposideros* was paraphyletic and members of the *H. commersoni* group fall outside typical *Hipposideros* (Foley *et al.*, 2015); this implies that they should be placed in a separate genus.

The genus *Hipposideros* contains some of the largest extant Yinpterochiroptera species, which can attain a body mass of 180 g (Vaughan, 1977). The life history and evolution of large-bodied hipposiderids is of interest to biologists because of their adaptations to persist in seasonal, tropical environments (Vaughan, 1977; McWilliam, 1982; Cotterill and Fergusson, 1999). *Hipposideros vittatus* from mainland Africa has a large gape and powerful bite (Cotterill and Fergusson, 1999) and it is a specialized predator of large arthropod prey with hard exoskeletons (Vaughan, 1977). Marked seasonal fluctuations in prey abundance of large African hipposiderids, resulting in temporary food shortages during the cool dry season, has considerable influence on their life history strategies. These seasonal differences have been invoked to explain local migrations to areas with greater food sources (Vaughan, 1977; McWilliam, 1982) or lower metabolic rates during periods of food shortage (Churchill *et al.*, 1997).

On the island of Madagascar, the genus *Hipposideros* is the sole representative of the family Hipposideridae, and by a single extant endemic taxon, *H. commersoni* (Simmons, 2005; Foley et al., 2015), and a subfossil, *H. besaoka* (Samonds, 2007). Records of *Hipposideros* from subfossil deposits are known from several sites on Madagascar (Goodman and Jungers, 2014). Samonds (2007) identified *H. commersoni* and *H. besaoka*, which she described as new to science from deposits dated to between 10,000 and 80,000 years ago. The two species, *H. besaoka* and *H. commersoni*, which were sympatric and presumably living in the cave during the same period, show a small amount of overlap in different dental measurements, which is not related to sexual dimorphism in the latter (Samonds, 2007).

Hipposideros commersoni s.s. is largely distributed in different bioclimatic zones of Madagascar and utilizes open woodland, degraded habitats, and forested areas from sea level to 1325 m (Goodman and Ramasindrazana, 2013). Its diet (mostly Coleoptera) and activity in

western Madagascar change seasonally and may be related to possible intra-island movements (Razakarivony *et al*., 2005; Rakotoarivelo *et al*., 2007, 2009; Kofoky *et al*., 2007). In southern Madagascar, *H. commersoni* is consumed by local people in the form of bush meat to supplement their diet, particularly during periods of food shortage and coinciding with the end of the wet season when these bats have considerable fat deposits (Goodman, 2006).

Kofoky *et al*. (2007) reported that *H. commersoni* was abundant in the Tsingy de Bemaraha National Park in October but very rare in the same area during July. In the Mahafaly Plateau, a local hunter noted that after the end of March few *H. commersoni* exit the cave until September (Goodman, 2006). However, it is unclear if this species remains inactive within caves or local populations migrate to other sites. On the basis of morphology and bioacoustic data (Ranivo and Goodman, 2007; Ramasindrazana *et al*., 2015) there is some evidence that *H. commersoni* as currently defined represents a highly variable taxon or contains a cryptic species. However, these preliminary results need to be examined in detail with increased samples taken across a greater geographical area, and most importantly tested with different molecular tools.

AIMS OF THIS STUDY

This study endeavours to understand the phylogeographical patterns of *Hipposideros commersoni* s.s. across the western portion of Madagascar and patterns of intra-island dispersal, as well at a broader geographical scale the evolutionary relationships of Afro-Malagasy members of this species group, including their colonization history of Madagascar. Datasets include molecular genetics to examine the phylogeographic and phylogenetic history of this species, as well as an overlay of external and craniodental measurements to examine morphological variation.

Specific aims were as follows:

(i) Investigate genetic and morphological variation in *H. commersoni* based on samples obtained from the western half of Madagascar within and outside dry forest formations, as well as to explore aspects of their phylogenetic history and to help resolve the species relationships of the different morphotypes recovered by Ranivo and Goodman (2007) (Chapter 1).

(ii) Determine how many species of *Hipposideros* currently occur on the island using external and craniodental measurements and morphological characters overlaid on phylogenetic data. Further, if cryptic species are identified, can subfossil remains of *H. besaoka* be confidently assigned based on craniodental morphology to one of these extant groups? (Chapter 2)

(iii) Investigate the fine-scale phylogeographic history of *H. commersoni* across western Madagascar. If geographic structure is found, tests will be conducted to see if this is consistent with previously identified bioclimatic zones (Chapter 3).

REFERENCES

Bates, P. J. J., Rossiter, S. J., Suyanto, A., Kingston, T. 2007. A new species of *Hipposideros* (Chiroptera: Hipposideridae) from Sulawesi. *Acta Chiropterologica*, 9: 13-26.

Churchill, S., Draper, R., Marais, E. 1997. Cave utilisation by Namibian bats: Population, microclimate and roost selection. *South African Journal of Wildlife Research*, 27 (2): 44-50.

Cotterill, F. P. D., Fergusson, R. A. 1999. Reproduction ecology of Commerson's leaf-nosed bats *Hipposideros commersoni* (Chiroptera: Hipposideridae) in south-central Africa:

Interactions between seasonality and large body size and implications for conservation. *South African Journal of Zoology*, 34 (1): 53–63.

Foley N. M, Thong V. D., Soisook P., Goodman S. M., Armstrong K. N., Jacobs D. S., Puechmaille S. J., Teeling E. C. 2015. How and why overcome the impediments to resolution: Lessons from rhinolophid and hipposiderid bats. *Molecular Biology and Evolution,* 32: 313–333.

Goodman, S. M. 2006. Hunting of Microchiroptera in south-eastern Madagascar. *Oryx,* 40: 1-4.

Goodman, S. M., Ramasindrazana, B. 2013. Chauves-souris ou ordre des Chiroptera/Bats or the Order Chiroptera. In *Atlas of selected land vertebrates of Madagascar*, eds. S. M. Goodman and M. J. Raherilalao, pp 169-209. Association Vahatra, Antananarivo.

Goodman, S. M., Jungers, W. L. 2014. *Extinct Madagascar: Picturing the island's past.* The University of Chicago Press, Chicago and London. 206 pp.

Guillén-Servent, A., Francis, C. M. 2006. A new species of bat of the *Hipposideros bicolor* group (Chiroptera: Hipposideridae) from Central Laos, with evidence of convergent evolution with Sundaic taxa. *Acta Chiropterologica,* 8 (1): 39-61.

Hill, J. E. 1963. A revision of the genus *Hipposideros*. *Bulletin of the British Museum (Natural History), Zoological Series*, 11: 1–129.

Kofoky, A., Andriafidison, D., Ratrimomanarivo, F., Razafimanahaka, H. J., Rakotondravony, D., Racey, P. A., Jenkins, R. K. B. 2007. Habitat use, roost selection and conservation of bats in Tsingy de Bemaraha National Park, Madagascar. *Biodiversity and Conservation,* 16(4): 1039-1053.

Koopman KF. 1994. Chiroptera: Systematics. In *Handbuch der Zoologie*, vol. VII, eds J. Niethammer, H. Schliemann, D. Starck, pp. 100–109. Walter de Gruyter, Berlin.

MacDonald D. W. 2006. *The encyclopedia of mammals*. Oxford University Press, Oxford.

McWilliam, A. N. 1982. *Adaptive responses to seasonality in four species of insectivorous bats in coastal Kenya*. Unpublished PhD thesis, University of Aberdeen, Aberdeen.

Murray, S. W., Campbell, P., Kingston, T., Zubaid, A., Francis, C. M., Kunz, T. H. 2012. Molecular phylogeny of hipposiderid bats from southeast Asia and evidence of cryptic diversity. *Molecular Phylogenetics and Evolution*, 62(2): 597–611.

Nowak, R. M. 1999. *Walker's mammals of the world*. The Johns Hopkins University Press, Baltimore.

Peterson, R. L, Eger, J. L., Mitchell, L. 1995. Chiroptères. *Faune de Madagascar*, 84: 1–204.

Pye, J. D. 1972. Bimodal distribution of constant frequencies in some hipposiderid bats (Mammalia: Hipposideridae). *Journal of Zoology*, 166: 323–335.

Rakotoarivelo, A. R., Ranaivoson, N., Ramilijaona, O., Kofoky, A. F., Racey, P. A., Jenkins, R. K. B. 2007. Seasonal food habits of five sympatric forest microchiropterans in western Madagascar. *Journal of Mammalogy*, 88(4): 959-966.

Rakotoarivelo, A. R., Ralisata, M., Ravoahangimalala, O. R., Rakotomalala, M. R., Racey, P. A., Jenkins, R. K. B. 2009. The food habits of a Malagasy giant: *Hipposideros commersoni* (E. Geoffroy, 1813). *African Journal of Ecology*, 47(3): 283-288.

Ramasindrazana, B., Rakotondramanana, C.F., Schoeman, M.C., Goodman, S.M. 2015. Evidence of echolocation call divergence in *Hipposideros commersoni* sensu stricto (E. Geoffroy, 1803) from Madagascar and correlation with body size. *Acta Chiropterologica*, 17(1): 85–94.

Ranivo, J., Goodman, S. M. 2007. Patterns of ecomorphological variation in the bats of western Madagascar: Comparisons among and between communities along a latitudinal gradient. *Mammalian Biol*ogy, 72 (1): 1–13.

Razakarivony, V. R., B. Rajemison, S. M. Goodman. 2005. The diet of Malagasy Microchiroptera based on stomach contents. *Mammalian Biology*, 70(5): 312-316.

Samonds, K. E. 2007. Late Pleistocene bat fossils from Anjohibe Cave, northwestern Madagascar. *Acta Chiropterologica*, 9: 39–65.

Simmons, N. B. 2005. Order Chiroptera. In: *Mammal species of the world: A taxonomic and geographical reference*, eds. D. E. Wilson and D. M. Reeder, 3rd edition, pp. 315–529. Johns Hopkins University Press, Baltimore.

Simmons, N. B., Geisler, J. H. 1998. Phylogenetic relationships of *Icaronycteris*, *Archeonycteris*, *Hassianycteris* and *Palaeochiropteryix* to extant bat lineages, with comments on the evolution of echolocation and foraging strategies in Microchiroptera. *Bulletin of the American Museum of Natural History*, 235: 1-182.

1 Springer, M. S., Teeling, E. C., Madsen, O., Stanhope, M. J., de Jong, W. W. 2001. Integrated
2 fossil and molecular data reconstruct bat echolocation. *Proceedings of the National Academy of*
3 *Sciences*, 98(11): 6241-6246.

4 Tate, G. H. H. 1941. A review of the genus *Hipposideros* with special reference to Indo-
5 Australian species. *Bulletin of the American Museum of Natural History*, 78: 353–393.

6 Vaughan, T. A. 1977. Foraging behaviour of the giant leaf-nosed bat (*Hipposideros*
7 *commersoni*). *East African Wildlife Journal*, 15: 237-249.

8

9

CHAPTER ONE

Cryptic diversity in *Hipposideros commersoni* sensu stricto (Chiroptera: Hipposideridae) in the western portion of Madagascar

ABSTRACT

The Commerson's leaf-nosed bat, *Hipposideros commersoni* sensu stricto, is endemic to Madagascar and is relatively common in the western portion of the island, where it is found in areas, including forested zones, from sea level to 1325 m. A previous study on morphological patterns of geographic variation within the species highlighted the presence of two distinct morphotypes; larger individuals in the north portion of the island and smaller individuals in the south. The main aim of this study was to use a combination of craniodental morphology and molecular data (mitochondrial and nuclear) to test previous hypotheses based on morphology and clarify the evolutionary history of the species group. We sequenced mitochondrial and nuclear genes from *H. commersoni* obtained from the western portion of Madagascar, and compared them with other African species as outgroups. We analyzed the sequence data using Maximum Likelihood and Bayesian phylogenetic inference. Divergence dates were estimated using Bayesian molecular clock approach. Variation in craniodental variables was also assessed from sequenced individuals. The molecular analyses suggest that *H. commersoni* is not monophyletic, with strong support for the presence of several independently evolving lineages. Two individuals amongst those sequenced from Isalo (south central) and Itampolo (southwest) form a separate clade (Clade A), distinct from other *H. commersoni*, and sister to continental African *H. vittatus* and *H. gigas*. Within the *H. commersoni* clade, the molecular data support two geographically distributed clades; one from the south (Clade B) and the other from the north (Clade C), which diverged approximately 3.38 million years ago. Morphometric data were consistent with the molecular analyses, suggesting a north–south break within *H. commersoni*. However, at some localities, animals from both clades occurred in sympatry and these individuals could not be differentiated based on external and craniodental measurements. Using a combination of molecular and morphological characters, this study presents evidence of cryptic diversity in *H. commersoni* on Madagascar. Further fine-scale phylogeographic studies are needed to resolve fully the systematics of *H. commersoni*. This study highlights the utility of

the combined approach in employing both morphological and molecular data to provide insights into the evolutionary history of Malagasy population currently assigned to *H. commersoni*.

Keywords: *Dry forest, Phylogeny, Paraphyly, Evolutionary history, Systematics, Morphology*

Introduction

Members of the Family Hipposideridae, known as Old World leaf-nosed bats, are one of the most widespread and abundant groups of insectivorous bats and inhabit tropical and subtropical regions of Africa, the Middle East, Asia and Australia [1]. To a large extent, species within this genus have been defined based on their external and craniodental morphology. In a recent summary, 70 species of *Hipposideros* were recognized [1], subsequently numerous other taxa have been described (e.g. [2–5]) and the taxonomy of the group, predominantly at the species level, is far from resolved. As a tool to understand the evolutionary history of members of this genus, closely related species are often placed in morphological species groups (e.g., [1, 6]). As currently delineated, the *H. commersoni* group includes the Afro-Malagasy taxa *H. commersoni* (É. Geoffroy, 1813), described from Madagascar, and *H. thomensis* (Bocage, 1891), *H. gigas* (Wagner, 1845) and *H. vittatus* (Peters, 1852), from continental Africa and offshore islands. The last-named three forms were previously considered subspecies of *H. commersoni* sensu lato, but were recently raised to species rank [1] based on reputed morphology and echolocation call differences [7–9]). As members of the *H. commersoni* group s.l. have to date not been the subject of a detailed phylogenetic study, it is unclear if these taxonomic changes reflect the evolutionary relationships within this portion of the genus or are examples of morphological convergence [10].

Hipposideros commersoni sensu stricto is a widespread endemic to Madagascar and can be found from sea level to 1325 m, generally in forested zones [11]. Its diet (mostly Coleoptera) and activity in western Madagascar may change seasonally and may be related to possible intra-island movements [12–15]. On the basis of current information, Malagasy populations of *H. commersoni* demonstrate considerable geographic variation in morphological measurements and certain patterns cannot be explained by simple clines [16].

In this study, we examine genetic and morphological variation in *H. commersoni* using samples obtained from different areas of Madagascar within and outside dry forest formations, specifically the western half of the island, to explore aspects of their phylogenetic history and to help resolve the systematic relationships of the different morphotypes recovered by Ranivo and Goodman [16].

Methods

Morphological and molecular sampling

In this paper, reference to *Hipposideros commersoni* is restricted to Malagasy populations and, hence, sensu stricto. A total of 22 *H. commersoni* (20 females and two males) were included in the molecular portion of this study (Table 1). During the past two decades intensive bats surveys were carried out by different researchers across Madagascar, but with a distinct bias towards the west, where there are often extensive cave systems used as day roost sites for *Hipposideros*. The collection of *H. commersoni* specimens and associated tissues were greatly biased in this context. This species is present in eastern part of Madagascar but only a few specimens were available. Morphological analyses were conducted only on the 20 females. These samples come from collections made over the past 15 years from 11 localities across the western portion of Madagascar (Fig. 1). All voucher specimens are cataloged in the Field Museum of Natural History (FMNH) or Université d'Antananarivo, Département de Biologie Animale (UADBA). Samples used in the molecular study included the aforementioned material, as well as additional tissue samples of *H. vittatus* (n = 7) and *H. gigas* (n = 1), two morphologically similar species [17], from the FMNH and the American Museum of Natural History (AMNH) collections (Table 1, Fig. 1).

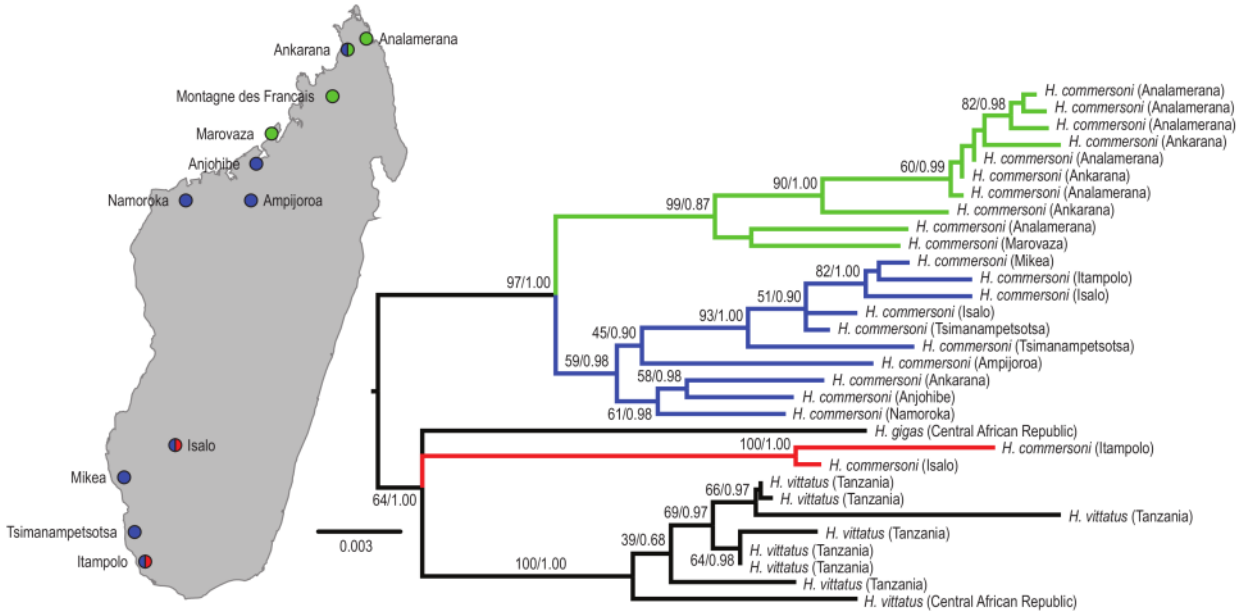

Fig. 1 Geographical distribution of *Hipposideros commersoni* specimens analysed in the present study (left). Localities are colour-coded according to the main phylogenetic lineages (red = Clade A, blue = Clade B, green = Clade C). Maximum likelihood tree (right) inferred from the combined analysis of molecular data (two mtDNA [CR and Cyt b], two nuclear introns [bSTAT and OSTA5]). Maximum likelihood bootstrap support and Posterior probability values (in that order) are shown at the nodes

1

2

Table 1 Details of specimens included in the molecular analysis (n = 22, 20 females and 2 males). The *Hipposideros commersoni* specimens are all from Madagascar; more precise details on collection localities are presented in Appendix 1

Species	Museum number	GenBank numbers				Collection locality
		CR	*Cyt b*	bSTAT	OSTA5	
Hipposideros commersoni	FMNH 169707	KT371749	KT5838015	KT583770	KT437663	Andrafiabe, Ankarana
Hipposideros commersoni	FMNH 175777	KT371750	KT5838022	KT583771	KT437664	Andranomavo, Namoroka
Hipposideros commersoni	FMNH 175966	KT371751	KT5838023	KT583772	KT437665	Menamaty, Isalo
Hipposideros commersoni	FMNH175970	KT371752	KT5838011	KT583773	KT437666	Berenty-Betsileo, Isalo
Hipposideros commersoni	FMNH 176155	KT371753	KT5838024	KT583774	KT437667	Ankiloaka, Mikea Forest
Hipposideros commersoni	FMNH 177302	KT371754	KT5838025	KT583775	KT437668	Ampijoroa
Hipposideros commersoni	FMNH 178806	KT371755	KT5838016	KT583776	KT437669	Bazaribe Cave, Analamerana
Hipposideros commersoni	FMNH 178808	KT371756	KT5838017	KT583777	KT437670	Bazaribe Cave, Analamerana
Hipposideros commersoni	FMNH 178809	KT371757	KT5838018	KT583778	KT437671	Bazaribe Cave, Analamerana
Hipposideros commersoni	FMNH 178810	KT371758	KT5838019	KT583779	KT437672	Bazaribe Cave, Analamerana
Hipposideros commersoni	FMNH 178811	KT371759	KT5838020	KT583780	KT437673	Bazaribe Cave, Analamerana
Hipposideros commersoni	FMNH 178815	KT371760	KT5838021	KT583781	KT437674	Bazaribe Cave, Analamerana
Hipposideros commersoni	FMNH 178812	KT371761	KT5838026	KT583782	KT437675	Bazaribe Cave, Analamerana
Hipposideros commersoni	FMNH 183934	KT371762	KT5838027	KT583783	KT437676	Mitoho Cave, Tsimanampetsotsa
Hipposideros commersoni	FMNH 184170	KT371763	KT5838028	KT583784	KT437677	Androimpano Cave, Itampolo
Hipposideros commersoni	FMNH 184173	KT371764	KT5838010	KT583785	KT437678	Androimpano Cave, Itampolo,
Hipposideros commersoni	FMNH 184030	KT371765	KT5838012	KT583786	KT437679	4.2 km SE Marovaza, in cave
Hipposideros commersoni	FMNH 183980	KT371766	KT5838013	KT583787	KT437680	Ampitiliantsambo Forest, Montagne de Français
Hipposideros commersoni	FMNH 217940	KT371767	KT5838031	KT583788	KT437681	Ranohira, Isalo
Hipposideros commersoni	UADBA 32987	KT371768	KT5838014	KT583789	KT437682	Andrafiabe, Ankarana
Hipposideros commersoni	FMNH 221308	KT371769	KT5838029	KT583790	KT437683	Andrafiabe, Ankarana
Hipposideros commersoni	UADBA32916	KT371770	KT5838030	KT583791	KT437684	Anjohibe Cave, Antanamarina,
Hipposideros vittatus	FMNH 192800	KT371772	KT583803	KT583792	KT437685	Kasinji Region, Pemba Island, Tanzania

Hipposideros vittatus	FMNH 192857	KT371773	KT583804	KT583793	KT437686	Kasinji Region, Pemba Island, Tanzania
Hipposideros vittatus	FMNH 192858	KT371774	KT583805	KT583794	KT437687	Kasinji Region, Pemba Island, Tanzania
Hipposideros vittatus	FMNH 192859	KT371775	KT583806	KT583795	KT437688	Kasinji Region, Pemba Island, Tanzania
Hipposideros vittatus	FMNH 192860	KT371776	KT583807	KT583796	KT437689	Kasinji Region, Pemba Island, Tanzania
Hipposideros vittatus	FMNH 192865	KT371777	KT583808	KT583797	-	Kasinji Region, Pemba Island, Tanzania
Hipposideros vittatus	FMNH 192866	KT371778	KT583809	KT583798	KT437690	Kasinji Region, Pemba Island, Tanzania
Hipposideros gigas	AMNH 269871	KT371748	KT583801	KT583799	KT437691	Dzanga Sangha Forest Reserve, Central African Republic
Hipposideros vittatus	AMNH 269879	KT371771	KT583802	KT583800	KT437692	Dzanga Sangha Forest Reserve, Central African Republic

Collection numbers are those assigned to each specimen by museums FMNH (Field Museum of Natural History), AMNH (American Museum of Natural History) and UADBA (Université d'Antananarivo, Département de Biologie Animale; – = missing data.

DNA sequencing

Genomic DNA was isolated using the NucleoSpin® Tissue kit (Macherey-Nagel, Germany), following the manufacturers protocol for tissue samples. Two mitochondrial (mtDNA) and two nuclear intron (ncDNA) markers were amplified. PCR reactions included a negative control (dH_2O used in both DNA extraction) to check for possible contamination.

The cytochrome b gene (*Cyt b*) was amplified using two sets of nested primers. The primers L14724AG (5′–ATG ATA TGA AAA ACC ATC GTT G–3′; [4]) and H15915 (5′–TCT CCA TTT CTG GTT TAC AAG AC–3′; [18]) were used to amplify a 1200 bp segment of *Cyt b*. In specimens in which L14724AG and H15915 did not amplify, the primers JorF (5′-GAC CTT CCA ACT CCC TCA AGC AT-3′; designed for study) and H15553 (5′–TAG GCA AAT AGG AAA TAT CAT TCT GGT–3′; [18]) were used to amplify a smaller 700 bp segment. The hypervariable portion of the control region (CR) of the mitochondrial genome was amplified in all specimens as a single fragment using primers P (5′–TCC TAC CAT CAG CAC CCA AAG C– 3′) and E (5′–CCT GAA GTA GGA ACC AGA TG–3′; [19]). The 16th intron of the signal

transducer and activator of transcription 5A (STAT) was amplified using previously published primers (bSTATa 5′–GAA GAA ACA TCA CAA GCC CC–3′, bSTATb 5′–AGA CCT CAT CCT TGG GCC–3′; [20, 21]). The 5th intron of the organic solute transporter subunit alpha gene (OSTA5) was amplified using the primers OSTA5F (5′–TGM WGG YCA TGG TGG AAG GCT TTG–3′) and OSTA5R (5′–AGA TGC CRT CRG GGA YGA GRA ACA–3′; [22]). The STAT marker was used based on the work of Eick et al. [20], who found high levels of intraspecific divergence for this marker in 58 bat species. Igea et al. [22] identified the intron OSTA5 to be an adequate marker for analyses of species delimitation, gene flow and genetic differentiation within two bat species. Cycle sequencing was performed using BigDye Chemistry (Version 3.1, Applied Biosystems, USA), and products analyzed on a 3100 ABI automated sequencer (Applied Biosystems). All heterozygous sites in the ncDNA were coded using the IUB code. All sequences were first aligned using ClustalW [23] as implemented in BioEdit [24], and thereafter manually to optimize homology. All new sequences were deposited in GenBank (Table 1).

Sequence analyses

The four markers (CR, *Cyt b*, STAT and OSTA5) were analyzed separately and then combined into a single data set. Gaps were treated as missing data. In addition, the markers were concatenated and analyzed according to origin of marker (mtDNA or nucDNA). The number of variable sites, number of parsimony informative sites and nucleotide frequencies were estimated for each data matrix in MEGA 6 [25].

Phylogenetic reconstruction was performed using both maximum likelihood (ML) and Bayesian (Bayes) approaches using the programs Garli 2.0 [26] and MrBayes 3.2 [27], respectively. The most appropriate substitution model for each gene (CR - HKY + I + G, *Cyt b*-HKY+I, STAT - TIM1 + I, OSTA5 - TIM1ef + I) was selected using the Akaike information criterion (AIC) as implemented in jModelTest [28, 29]. For the concatenated data sets, partitioned analyses were conducted, with data partitioned by gene, with the parameters of nucleotide substitution models unlinked across partitions. Each ML analysis was initiated from a random starting tree, with nodal support assessed using 1000 bootstrap replicates. Two independent Bayes runs of 5 million generations each were performed; each run consisted of four Monte Carlo Markov chains (MCMC), with topologies sampled every 250 generations. The program Tracer 1.6 [30] was used to determine that the effective sample size (ESS) had reached > 200 for all parameters. A 50 % majority rule consensus tree was constructed using the

CONSENSE program in the PHYLIP package [31]. In each simulation the first 20 % of generations were discarded as burn-in, after a pilot run to determine that this was sufficient to achieve stationarity.

Molecular dating

No Rhinolophidae or Hipposideridae fossils are known from before the middle Eocene, but fossils referable to both families are reported from the middle to late Eocene of Europe [32, 33], including *H. schlosseri* from the late Eocene of France [34]. As fossil calibration points are not available for *H. commersoni* s.l., we expanded the taxonomic sampling used in the molecular clock analysis to allow the use of fossil calibration points. *Cyt b* sequences were downloaded from GenBank for six species of *Hipposideros*: *H. armiger* (DQ865345), *H. pratti* (EF544427), *H.* aff. *ruber* (EU934485), *H.* aff. *caffer* (EU934461), *H. gigas* (EU934469) and *H. cyclops* (EU934466), as well as eight species and 12 individuals of the family Rhinolophidae considered as sister to the Hipposideridae [35, 36]: *R. mossambicus* (JQ929291, JQ929299), *R. eloquens* (JQ929284, JQ929285), *R. hildebrandtii* (JQ929297, JQ929298), *R. darlingi* (EU436675), *R. fumigatus* (FJ457614), *R. landeri* (EU436668, FJ457612), *R. ruwenzorii* (EU436679) and *R. maclaudi* (FJ185203). As calibration point, we used a minimum of 37 Mya and maximum of 55 Mya for the split between the Rhinolophidae and the Hipposideridae [20, 37, 38].

Divergence dates between clades were estimated from the expanded Cyt b data set using an uncorrelated relaxed lognormal Bayesian molecular clock approach [39], as implemented in BEAST 2.1.3.0 [40]. The HKY + I substitution model was used, with the Yule speciation model as tree prior. As an alternative to fossil calibrated estimate of divergence times, an additional molecular clock analysis was conducted using a fixed mean substitution rate of $1.30 \times 10{-}8$ subs/site/year [5, 41]. This analysis was performed using the strict molecular clock model in BEAST. All other parameters were the same as in previous analysis. The MCMC chains were run for 30 million generations, with topologies and parameters logged every 1500 generations. Results were evaluated using Tracer v1.6 [30]. The Effective Sample Size (ESS) values were >200 for all parameters, suggesting the MCMC chains had sufficiently converged [40]. After discarding the first 25 % of generations as burn-in, the maximum clade credibility tree was constructed using TreeAnnotator 1.7.4 (available in the BEAST package), and then visualized with FigTree 1.3.1 [42].

Morphological measurements

The following standard external measurements were taken from specimens collected in the field before their preparation using a millimeter ruler accurate to the nearest 0.5 mm: total length (TL), tail length (TAIL), hind foot length (HF) (not including claw), ear length (EAR) and forearm length (FA). Further, body mass (WT) was recorded in grams using a spring balance accurate to the nearest 0.5 g.

Cranial and dental measurements were obtained from cleaned skulls of voucher specimens using digital calipers accurate to the nearest 0.1 mm and following for the most part Freeman [43]: cranial — greatest skull length (SL), condyle-basal length (CBL), greatest zygomatic breadth (ZYGO), minimum interorbital width (IOW), greatest mastoid breadth (MAST), rostrum length (ROST), palatal length (PAL); and dental — total tooth row (C1-M3), upper molar row (UP MOL R), width at upper canines (C1-C1), width at upper posterior molars (M3-M3), height upper canine (UP CANIN), dentary length (DENT LEN), moment arm of temporal (MOM1 COR), total lower tooth row (I1-M3) and lower tooth row (LOWER TR). Only adult specimens were used in this study, as defined by the eruption of all permanent teeth (often showing some wear), the complete ossification of the basiosphenoid suture, and the development of the sagittal crest. All external and craniodental measurements used in the analyses were made by a single individual (SMG). The number of adult male *H. commersoni* available in the morphometric dataset was limited, and given there is evidence of sexual dimorphism in this species [16, 44], males were excluded from the morphometrics analyses. Intact skulls from 20 adult females were included in this study from 13 localities spanning the latitudinal distribution of *H. commersoni* in western Madagascar.

Statistical analyses

Shapiro–Wilk's test and Levene's test were implemented to assess the assumptions of normality and equality of variances of variable characters in the dataset. Analysis of Variance (ANOVA) was carried out using post-hoc Tukeytests, to assess morphological and craniodental differences between the derived genetic clades.

Principal component analysis (PCA) was conducted separately on external and craniodental measurements to examine possible segregation of the different molecular clades, as well as geographic variation in H. commersoni. Further hierarchical cluster analysis was implemented using Ward's method on both measurement data sets to provide additional confirmation of the factor loadings obtained and to identify natural groupings among samples

(Tables 2 and 3) [45, 46]. Data were log-transformed to improve normality and homoscedasticity. All statistical analyses were carried out using SPSS (version 21.0, IBM SPSS Statistics).

Results

DNA sequencing

The four genetic markers were successfully amplified for all 31 taxa included in the molecular portion of the study (Table 1). The aligned sequence data for each marker included (Table 1): CR, 481 bp (114 variable sites); *Cyt b*, 705 bp (60 variable sites); STAT, 476 bp (six variable sites); and OSTA5, 676 bp (nine variable sites). The nucleotide composition and the levels of variation of the two marker systems (mtDNA vs nucDNA) differed (Table 4). The mtDNA partition contained the highest number of variable characters (174 variable sites), while the ncDNA data was more conserved (15 variable sites). For the STAT gene, only eight unique haplotypes were identified. The haplotypic diversity for this dataset is high (Hd = 0.80), but the nucleotide diversity is low (π = 0.00274). For OSTA5 gene, 10 unique haplotypes were identified. Once again low levels of nucleotide variability were observed (π = 0.00264). As expected, CR contained the highest proportion of variable characters (24 % variable characters) followed by Cyt b (9 % variable characters).

Phylogenetic analysis

The phylogenetic analysis of each nuclear marker independently resulted in largely unresolved trees, which is not surprising given the few number of variable characters observed (Additional file 1: Figure S3 and S4; Table 4). The mtDNA marker topologies were better resolved (Additional file 1: Figure S1 and S2). There was no significant (ML bootstrap > 70 %; Bayesian posterior probability >95 %) conflict among the topologies recovered by the independent analysis of the four molecular markers [47] and the molecular data were concatenated (2336 bp, 118 variable characters). The ML and Bayesian analyses of the concatenated data matrix (mtDNA + ncDNA; Fig. 1) did not recover *H. commersoni* as a single monophyletic lineage. Two *H. commersoni* specimens (collected from the Isalo National Park, FMNH 175970, and from Itampolo, FMNH 184173) were placed in close association (ML bootstrap, 64; Bayes' posterior probability, 1.00) to African *H. gigas* and *H. vittatus* (Clade A; Fig. 1). Clade A is genetically distant from the other Malagasy *H. commersoni* specimens. This level of divergence (2.6 % between Clades A and C to 3.1 % between Clades A and B [Table 5]) based on *Cyt b* uncorrected mean pairwise divergence is notable given that other *H. commersoni* specimens collected from these two localities cluster within Clade B (ML bootstrap, 99; Bayesian posterior probability, 1.00) together with specimens from localities in the southwest (Fig. 1). Clade C consists exclusively of specimens collected from the north. Clades B and C form a well-

supported monophyletic lineage (ML bootstrap, 97; Bayes' posterior probability, 1.00), sister to the lineage which includes Clade A, *H. gigas* and *H. vittatus* (ML bootstrap, 64; Bayes' posterior probability, 1.00). These data strongly suggest the presence of several independently evolving lineages within *H. commersoni*. Clades B and C are geographically structured, with Clade C including specimens collected from northern Madagascar, while members of Clade B are more widely distributed in the south. Uncorrected pairwise sequence distances for the two mtDNA regions (CR and Cyt b) are presented in Table 5. Genetically, Clade A is as distant from the *H. gigas*-*H. vittatus* species pair (respectively 3.2 % and 2.9 %) as it is from other *H. commersoni* placed in Clades B and C, again highlighting the uniqueness of this lineage.

Molecular clock dating

The maximum clade probability tree (Fig. 2) inferred in BEAST supports the Garli and MrBayes phylogenies. Our analyses recovered *H. commersoni* Clade A as basal to all other members of the *H. commersoni* species group (*H. commersoni* Clades B & C, *H. gigas* and *H. vittatus*). This suggests that *H. commersoni* Clades B and C are more closely related to the African taxa *H. gigas* and *H. vittatus* than to other Malagasy *H. commersoni* (Clade A). Molecular clock estimates using fossil calibration suggest that Clade A diverged from its sister taxa (*H. vittatus*, *H. gigas*, *H. commersoni* Clade B and C) during the Miocene (5.81 MYA; 95 % HPD 2.24–13.93). This divergence event is older than the separation of other established species groups, for example *Rhinolophus mossambicus* and *R. fumigatus*, which our molecular clock estimates suggests diverged 4.80 MYA (95 % HPD 1.90–9.45), and *R. ruwenzorii* and *R. maclaudi*, which diverged 3.86 MYA (95 % HPD 1.11–8.54) [37]. Clades B and C of the *H. commersoni* group last shared a common ancestor during the Pliocene (3.38 MYA; 95 % HPD 1.32–8.48, Fig. 2). The estimated divergence times using the substitution rate calibrated molecular clock resulted in more recent divergence dates (Additional file 2: Figure S5). For example, molecular clock estimates suggest that Clade A diverged from its sister taxa 4.20 MYA (95 % HPD 1.99–13.73) and the two sister Clades B & C shared their last common ancestor 2.55 MYA (95 % HPD 1.15–7.89, Table 6). The 95 % HPD intervals for divergence events from both analyses (fossil calibrated and substitution rate calibrated) were broad and did show overlap. From Taylor et al. [37], *R. mossambicus* and *R. fumigatus*, diverged 6.96 MYA, which is older than our estimate and *R. ruwenzorii* and *R. maclaudi* about 2.99 MYA, which is more recent than our estimate. We suggest that using a calibration point allowed BEAST to estimate a more realistic clock rate. The substitution rate of 1.0 in the fossil calibrated clock allowed the determination of relative rates for each recovered clade.

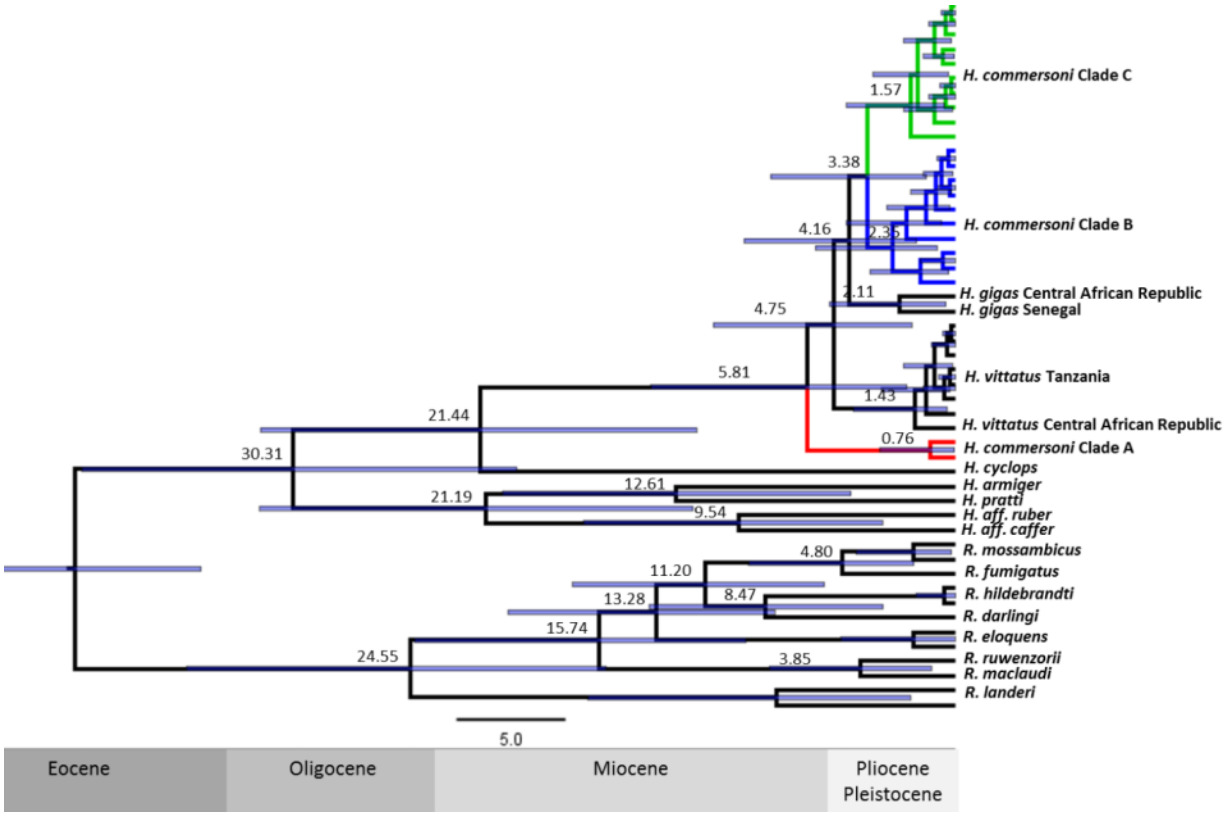

Fig. 2 Maximum clade probability tree, inferred from the analysis of Cyt b data based on fossil calibration. Values at nodes indicate the posterior mean divergence dates in millions of years before present. Shaded bars indicate the 95 % highest posterior density (HPD) credibility intervals

1

2

Morphometrics

As Clade A was comprised of two individuals, statistical comparisons were made only between animals belonging to Clades B and C. Shapiro–Wilk's test ($P > 0.05$) and a visual inspection of their histograms showed that the variable characters in the dataset were normally distributed. Levene's test verified the equality of variances in the samples ($P > 0.05$).

Analysis of variance (ANOVA) revealed significant variation in four of six external variables and 15 of 16 craniodental variables when taxa were sorted into Clades A, B or C following the results of molecular analyses (Table 7). Clade A is morphologically similar to Clade B, but is morphologically differentiated from Clade C (Table 7). The larger Clade C bats had significantly greater total length, tail length, ear length and forearm length than specimens assigned to Clade B, yet there were no significant differences in hindfoot length and body mass between the clades (Table 7). In parallel, craniodental measurements were significantly larger in Clade C than Clade B, except minimum interorbital width (Table 7).

The first two unrotated principal components (PC1 and PC2) explained 67.6 % of the total variance in external measurements (Fig. 3a) and 88.2 % of total variance in craniodental morphology (Fig. 3b). PCA plots of external and craniodental variables recovered Clades B and C as two distinct groups with little overlap. In contrast, individuals of Clades A and B overlapped in morphological variables. Because several of the external morphology variables and most of the craniodental variables loaded high on PC1, we interpreted this component as a proxy for size. Both sets of variables suggest that *H. commersoni* Clades A and B are smaller than those from Clade C (Fig. 3). In the case of external measurements, PC2 showed an inverse relationship between tail length and hind foot length – bats that had high loadings on PC2 had a relatively long tail but short hind foot, whereas bats that had low loadings on PC2 had a relatively short tail but long hind foot (Table 8). In the case of craniodental variables, PC2 indicated skull robustness (Table 9) - bats that loaded high on PC2 had a relatively larger interorbital width than bats that loaded low on PC2.

Two major clusters were recovered from the dendrograms produced by the hierarchical cluster analyses of external and craniodental variables, supporting the PCA analysis. The first cluster, recovered in both dendrograms, included all eight individuals from northern Madagascar assigned to Clade C and two animals genetically assigned to Clade B (FMNH 221308 from Ankarana and FMNH 175777 from Namoroka). The second cluster contained the smaller southern individuals from Clades A and B (Fig. 4), which confirms that the two

genetically divergent animals belonging to Clade A are morphologically similar to animals from Clade B.

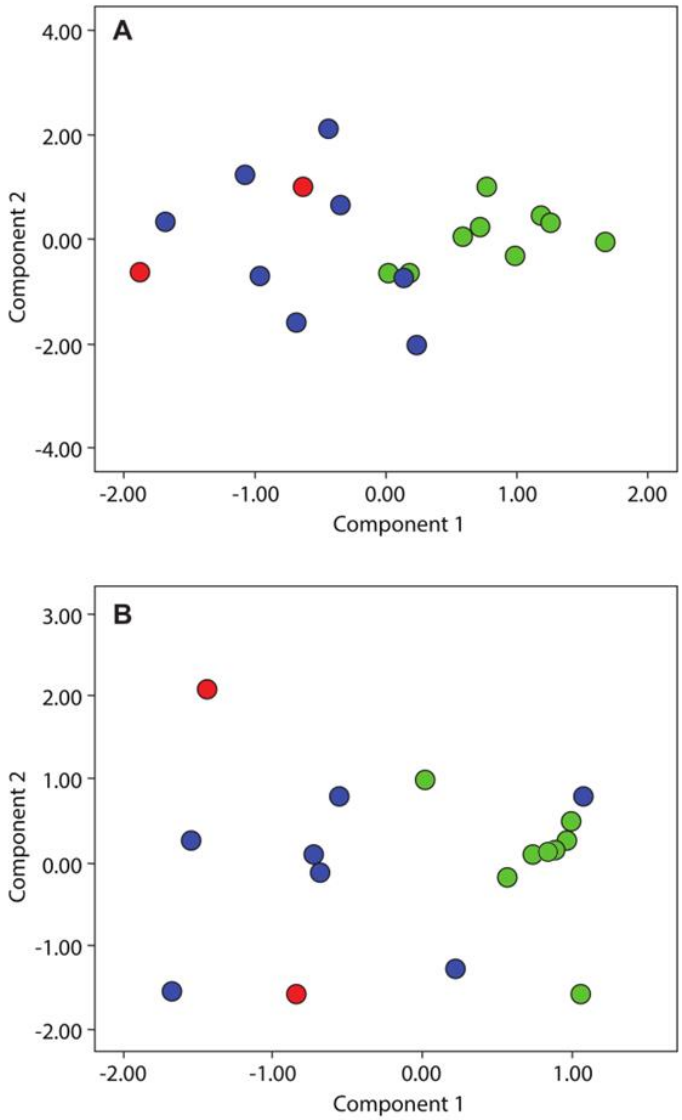

Fig. 3 Principal component analyses of female *Hipposideros commersoni* for **a** log-transformed external variables for 19 specimens and **b** log-transformed craniodental variables for 17 specimens (red = Clade A, blue = Clade B, green = Clade C)

1

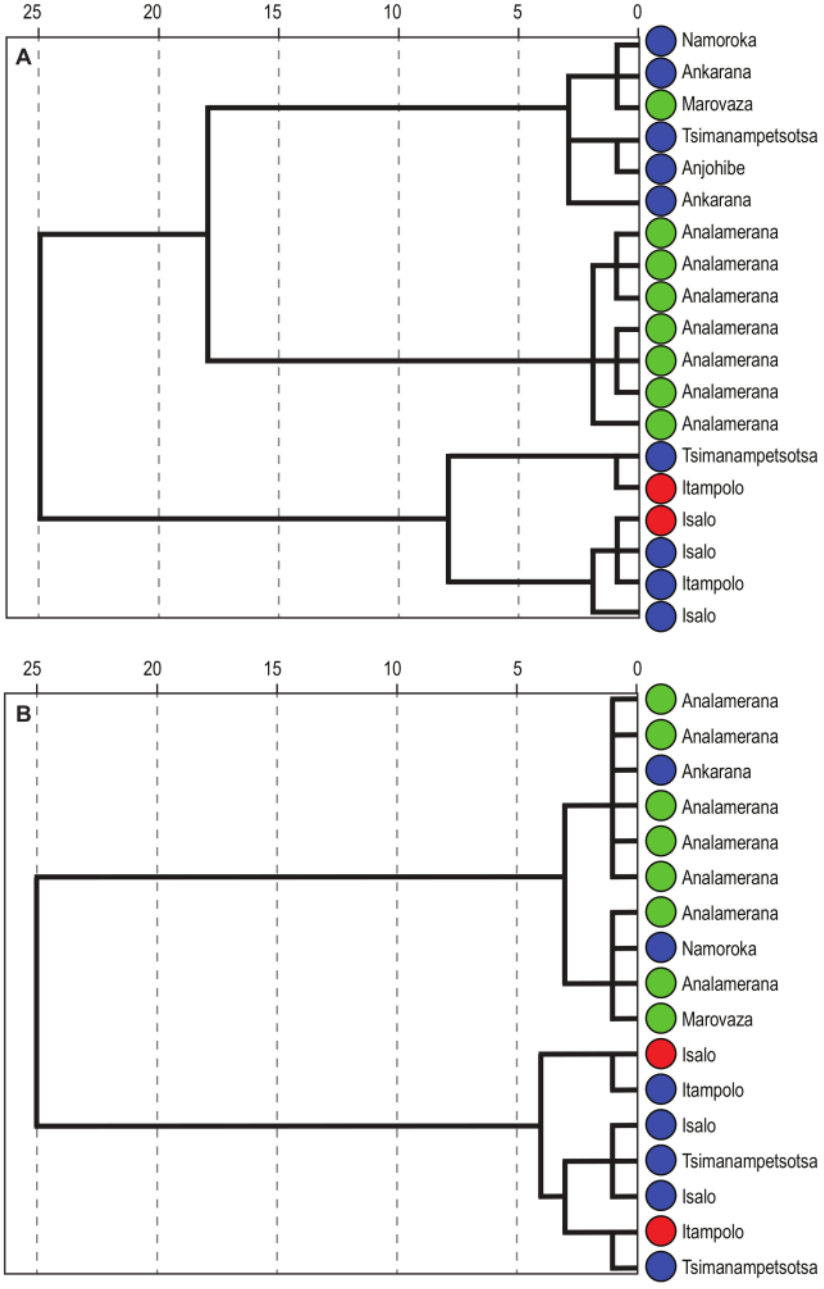
25
20
15
10
5
0
A
Namoroka
Ankarana
Marovaza
Tsimanampetsotsa
Anjohibe
Ankarana
Analamerana
Analamerana
Analamerana
Analamerana
Analamerana
Analamerana
Analamerana
Tsimanampetsotsa
Itampolo
Isalo
Isalo
Itampolo
Isalo
25
20
15
10
5
0
B
Analamerana
Analamerana
Ankarana
Analamerana
Analamerana
Analamerana
Analamerana
Namoroka
Analamerana
Marovaza
Isalo
Itampolo
Isalo
Tsimanampetsotsa
Isalo
Itampolo
Tsimanampetsotsa

Fig. 4 Hierarchical clustering dendrogram for **a** log-transformed external variables for 19 specimens and **b** log-transformed craniodental variables of 17 female *Hipposideros commersoni*. Collection locality information is assigned to each individual and color-coding is based on main lineages recovered by molecular data

Table 2 Reformed agglomeration table from hierarchical cluster analysis using Ward's method of log-transformed external measurements of *Hipposideros commersoni* s.s.

No. of clusters	Agglomeration last step	Coefficients this step	Change
2	36.000	21.500	14.500
3	21.500	11.308	10.192
4	11.308	6.921	4.387
5	6.921	5.562	1.359
6	5.562	4.286	1.276

Table 3 Reformed agglomeration table from hierarchical cluster analysis using Ward's method of log-transformed craniodental measurements of *Hipposideros commersoni* s.s.

No. of clusters	Agglomeration last step	Coefficients this step	Change
2	0.252	0.143	0.109
3	0.143	0.102	0.041
4	0.102	0.072	0.030
5	0.072	0.059	0.013
6	0.059	0.046	0.013

Table 4 Characteristics of datasets used in this study. Patterns of sequence variability are presented for two mtDNA regions (CR and *Cyt b*), two nuclear introns (bSTAT and OSTA5) and the combined data matrix. The total number of nucleotide sites, variable and parsimony informative sites, as well nucleotide frequencies are given for each partition and the combined data matrix

Gene	**Total number of individuals**	**Total sites**	**Variable sites**	**Parsimony informative sites**	**Nucleotide frequencies**			
					%A	**%T**	**%C**	**%G**
CR	31	481	114	72	32.73	27.24	25.74	14.29
Cyt b	31	705	60	38	26.90	27.06	30.86	15.17
bSTAT	31	476	6	2	20.17	27.91	28.77	23.14
OSTA5	31	676	9	6	23.85	25.46	27.04	23.65
Supermatrix	31	2336	189	118	25.87	26.84	28.26	19.03

Table 5 Uncorrected mean pairwise distances based on analyses of the CR (below the diagonal) and *Cyt b* gene (above the diagonal) between major lineages of *Hipposideros commersoni* s.s. (Clades A, B, C) identified in the molecular analyses, *H. gigas* and *H. vittatus*

	Clade A	**Clade B**	**Clade C**	***H. gigas***	***H. vittatus***
Clade A		0.031	0.026	0.032	0.029
Clade B	0.072		0.019	0.031	0.028
Clade C	0.101	0.058		0.025	0.026
H. gigas	0.072	0.083	0.096		0.029
H. vittatus	0.074	0.077	0.090	0.069	

Table 6 Divergence dates between major lineages of *Hipposideros commersoni* s.s. (Clades A, B, C) and *H. gigas* and *H. vittatus*. Two molecular clock analyses were conducted. Fossil-calibrated values were estimated using a Bayesian lognormal relaxed-clock model, while the substitution rate calibrated values were estimated using the strict molecular clock model using a fixed mean substitution rate of 1.30 X 10^{-8} subs/site/year. The mean estimated values and the 95% highest posterior density (HPD) ranges are given for the two molecular clocks. See Figure 2 for the corresponding maximum clade probability trees.

	Divergence times using fossil calibration point		**Divergence times using fixed mean substitution rate**	
Node:	**Mean**	**95% HPD (Mya)**	**Mean**	**95% HPD (Mya)**
Clade A	5.80	2.24-13.93	4.20	1.97-13.73
H. vittatus	4.75	2.01-11.09	3.68	1.80-10.88
H. gigas	4.16	1.77-9.68	3.17	1.50-9.00
Clade B & C	3.38	1.32-8.48	2.55	1.15-7.99

Table 7 Summary of body mass, external body and craniodental measurements, and results of one-way ANOVAs and Tukey *post hoc* tests for *Hipposideros commersoni* s.s. based on the molecular clades defined in this study. See materials and methods for definitions of variable acronyms. ns = not significant

Variable		**Clade A**	**Clade C**	**Clade B**	**One-way ANOVA**		**Post hoc Tukey tests**
					$F_{(2, 16)}$	**P**	
TL					6.50	0.01	*P* = 0.03; Clade B < C
	N	2	9	8			
	Mean	121.0	133.6	125.6			
	Std. Deviation	-	4.50	7.23			
	Minimum	119	125	115			
	Maximum	123	138	137			
TAIL					7.03	0.006	*P* = 0.006; Clade B < C
	N	2	9	8			

	Mean	32	36.8	31.0			
	Std. Deviation	-	2.91	3.66			
	Minimum	30	31	25			
	Maximum	34	41	35			
HF					1.51	ns	ns
	N	2	9	8			
	Mean	14.5	15.8	14.8			
	Std. Deviation	0.71	0.44	1.98			
	Minimum	14	15	13			
	Maximum	15	16	18			
					10.16	0.01	*P* = 0.02;
EAR							Clade B < C
	N	2	9	8			

	Mean	26.5	30.7	28.6			
	Std. Deviation	-	0.71	1.85			
	Minimum	26	30	26			
	Maximum	27	32	31			
					6.41	0.009	*P* = 0.02;
FA							Clade B < C
	N	2	9	8			
	Mean	80.5	86.4	82.3			
	Std. Deviation	-	2.88	2.96			
	Minimum	80	82	79			
	Maximum	81	91	87			
WT					0.20	ns	ns
	N	2	9	8			

	Mean	40.5	42.11	39.69			
	Std. Deviation	-	5.07	7.40			
	Minimum	26	30	29			
	Maximum	55	47	49			
					$F_{(2, 14)}$	P	
					9.82	0.002	*P* = 0.011;
SL							Clade B < C
	N	2	8	7			
	Mean	26.95	29.72	28.08			
	Std. Deviation	-	0.67	1.20			
	Minimum	26.5	28.2	26.6			
	Maximum	27.4	30.5	29.9			
					9.68	0.002	*P* = 0.009;
CBL							Clade B < C
	N	2	8	7			

	Mean	23.9	26.34	24.78			
	Std. Deviation	-	0.60	1.12			
	Minimum	23.6	25.1	23.4			
	Maximum	24.2	27.1	26.6			
ZYGO					6.32	0.01	ns
	N	2	8	7			
	Mean	14.1	15.65	14.83			
	Std. Deviation	-	0.59	0.64			
	Minimum	13.6	15	14.1			
	Maximum	14.6	16.8	15.8			
IOW					0.36	ns	ns
	N	2	8	7			

	Mean	2.9	3.01	2.93			
	Std. Deviation	-	0.13	0.26			
	Minimum	2.6	2.8	2.6			
	Maximum	3.2	3.2	3.3			
					5.91	0.034	*P* = 0.014;
MAST							Clade B < C
	N	2	8	7			
	Mean	12.2	13.67	12.91			
	Std. Deviation	-	0.51	0.69			
	Minimum	11.7	12.9	12.2			
	Maximum	12.7	14.4	13.9			
					4.34	0.034	*P* = 0.038;
ROST							Clade B < C
	N	2	8	7			

	Mean	10.95	11.70	10.94			
	Std. Deviation	-	0.38	0.68			
	Minimum	10.7	11	10.1			
	Maximum	11.2	12.1	12			
PAL					4.34	0.028	ns
	N	2	8	7			
	Mean	3.65	4.47	4.07			
	Std. Deviation	-	0.27	0.43			
	Minimum	3.2	4	3.7			
	Maximum	4.1	4.8	4.9			
					10.97	0.001	*P* = 0.004;
C1-M3							Clade B < C
	N	2	8	7			

	Mean	9.45	10.55	9.79			
	Std. Deviation	-	0.26	0.50			
	Minimum	9.3	10	9.3			
	Maximum	9.6	10.8	10.8			
					9.79	0.002	*P* = 0.003;
UP MOL R							Clade B < C
	N	2	8	7			
	Mean	7.35	7.87	7.36			
	Std. Deviation	-	0.17	0.31			
	Minimum	7.3	7.6	7			
	Maximum	7.4	8.2	8			
					11.69	0.001	*P* = 0.002;
C1-C1							Clade B < C
	N	2	8	7			

	Mean	6.90	8.16	7.17			
	Std. Deviation	-	0.46	0.45			
	Minimum	6.6	7.3	6.7			
	Maximum	7.2	8.7	7.9			
					7.33	0.007	*P* = 0.011;
M3-M3							Clade B < C
	N	2	8	7			
	Mean	9.85	10.82	10.03			
	Std. Deviation	-	0.24	0.64			
	Minimum	9.7	10.4	9.2			
	Maximum	10	11.1	11			
UP CANIN					4.50	0.031	ns
	N	2	8	7			

	Mean	4.35	5.09	4.60			
	Std. Deviation	-	0.26	0.45			
	Minimum	3.9	4.7	3.8			
	Maximum	4.8	5.4	5.3			
					8.46	0.004	*P* = 0.011;
DENT LEN							Clade B < C
	N	2	8	7			
	Mean	17.75	19.57	18.33			
	Std. Deviation	-	0.48	0.95			
	Minimum	17.6	18.5	17.1			
	Maximum	17.9	20	19.6			
MOM1 COR					4.01	0.042	ns
	N	2	8	7			

	Mean	5.65	6.22	5.76			
	Std. Deviation	-	0.21	0.49			
	Minimum	5.5	6.0	5.0			
	Maximum	5.8	6.6	6.4			
					7.78	0.005	*P* = 0.014;
I1-M3							Clade B < C
	N	2	8	7			
	Mean	11.75	12.99	12.13			
	Std. Deviation	-	0.30	0.70			
	Minimum	11.6	12.5	11.1			
	Maximum	11.9	13.3	13.2			
					11.20	0.001	*P* = 0.003;
LOWER TR							Clade B < C
	N	2	8	7			

Mean	10.70	11.87	10.97
Std. Deviation	-	0.27	0.57
Minimum	10.5	11.5	10.2
Maximum	10.9	12.2	11.9

Table 8. Character loading for the first three components in a Principal Component (PC) analysis based on external measurements of *Hipposideros commersoni*

Variable	PC1	PC2	PC3
TAIL	0.543	0.566	0.518
HF	0.541	-0.657	0.263
EAR	0.850	-0.197	-0.185
FA	0.824	-0.317	-0.172
TL	0.774	0.308	0.265
WT	0.519	0.461	-0.636

Table 9. Character loading for the first three components in a Principal Component (PC) analysis based on craniodental measurements of *Hipposideros commersoni*

Variable	PC1	PC2	PC3
SL	0.980	-0.140	-0.026
CBL	0.980	-0.110	-0.034
ZYGO	0.898	-0.288	0.171
IOW	0.396	0.805	0.315
MAST	0.909	-0.264	0.048
ROST	0.800	0.051	0.446
PAL	0.865	-0.315	0.019
C1-M3	0.972	0.039	-0.071
UP MOL R	0.869	0.258	0.021
C1-C1	0.925	-0.222	-0.129
M3-M3	0.976	0.034	0.010
UP CANIN	0.688	0.578	-0.342
DENT LEN	0.977	-0.038	-0.082
MOM1 COR	0.908	-0.035	0.200

Discussion

This study combines evidence from molecular (mtDNA and ncDNA) and morphological characters to provide support for the reciprocal monophyly of several independently evolving lineages within *Hipposideros commersoni*, occurring on Africa and nearby islands, as well on Madagascar. One of the principal questions addressed is the evolutionary history and systematic relationships of Malagasy populations currently assigned to *H. commersoni*, as well as African populations currently placed within the *H. commersoni* species group [1].

The results suggest that previous taxonomic treatments of the group underestimated species diversity of *H. commersoni* and that a cryptic species appears to be present. Although our geographic sampling did not cover the complete range of this species, specifically the eastern portion of the island, the results indicate nonmonophyly with respect to Madagascar of different recovered Malagasy clades.

Single locus or multilocus molecular data and/or morphological differences have been used previously to identify cryptic species diversity in southeast Asian [10, 48, 49] and African [50, 51] hipposiderids. Based on an analysis of the *H. larvatus* species complex using mitochondrial control region markers, morphology and bioacoustics two forms were identified (*H. khasiana* and *H. grandis*) that were differentiated based on haplotypic structure and phonics [52]. In another example, *H. khaokhouaensis* from Laos is similar in general body size and shape to its sister species *H. rotalis*, but differs in aspects of the noseleaf, skull structure related to bioacoustics and echolocation frequency [4]. The phylogenetic relationships within the African *H. ruber* species complex were investigated [51] using *Cyt b* to determine the taxonomic status of two divergent genetic forms often found in sympatry in Senegal, which might represent cryptic species despite being morphologically indistinguishable. However, in this latter case, absence of nuclear gene flow between these two reputed forms remains to be investigated to demonstrate their reproductive isolation.

All *H. commersoni* sequenced in the current study were from the western half or extreme north of Madagascar. The molecular analyses presented herein indicate that *H. commersoni* as currently diagnosed is not monophyletic with respect to Madagascar, and with strong support for the presence of divergent lineages. As two individuals from Isalo (FMNH 175970) and Itampolo (FMNH 184173) form a well-supported monophyletic group (Clade A), basal to African *H. vittatus* and *H. gigas*, and separate from the balance of Malagasy *H. commersoni* (Clades B and C), a single origin of this species complex on the island is not supported. The long branches separating these clades (ranging from 2.6 to 3.2 % uncorrected

sequence divergence) indicate relatively deep independent evolutionary trajectories of several million years based on molecular clock inferences. Although Clade A was only significantly supported by the mitochondrial data, this is not surprising, given the relatively conservative nature of the nuclear markers sequenced. The absence of haplotype sharing in OSTA5 gene for Clades B and C, however, does indicate at least some degree of genetic isolation between these two groups. These results indicate that members of the *H. commersoni* species group do not represent a single widespread Afro-Malagasy taxon. Furthermore, the molecular data support a certain level of divergence between Clades B (in the north) and C (in the south). Additional samples are needed to ascertain whether the recovered phylogeny is an artefact of sampling or the result of isolation by distance. The sequence divergence of Clade A with respect to the balance of *H. commersoni* (Clades B and C) is comparable with that observed between African *H. vittatus* and *H. gigas*, and based on the molecular clock analysis, it is estimated that the Clade A lineage diverged from its sister taxa during the Miocene.

Genetic divergence in mitochondrial genes varies widely among species. Avise [53] highlighted that due to the matrilineal nature of inheritance of mitochondrial genes, relatively deep divergences do not necessarily correspond to species boundaries. Further, significant nuclear gene flow may occur among divergent mitochondrial phylogroups. Using the published literature, Baker and Bradley [54] found an interval of 3.3–14.7 % uncorrected genetic distance between sister species of bats, and distances ranging from 0.6–2.3 % encompassing intraspecific variation. These values have been corroborated by recent studies of cryptic species of Asian *Hipposideros*, which show three different levels of interspecific divergences: 1) as low as 3.9 %, with supporting evidence from external and craniodental morphology, as well as bioacoustics [4]; 2) an intermediate level of 6.5 %, with corroborating evidence from bioacoustics [55]; and 3) as high as 13.4 %, with corroborating evidence from bioacoustics [52]. The sequence divergence values recovered in the current study separating Clade A from other *H. commersoni* (Clades B and C) suggest that previous taxonomic conclusions underestimated the species diversity of Malagasy bats currently classified as *H. commersoni*.

Within the portion of the phylogeny composed of most individuals assigned to *H. commersoni*, the molecular data support two largely geographically non-overlapping clades: a northern group (Clade C) with a relatively limited range and a southern group with a broader geographical distribution (Clade B). The molecular clock analyses indicate that these two clades diverged from one another approximately 3.38 MYA. Morphometric analyses are generally consistent with the molecular data, suggesting a north–south break between animals assigned to Clades B and C. The exception was in Ankarana (far north), where the two lineages co-occur

but individuals from each clade could not be differentiated based on multivariate analyses of external and craniodental measurements (Fig. 4). Patterns of morphological variation were not uniform or falling along well-defined clines, such as latitude, and members of these two clades do not completely separate from one another. In term of genetics, based on currently available samples, Clades B and Clade C are differentiated, for example, the uncorrected *Cyt b* sequence divergence is 1.9 %. In the case of the two individuals falling within Clade A, they are genetically distinct from those in Clade B, but show no apparent morphological differentiation. Hence, we interpret this variation as some form of incipient speciation between animals assigned to Clades B and C.

Ramasindrazana et al. [44] have recently analyzed echolocation calls of animals referred to as *H. commersoni* captured in western Madagascar. They found latitudinal variation - animals from the north being larger and emitting lower call frequencies and those from the south smaller and emitting higher call frequencies. On average, females, referred to as *H. commersoni*, from the north (Ankarana) deviate from the allometric relationship with lower resting frequency of echolocation calls than predicted from body size. These authors suggested that this pattern might be explained by either regional variation in bioacoustics, intra-island migratory movements or the presence of a cryptic species. The animals that deviated from the pattern were not sequenced in this current study and no further interpretation can be offered.

Evolution of Malagasy *Hipposideros*

A particularly striking result of the current analyses is the existence of a previously unrecognized clade of Malagasy *H. commersoni* (Clade A), estimated to have diverged from sister taxa (Malagasy *H. commersoni* Clades B and C, and African *H. gigas* and *H. vittatus*) during the late Miocene (5.81 MYA). *Hipposideros gigas* and *H. vittatus* are more closely related to *H. commersoni* Clades B and C, suggestive of two dispersal hypotheses. The first scenario is that Clade A and Clade B-C originated from two independent African mainland-to-Madagascar dispersal events, with Clade A arriving on the island during the Miocene (approximately 5.8 MYA) and Clade B-C more recently (approximately 3.38 MYA). A second hypothesis is that the *H. commersoni* group evolved on Madagascar and at some point after the end of the Miocene, a population related to Clade A crossed the Mozambique Channel and colonized the African continent leading to two recognized extant forms, *H. vittatus* and *H. gigas*, that are morphologically and karyologically similar [17, 36]. Following this second

hypothesis, speciation took place within the Malagasy population, giving rise to Clades B and C representing the most recent branch of this lineage.

Madagascar was cooler and drier during periods of Pleistocene glaciation, which led to habitat shifts and forced some taxa to retreat into refugia [56–58], in different high mountain areas [59]. Expansion from refugia would have occurred during warmer periods. *Hipposideros* bones from relatively recent geological deposits are known from several sites on the island [60]. Subfossils from Tsimanampetsotsa, extreme southwest, identified as *Hipposideros* were slightly smaller than typical *H. commersoni* [61], which occur in this region today [11]. Samonds [62] conducted research on *Hipposideros* subfossils from Anjohibe Cave in the northwest of Madagascar, and the excavated fossils were dated between 10,000 and 80,000 years ago. Samonds [62] identified three morphological forms of *Hipposideros* from these deposits: 1) those fitting with extant *H. commersoni*; 2), *H. besaoka*, which was described as a new species, being larger and more robust than *H. commersoni*; and 3), *Hipposideros* sp. cf. *H. commersoni*, which appeared to have some dental differences from modern *H. commersoni*. *Hipposideros besaoka* and *H. commersoni* were sympatric and presumably living in the Anjohibe Cave during the same period, and they show a small amount of overlap in some dental measurements, not related to sexual dimorphism [62]. Our morphological and molecular data support parallel results in modern populations of *H. commersoni*, with Clades B and C known to occur in sympatry at one northern locality. This raises the intriguing possibility that one of the phylogenetic clades identified in this paper (Clade B or Clade C), might be referable to *H. besaoka* and, in this case, this species is not extinct. Further fine-scale phylogeographic studies using variable nuclear markers such as microsatellites are needed to clarify species boundaries and give a greater understanding of the processes underpinning the evolution of these taxa across Madagascar.

Geographically correlated population structure

Within *H. commersoni* (Clade B-C), the molecular data support two regionally associated clades: a small-bodied southern group with a broad geographical distribution (Clade B) and a large-bodied northern group (Clade C) with a relatively limited range. The molecular clock analyses indicate that these two clades diverged from one another approximately 3.38 MYA. Morphometric data are consistent with the molecular data, suggesting a north–south break in distribution. These two lineages are not completely allopatric. In Ankarana, sequenced individuals assigned to these two genetic clades could not be distinguished using external and

craniodental measurements (Fig. 3). The morphometric data in the present study are consistent with conclusions of a previous study on geographic variation in morphology of this taxon in western Madagascar [16]. Specimens grouped into two distinct morphotypes, a larger morphotype found in northern Madagascar (from Analamerana to Ankarana and south to Bemaraha) and a smaller morphotype widely distributed in the south, from Isalo to Tsimanampetsotsa. Ranivo and Goodman [16] found that male *H. commersoni* do not show the same pattern and are largely homogenous in size across these zones.

At least three other Malagasy bat species, *Paratriaenops furculus* [63], *Chaerephon leucogaster* [64] and *Myotis goudoti* [65] show similar haplotypic segregation along a latitudinal gradient. However, the latitudinal distribution of different clades and the calculated expansion periods of the other species differ from late Pleistocene in *M. goudoti* to early Holocene in *C. leucogaster*, suggesting that no common historical process underlies the different demographic events between these taxa [64, 65].

Ranivo and Goodman [16] found both *H. commersoni* morphotypes in Isalo. The morphologically divergent animals from Isalo included two specimens (FMNH 175973 and 175975) that were collected on the same day and at the same cave site as the Isalo specimen (FMNH 175970) analyzed in our molecular study, which falls into Clade A. This latter specimen morphologically aligns with the smaller southern individuals, while FMNH 175973 and 175975 are of the larger northern morphotype. This may indicate some form of intraisland movements.

In eastern Africa, seasonal fluctuations in abundance of prey utilized by large hipposiderids are pronounced, which can result in food shortages during the cool dry season. These shifts in the resource base have been invoked to explain local seasonal movement in *H. vittatus*/*H. gigas* to areas with greater food abundance [7, 66]. It is unclear if *H. commersoni* remains inactive in caves during times of resource shortage or if local populations migrate to other sites. Large hipposiderid bats have high wing loading and low to medium aspect ratios [67], which may favor relatively quick, long-distance movements, allowing certain populations to track food resources [68, 69]. The colonization and speciation history of *H. commersoni* on Madagascar, as represented by a single species occurring on the island, is certainly more complex than currently understood. Further studies including increased spatial sampling and the use of additional molecular markers particularly faster evolving nuclear markers are needed to fully resolve the evolutionary history and associated systematics of the different clades occurring on Madagascar.

Conclusions

This study provides evidence, particularly from mitochondrial data, for the existence of at least two sympatrically occurring species of the genus *Hipposideros* on Madagascar. Absence of nuclear gene flow between groups remains to be established to verify their reproductive isolation, yet the lack of haplotype sharing in OSTA5 for Clades B and C indicates some degree of genetic isolation between these clades. Subfossil evidence indicates that in the recent geological past two species, *H. commersoni* and the presumed extinct *H. besaoka*, occurred in sympatry [62]. Given that we have recovered two genetically distinct lineages of *H. commersoni* (Clades B and C) living on occasion in sympatry, this might indicate that one of them is *H. besaoka* and, hence, still extant. A detailed morphological comparison of the type series of Samonds' [62] *H. besaoka* with modern *H. commersoni* represented in our data is needed to test this intriguing possibility and crucial before the description of a possible undescribed species.

References

1. Simmons NB. Order Chiroptera. In: Wilson DE, Reeder DM, editors. Mammal species of the World: a taxonomic and geographic reference. 3rd ed. Baltimore: Johns Hopkins University Press; 2005. p. 312–529.

2. Bates PJJ, Rossiter SJ, Suyanto A, Kingston T. A new species of *Hipposideros* (Chiroptera: Hipposideridae) from Sulawesi. Acta Chiropterologica. 2007;9(1):13–26.

3. Douangboubpha B, Bumrungsri S, Satasook C, Soisook P, Si Si Hla B, Aul B, et al. A new species of small *Hipposideros* (Chiroptera: Hipposideridae) from Myanmar and a revaluation of the taxon *H. nicobarulae* Miller, 1902 from the Nicobar Islands. Acta Chiropterologica. 2011;13(1):61–78.

4. Guillén-Servent A, Francis CM. A new species of bat of the *Hipposideros bicolor* group (Chiroptera: Hipposideridae) from Central Laos, with evidence of convergent evolution with Sundaic taxa. Acta Chiropterologica. 2006;8:39–61.

5. Thong VD, Puechmaille SJ, Denzinger A, Bates PJJ, Dietz C, Csorba G, et al. Systematics of the *Hipposideros turpis* complex and a description of a new subspecies from Vietnam. Mamm Rev. 2012;42:166–92.

6. Koopman KF. Chiroptera: Systematics. In: Niethammer J, Schliemann H, Starck D, editors. Handbuch der Zoologie, vol. VII. Berlin: Walter de Gruyter; 1994. p. 100–9.

7. McWilliam AN. Adaptive responses to seasonality in four species of insectivorous bats in coastal Kenya. University of Aberdeen: PhD thesis; 1982.

8. Peterson RL, Eger JL, Mitchell L. Chiroptères. Faune de Madagascar. 1995;84:1–204.

9. Pye JD. Bimodal distribution of constant frequencies in some hipposiderid bats (Mammalia: Hipposideridae). J Zool. 1972;166:325–35.

10. Murray SW, Campbell P, Kingston T, Zubaid A, Francis CM, Kunz TH. Molecular phylogeny of hipposiderid bats from Southeast Asia and evidence of cryptic diversity. Mol Phylogenet Evol. 2012;62:597–611.

11. Goodman SM, Ramasindrazana B. Bats or the order Chiroptera. In: Goodman SM, Raherilalao MJ, editors. Atlas of selected land vertebrates of Madagascar. Antananarivo: Association Vahatra; 2013. p. 169–209.

12. Kofoky A, Andriafidison D, Ratrimomanarivo F, Razafimanahaka HJ, Rakotondravony D, Racey PA, et al. Habitat use, roost selection and conservation of bats in Tsingy de Bemaraha National Park, Madagascar. Biodivers Conserv. 2007;16(4):1039–53.

13. Rakotoarivelo AR, Ranaivoson N, Ramilijaona OR, Kofoky AF, Racey PA, Jenkins RKB. Seasonal food habits of five sympatric forest microchiropterans in western Madagascar. J Mamm. 2007;88:959–66.

14. Rakotoarivelo AR, Ralisata M, Ramilijaona OR, Rakotomalala MR, Racey PA, Jenkins RKB. The food habits of a Malagasy giant: *Hipposideros commersoni* (E. Geoffroy, 1813). Afr J Ecol. 2009;47(3):283–8.

15. Razakarivony VR, Rajemison B, Goodman SM. The diet of Malagasy Microchiroptera based on stomach contents. Mamm Biol. 2005;70(5):312–6.

16. Ranivo J, Goodman SM. Variation géographique de *Hipposideros commersoni* de la zone sèche de Madagascar (Mammalia, Chiroptera, Hipposideridae). Verhandlungen des naturwissenschaftlichen Vereins Hamburg. 2007;43:35–56.

17. Monadjem A, Taylor PJ, Cotterill FPD, Schoeman MC. Bats of southern and central Africa: a biogeographic and taxonomic synthesis. Johannesburg: University of the Witwatersrand; 2010.

18. Irwin DM, Kocher TD, Wilson AC. Evolution of the cytochrome b gene of mammals. J Mol Evol. 1991;32:128–44.

19. Wilkinson GS, Chapman AM. Length and sequence variation in evening bat d-loop mtDNA. Genetics. 1991;128:607–17.

20. Eick GN, Jacobs DS, Matthee CA. A nuclear DNA phylogenetic perspective on the evolution of echolocation and historical biogeography of extant bats (Chiroptera). Mol Biol Evol. 2005;22:1869–86.

21. Matthee CA, Burzlaft JD, Taylor JF, Davis SK. Mining the mammalian genome for artiodactyl systematics. Syst Biol. 2001;50:367–90.

22. Igea J, Juste J, Castresana J. Novel intron markers to study the phylogeny of closely related mammalian species. BMC Evol Biol. 2010;10:369.

23. Thompson JD, Gibson TJ, Plewniak F, Jeanmougin F, Higgins DG. The CLUSTAL_X windows interface: flexible strategies for multiple sequence alignment aided by quality analysis tools. Nucleic Acids Res. 1997;25(24):4876–82.

24. Hall TA. BioEdit: a user-friendly biological sequence alignment editor and analysis program for Windows 95/98/NT. Nucleic Acids Symp Ser. 1999;41:95–8.

25. Tamura K, Stecher G, Peterson D, Filipski A, Kumar S. MEGA6: Molecular Evolutionary Genetics Analysis version 6.0. Mol Biol Evol. 2013;30:2725–9.

26. Zwickl DJ. Genetic algorithm approaches for the phylogenetic analysis of large biological sequence datasets under the maximum likelihood criterion. Ph.D. dissertation: The University of Texas; 2006.

27. Ronquist F, Teslenko M, Van der Mark P, Ayres D, Darling A, Höhna S, et al. MrBayes 3.2: efficient Bayesian phylogenetic inference and model choice across a large model space. Syst Biol. 2012;61:539–42.

28. Darriba D, Taboada GL, Doallo R, Posada D. jModelTest 2: more models, new heuristics and parallel computing. Nat Methods. 2012;9(8):772.

29. Posada D, Crandall KA. Modeltest: testing the model of DNA substitution. Bioinformatics. 1998;14:817–8.

30. Rambaut A, Suchard MA, Xie D, Drummond AJ. Tracer v1.6; 2014. http://beast.bio.ed.ac.uk/Tracer (accessed October 2014).

31. Felsenstein J. PHYLIP (Phylogeny Inference Package). Distributed by the author. Seattle, WA: Department of Genome Sciences, University of Washington; 2005.

32. McKenna MC, Bell SK. Classification of mammals above the species level. New York: Columbia University Press; 1997.

33. Simmons NB, Geisler JH. Phylogenetic relationships of *Icaronycteris*, *Archaeonyteris*, *Hassianycteris* and *Palaeochiropteryx* to extant bat lineages, with comments on the evolution of echolocation and foraging strategies in Microchiroptera. Bull Amer Mus Nat Hist. 1998;235:1–182.

34. Sigé B. Le gisement du Bretou (Phosphorites de Quercy, Tarn-et-Garonne, France) et sa faune de Vertèbres de l'Éocène supérieur. Palaeontographica. 1988;205:69–102.

35. Foley NM, Thong VD, Soisook P, Goodman SM, Armstrong KN, Jacobs DS, et al. How and why overcome the impediments to resolution: lessons from rhinolophid and hipposiderid bats. Mol Biol Evol. 2015;32:313–33.

1 36. Koubínová D, Sreepada KS, Koubek P, Zima J. Karyotypic variation in rhinolophid and
2 hipposiderid bats (Chiroptera: Rhinolophidae, Hipposideridae). Acta Chiropterologica.
3 2010;12(2):393–400.

4 37. Taylor PJ, Stoffberg S, Monadjem A, Schoeman MC, Bayliss J, Cotterill FPD. Four new bat
5 species (*Rhinolophus hildebrandtii* complex) reflect Plio-Pleistocene divergence of dwarfs and
6 giants across an Afromontane archipelago. PLoS ONE. 2012;7(9), e41744.

7 38. Teeling EC, Springer MS, Madsen O, Bates P, O'Brien SJ, Murphy WJ. A molecular
8 phylogeny for bats Illuminates biogeography and the fossil record. Science. 2005;307:580–4.

9 39. Drummond AJ, Ho SYW, Phillips MJ, Rambaut A. Relaxed phylogenetics and dating with
10 confidence. PLoS Biol. 2006;4, e88.

11 40. Drummond AJ, Rambaut A. BEAST: Bayesian evolutionary analysis by sampling trees.
12 BMC Evol Biol. 2007;7:214.

13 41. Nabholz B, Glemin S, Galtier N. Strong variations of mitochondrial mutation rate across
14 mammals – the longevity hypothesis. Mol Biol Evol. 2008;25:120–30.

15 42. Rambaut A: FigTree; 2009. http://tree.bio.ed.ac.uk/software/figtree/ (accessed January
16 2012).

17 43. Freeman PW. A multivariate study of the family Molossidae (Mammalia, Chiroptera):
18 morphology, ecology, evolution. Fieldiana: Zoology, new series. 1981;7:1–171.

19 44. Ramasindrazana B, Rakotondramanana CF, Schoeman MC, Goodman SM. Evidence of
20 echolocation call divergence in *Hipposideros commersoni* sensu stricto (E. Geoffroy, 1803)
21 from Madagascar and correlation with body size. Acta Chiropterologica. 2015;17(1):85–94.

22 45. Anderberg MR. Cluster analysis for applications. New York: Academic; 1973.

23 46. Davis JC. Statistics and data analysis in geology. New York: John Wiley and Sons; 1973.

24 47. Taylor PJ, Kearney TC, Peterhans JCK, Baxter RM, Willows-Munro S. Cryptic diversity in
25 forest shrews of the genus *Myosorex* from southern Africa, with the description of a new species
26 and comments on *Myosorex tenuis*. Zool J Linnean Soc. 2013;169:881–902.

27 48 Esselstyn JA, Evans BJ, Sedlock JL, Anwarali Kahn FA, Heaney LR. Singlelocus species
28 delimitation: a test of the mixed yule-coalescent model, with an empirical application to
29 Philippine round-leaf bats. Proc R Soc B: Biol Sci. 2012;279:3678–86.

49. Lavery TH, Leung LK-P, Seddon JM. Molecular phylogeny of hipposiderid bats (Chiroptera: Hipposideridae) from Solomon Islands and Cape York Peninsula, Australia. Zoologica Scripta. 2014;43:429–42.

50. Vallo P, Guillén-Servent A, Benda P, Pires BD, Koubek P. Variation of mitochondrial DNA in the *Hipposideros caffer* complex (Chiroptera: Hipposideridae) and its taxonomic implications. Acta Chiropterologica. 2008;10:193–206.

51. Vallo P, Benda P, Martínková N, Kaňuch P, Kalko EKV, Červený J, et al. Morphologically uniform bats *Hipposideros* aff. *ruber* (Hipposideridae) exhibit high mitochondrial genetic diversity in southeastern Senegal. Acta Chiropterologica. 2011;13:79–88.

52. Thabah A, Rossiter SJ, Kingston T, Zhang S, Parsons S, Mya KM, et al. Genetic divergence and echolocation call frequency in cryptic species of *Hipposideros larvatus* s.l. (Chiroptera: Hipposideridae) from the Indo-Malayan region. Biol J Linn Soc. 2006;88:119–30.

53. Avise JC. Molecular markers, natural history, and evolution. 2nd ed. Massachusetts: Sinauer Associates; 2004.

54. Baker RJ, Bradley RD. Speciation in mammals and the genetic species concept. J Mamm. 2006;87:643–62.

55. Kingston T, Lara MC, Jones G, Akbar Z, Kunz TH, Schneider CJ. Acoustic divergence in two cryptic *Hipposideros* species: a role for social selection? Proc R Soc Lond. 2001;268:1381–6.

56. Burney DA. Climate change and fire ecology as factors in the Quaternary biogeography of Madagascar. In: Lourenço WR, editor. Biogéographie de Madagascar. Paris: Editions ORSTOM; 1995. p. 49–58.

57. Straka H. Histoire de la végétation de Madagascar oriental dans les dernières 100 millénaires. In: Lourenço WR, editor. Biogéographie de Madagascar. Paris: Editions ORSTOM; 1995. p. 75–89.

58. Wilmé L, Goodman SM, Ganzhorn JU. Biogeographic evolution of Madagascar's microendemic biota. Science. 2006;312:1063–5.

59. Vences M, Wollenberg KC, Vieites DR, Lees DC. Madagascar as a model region of species diversification. Trends Ecol Evol. 2009;24:456–65.

60. Goodman SM, Jungers WL. Extinct Madagascar: picturing the island's past. Chicago: The University of Chicago Press; 2014.

61. Sabatier M, Legendre S. Une faune à rongeurs et chiroptères Plio-Pléistocènes de Madagascar. Actes du 100e Congrès National des Sociétés Savantes, Montpellier, Section des Sciences. 1985;6:21–8.

62. Samonds KE. Late Pleistocene bat fossils from Anjohibe Cave, northwestern Madagascar. Acta Chiropterologica. 2007;9:39–65.

63. Russell AL, Ranivo J, Palkovacs EP, Goodman SM, Yoder AD. Working at the interface of phylogenetics and population genetics: a biogeographical analysis of *Triaenops* spp. (Chiroptera: Hipposideridae). Mol Ecol. 2007;16:839–51.

64. Ratrimomanarivo FH, Goodman SM, Stanley WT, Naidoo T, Taylor PJ, Lamb J. Geographic and phylogeographic variation in *Chaerephon leucogaster* (Chiroptera: Molossidae) of Madagascar and the western Indian Ocean islands of Mayotte and Pemba. Acta Chiropterologica. 2009;11:25–52.

65. Weyeneth N, Goodman SM, Ruedi M. Do diversification models of Madagascar's biota explain the population structure of the endemic bat *Myotis goudoti* (Chiroptera: Vespertilionidae)? J Biogeog. 2010;38:44–54.

66. Vaughan TA. Foraging behaviour of the giant leaf-nosed bat (*Hipposideros commersoni*). East Afr Wildlife J. 1977;15:237–49.

67. Norberg UM, Rayner JMV. Ecological morphology and flight in bats (Mammalia: Chiroptera): wing adaptations, flight performance, foraging strategy and echolocation. Philos Trans R Soc Lond B Biol Sci. 1987;316:335–427.

68. Bernard E, Fenton MB. Bat mobility and roosts in a fragmented landscape in Central Amazonia, Brazil. Biotropica. 2003;35:262–77.

69. Jones G, Rayner MV. Optimal flight speed in pipistrelle bats, *Pipistrellus pipistrellus*. In: Hanák V, Horáček I, Geisler J, editors. European bat research 1987.Prague: Charles University Press; 1989. p. 247–53.

Appendix 1. Collection details of specimens of *Hipposideros commersoni* s.s. included in analyses of external and cranio-dental morphometry and molecular variation. All listed specimens were included in the molecular analyses, and with the exception of those underlined, were also included in the morphometric craniodental analysis. For voucher specimens used in molecular analyses, clade assignments are given based on the supermatrix data presented in Figure 2. Localities correspond with those presented in Figure 1. Institutional acronyms are as follows: UADBA: Université d'Antananarivo, Département de Biologie Animale, Antananarivo; FMNH: Field Museum of Natural History, Chicago. Site acronyms: PN = Parc National, RNI = Réserve Naturelle Intégrale, RS = Réserve Spéciale, SF = Station Forestière.

Museum number	**Province/Locality (numbers in parentheses refer to those shown in Figure 1)**	**Clade (from Figure 2)**	**Latitude**	**Longitude**	**Collection date**	**Sex**	**Alt. (m)**
FMNH 169707	Antsiranana/RS d'Ankarana, 2.6 km E Andrafiabe, near Andrafiabe Cave	C	49.0567	-12.9317	November 2001	Female	50
FMNH 175777	Mahajanga/RNI de Namoroka, near source of Mandevy River, 32 km NW Andranomavo	B	45.345	-16.38	October 2002	Female	100
FMNH 175966	Fianarantsoa/just outside PN de l'Isalo, along Menamaty River, 8 km N Ranohira (RN7)	B	45.3917	-22.4856	December 2002	Female	700
FMNH 175970	Fianarantsoa/PN de l'Isalo, along Sahanafa River, 28 km SE Berenty-Betsileo	A	45.2933	-22.3167	December 2002	Female	550

FMNH 176155	Toliara/Forêt des Mikea, 9.5 km W Ankiloaka	B	43.5233	-22.7783	February 2003	Male	80
FMNH 177302	Mahajanga/SF d'Ampirojoa	B	46.81	-16.315	April 2003	Male	100
FMNH 178806	Antsiranana/RS d'Analamerana, Grotte de Bazaribe, 3.6 km SE Menagisy	C	49.47352	-12.7121	January 2004	Female	90
FMNH 178808	Antsiranana/RS d'Analamerana, Grotte de Bazaribe, 3.6 km SE Menagisy	C	49.47352	-12.7121	January 2004	Female	90
FMNH 178809	Antsiranana/RS d'Analamerana, Grotte de Bazaribe, 3.6 km SE Menagisy	C	49.47352	-12.7121	January 2004	Female	90
FMNH 178810	Antsiranana/RS d'Analamerana, Grotte de Bazaribe, 3.6 km SE Menagisy	C	49.47352	-12.7121	January 2004	Female	90
FMNH 178811	Antsiranana/RS d'Analamerana, Grotte de Bazaribe, 3.6 km SE Menagisy	C	49.47352	-12.7121	January 2004	Female	90
FMNH 178815	Antsiranana/RS d'Analamerana, Grotte de Bazaribe, 3.6 km SE Menagisy	C	49.47352	-12.7121	January 2004	Female	90
FMNH 183932	Toliara/PN de Tsimanampetsotsa, 6.5 km NE Efoetse, near Mitoho Cave	B	43.75	-24.05	October 2004	Female	50

FMNH 183934	Toliara/PN de Tsimanampetsotsa, 6.5 km NE Efoetse, near Mitoho Cave	B	43.75	-24.05	October 2004	Female	50
FMNH 184170	Toliara/Grotte d'Androimpano, 4.2 km NE Itampolo (village), on old road to Ejeda	B	43.96328	-24.6502	February 2005	Female	110
FMNH 184173	Toliara/Grotte d'Androimpano, 4.2 km NE Itampolo (village), on old road to Ejeda	A	43.96328	-24.6502	February 2005	Female	110
FMNH 184030	Mahajanga/4.2 km SE Marovaza, in cave	C	47.30797	-14.966	April 2005	Female	40
FMNH 183980	Antsiranana/Montagne de Français, Forêt d'Ampitiliantsambo	C	49.38453	-12.3371	January 2005	Female	210
FMNH 217940	Fianarantsoa/PN de l'Isalo, 10.5 km SW Ranohira, Hotel Jardin du Roi	B	45.29	-22.31	December 2011	Female	
UADBA 32987	Antsiranana/PN d'Ankarana, 2.6 km E Andrafiabe, in forest near AndrafiabeCave	C	49.05667	-13.93167	September 2012	Female	50
FMNH 221308	Antsiranana/PN d'Ankarana, 2.6 km E Andrafiabe, in forest near Andrafiabe Cave	B	49.05667	-13.93167	September 2012	Female	50
UADBA 32916	Mahajanga/Grotte d'Anjohibe, 3.7 km NE Antanamarina	B	46.88598	-15.53815	September 2012	Female	100

Additional file 1: Figures S1 to S4. Single-gene trees. Maximum likelihood tree inferred from CR (S1) , Cyt b (S2), bSTAT (S3) and OSTA5 (S4).

Posterior probability values and maximum likelihood bootstrap support (in that order) are shown at the nodes. S1) Maximum likelihood tree inferred from mtDNA control region data. Maximum likelihood bootstrap support and posterior probability values (in that order) are shown at the nodes. S2) Maximum likelihood tree inferred from mtDNA *Cyt b* data. Maximum likelihood bootstrap support and posterior probability values (in that order) are shown at the nodes. S3) Maximum likelihood tree inferred from nuclear intron bSTAT. Maximum likelihood bootstrap support and posterior probability values (in that order) are shown at the nodes. S4) Maximum likelihood tree inferred from the nuclear intron OSTA5. Maximum likelihood bootstrap support and posterior probability values (in that order) are shown at the nodes.

S1

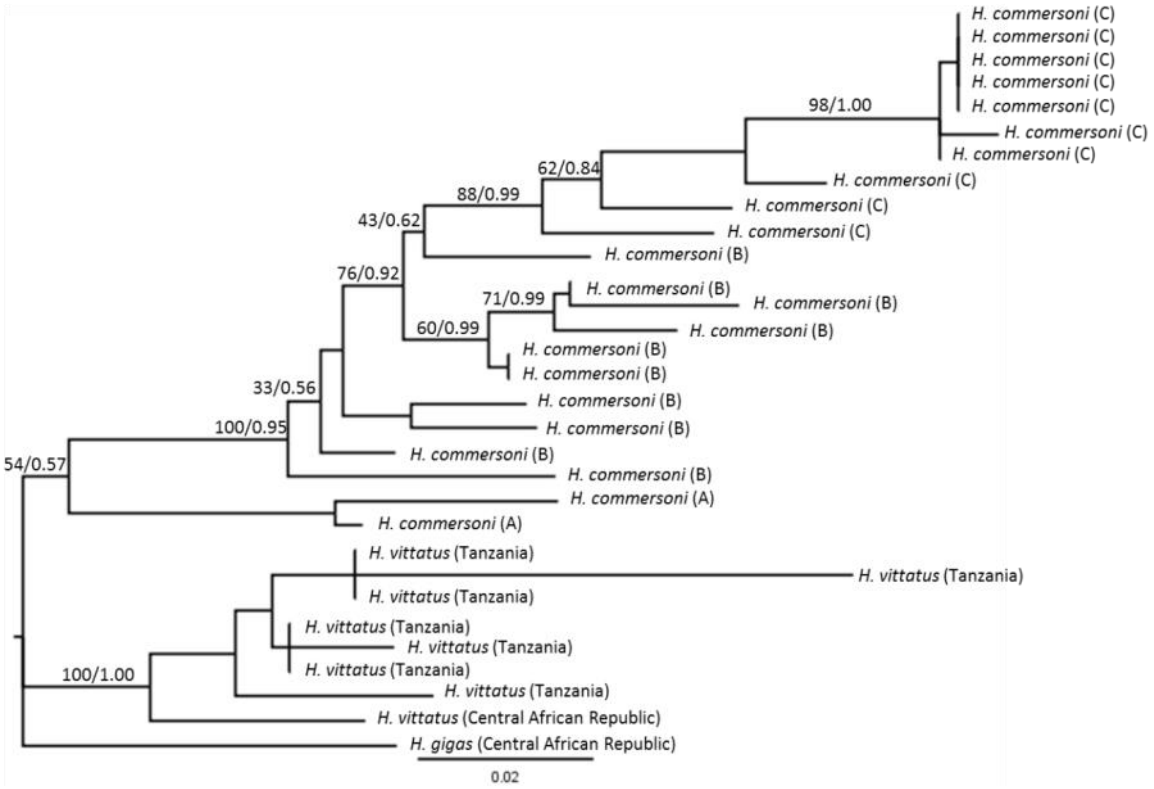

S2

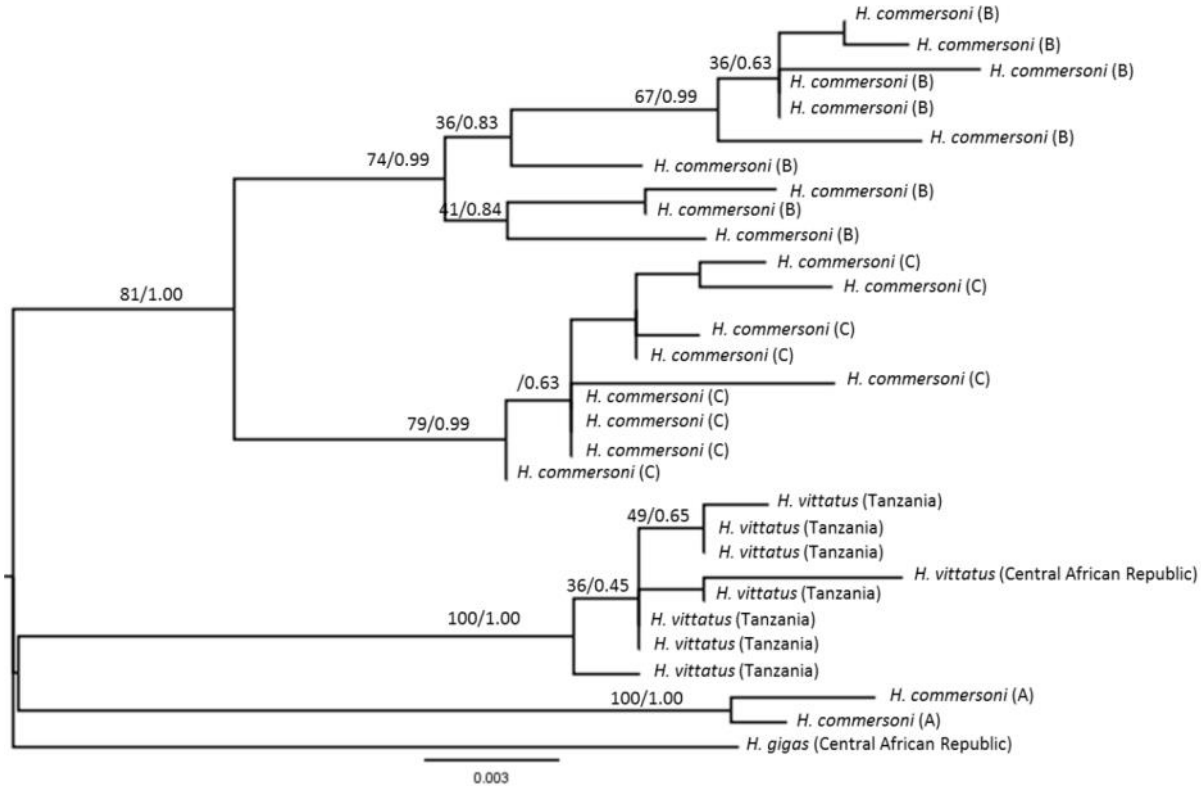
H. commersoni (B)
H. commersoni (B)
36/0.63
H. commersoni (B)
H. commersoni (B)
67/0.99
36/0.83
H. commersoni (B)
74/0.99
H. commersoni (B)
H. commersoni (B)
41/0.84
H. commersoni (B)
H. commersoni (C)
81/1.00
H. commersoni (C)
H. commersoni (C)
H. commersoni (C)
/0.63
H. commersoni (C)
H. commersoni (C)
79/0.99
H. commersoni (C)
H. commersoni (C)
H. vittatus (Tanzania)
49/0.65
H. vittatus (Tanzania)
H. vittatus (Tanzania)
H. vittatus (Central African Republic)
36/0.45
H. vittatus (Tanzania)
100/1.00
H. vittatus (Tanzania)
H. vittatus (Tanzania)
H. vittatus (Tanzania)
100/1.00
H. commersoni (A)
H. commersoni (A)
H. gigas (Central African Republic)
0.003

S3

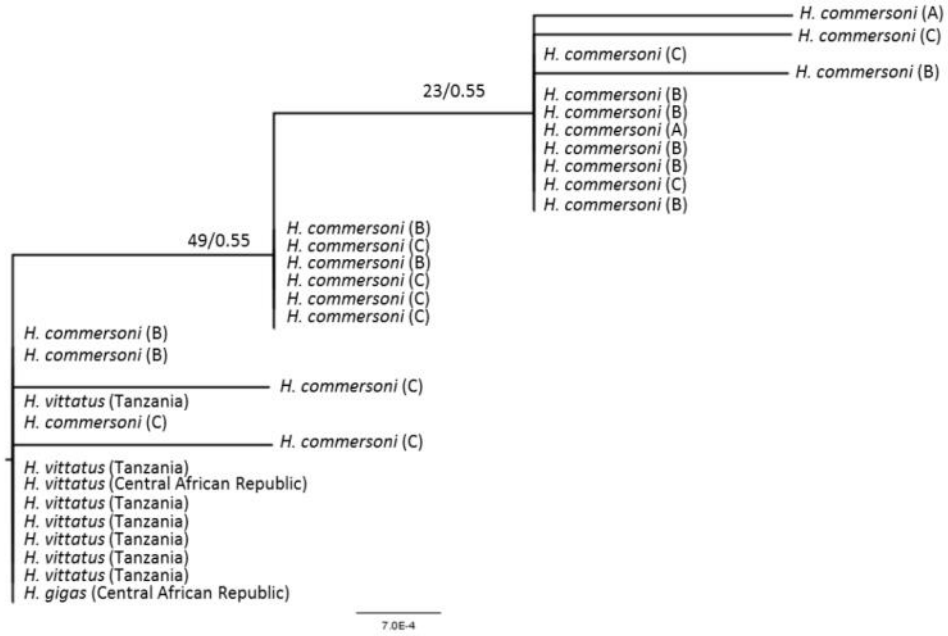
H. commersoni (A)
H. commersoni (C)
H. commersoni (C)
H. commersoni (B)
23/0.55
H. commersoni (B)
H. commersoni (B)
H. commersoni (A)
H. commersoni (B)
H. commersoni (B)
H. commersoni (C)
H. commersoni (B)
H. commersoni (B)
49/0.55
H. commersoni (C)
H. commersoni (B)
H. commersoni (C)
H. commersoni (C)
H. commersoni (C)
H. commersoni (B)
H. commersoni (B)
H. commersoni (C)
H. vittatus (Tanzania)
H. commersoni (C)
H. commersoni (C)
H. vittatus (Tanzania)
H. vittatus (Central African Republic)
H. vittatus (Tanzania)
H. vittatus (Tanzania)
H. vittatus (Tanzania)
H. vittatus (Tanzania)
H. vittatus (Tanzania)
H. gigas (Central African Republic)
7.0E-4

S4

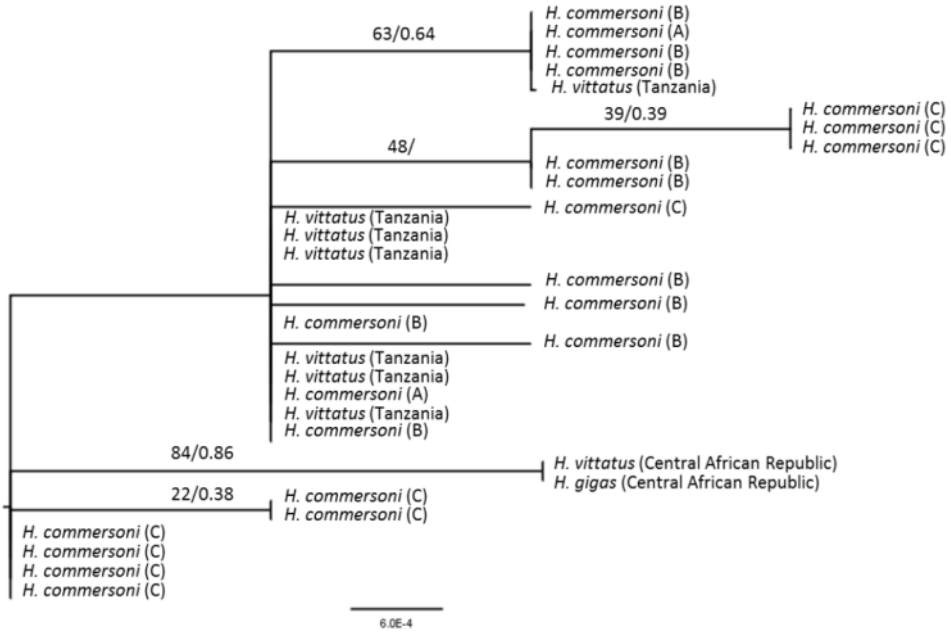
63/0.64
H. commersoni (B)
H. commersoni (A)
H. commersoni (B)
H. commersoni (B)
H. vittatus (Tanzania)
39/0.39
H. commersoni (C)
H. commersoni (C)
H. commersoni (C)
48/
H. commersoni (B)
H. commersoni (B)
H. commersoni (C)
H. vittatus (Tanzania)
H. vittatus (Tanzania)
H. vittatus (Tanzania)
H. commersoni (B)
H. commersoni (B)
H. commersoni (B)
H. commersoni (B)
H. vittatus (Tanzania)
H. vittatus (Tanzania)
H. commersoni (A)
H. vittatus (Tanzania)
H. commersoni (B)
84/0.86
H. vittatus (Central African Republic)
H. gigas (Central African Republic)
22/0.38
H. commersoni (C)
H. commersoni (C)
H. commersoni (C)
H. commersoni (C)
H. commersoni (C)
H. commersoni (C)
6.0E-4

Additional file 2: Figure S5. Alternative maximum clade probability tree, inferred from the analysis of Cyt b data. A strict molecular clock model with a fixed mean substitution rate of 1.30 × 10-8 subs/site/year was performed. Values at nodes indicate the posterior mean substitution rate (subs/site/year). Shaded bars indicate the 95% highest posterior density (HPD) credibility intervals.

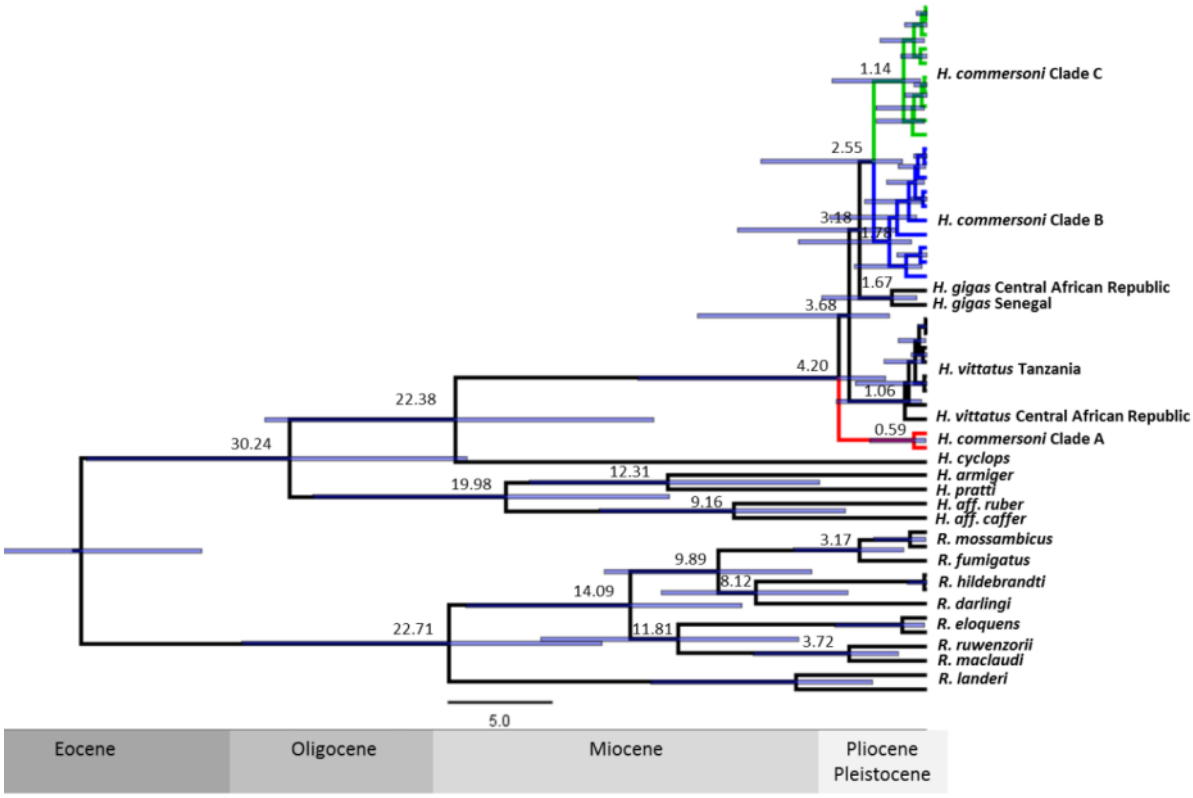

CHAPTER TWO

How many species of *Hipposideros* have occurred on Madagascar since the Late Pleistocene?

ABSTRACT

Populations of the Malagasy *Hipposideros commersoni* (Family Hipposideridae) are threatened by deforestation and hunting. Maximum likelihood and Bayesian analysis of 148 cytochrome b sequences found this species to be paraphyletic and composed of three well-supported monophyletic clades. Clades B and C form a monophyletic lineage which can be referred to as *H. commersoni*; these two clades are separated by 6% sequence variation. Clade A represents a distinct evolutionary lineage separate (9-11% average sequence divergence) from *H. commersoni* (clades B and C) and is named herein as a new species, *H. cryptovalorona*. In the phylogeny presented herein, this species is strongly associated with the out-group taxa *H. gigas* and *H. vittatus*, both restricted to Africa. External, cranial and dental measurements taken from the same individuals used in the molecular study indicate no clear distinction in morphology between these three clades; this includes noseleaf structure and craniodental characteristics. Principal component analyses showed limited separation of the three clades. Comparison to Quaternary fossil species from NW Madagascar, *H. besaoka*, found little morphological overlap between the three clades with this extinct species. Hence, at least three species of *Hipposideros* have occurred on Madagascar since the Late Pleistocene, two extant (*commersoni* s.s. and *cryptovalorona*) and one extinct (*besaoka*).

ADDITIONAL KEYWORDS: *Madagascar – cryptic species – genetics – cranial – dental – morphology – phylogeny – new species.*

INTRODUCTION

The Family Hipposideridae, known as Old World leaf-nosed bats, has a broad distribution, occurring in tropical and subtropical regions of Africa (including offshore islands), Madagascar, the Middle East, Asia and Australia. The genus *Hipposideros* Gray, 1831, is one of the more widespread and abundant genera of insectivorous bats in the Old World. In a synthesis published over a decade ago, 70 species, largely defined based on external and craniodental morphology, were recognized (Simmons, 2005) and subsequently several other taxa have been described (e.g. Guillen-Servent & Francis, 2006; Bates *et al*., 2007; Douangboubpha *et al.*, 2011; Thong *et al*., 2012a, 2012b). On the basis of largely molecular inference, other cryptic species have been uncovered and remain to be named (e.g. Koubinova *et al*., 2010; Vallo *et al.*, 2011; Esselstyn *et al.*, 2012; Murray *et al.*, 2012). There is a growing number of cryptic species of hipposiderid bats that have been identified by differences in call frequency (e.g., Pye, 1972; Francis, Kock & Habersetzer, 1999; Kingston *et al*., 2001; Thabah *et al*., 2006; Lavery *et al.*, 2014). Indeed, acoustic divergence in cryptic bat species may be more likely to occur in high duty cycle echolocating taxa such as the Hipposideridae, and, amongst this bat family, acoustic signatures are reliable indicators of species identity (Jones & Barlow, 2004). However, the recognition of morphologically similar taxa can be easily confounded with animals in the hand, specifically cryptic species, as at certain sites in tropical regions species richness of members of this genus can be considerable, such as on Mt. Nimba in West Africa with seven sympatric taxa (Monadjem *et al*., 2013) or the Tai and Comoe National Parks of Cote d'Ivoire with five and six species, respectively (Fahr & Kalko, 2011).

One extant species has been recognized from Madagascar, *H. commersoni* (E. Geoffroy St. Hilaire, 1813), which occurs in different biomes on the island and across an elevational range from sea-level to 1325 m asl (Goodman & Ramasindrazana, 2013). It has a rather convoluted taxonomic history. The nominate form of this large-bodied species was described from Madagascar, based on illustrations and manuscript notes of Philibert Commerson (1727-1773), a naturalist who explored different western Indian Ocean islands. Subsequently, a number of African taxa showing morphological similarity to the Madagascar form were named. In his synopsis of bats of the world, Koopman (1994) recognized the following taxa – *H. c. commersoni* on Madagascar, *H. c. marungensis* (Noack, 1887) in eastern Africa from Ethiopia south to northeast South Africa, *H. c. niangarae* J.A. Allen, 1917, in northeastern Zaire, *H. c. gigas* (Wagner, 1845) in western Africa from Senegal and Central African Republic south to Namibia and *H. c. thomensis* (Bocage, 1891) from Sao Tome Island in the Gulf of Guinea. In a recent molecular phylogeny, it was found that the genus *Hipposideros* was paraphyletic and

members of the *H. commersoni* group fall outside typical *Hipposideros* (Foley *et al*., 2015); this implies that they should be placed in a separate genus.

In their review of the Madagascar bat fauna, Peterson, Eger & Mitchell (1995), compared size differences between animals they named *H. c. commersoni* from Madagascar, *H. c. marungensis* from East Africa and *H. c. thomensis* from Sao Tome. On the basis of a phenetic analysis they concluded that these three taxa were valid. In an earlier revision of the genus, Hill (1963) also followed the multi-subspecies concept and recognized the following forms: *H. c. commersoni* from Madagascar, *H. c. marungensis* from East Africa, Zanzibar, Malawi, Zambia and southwestern Africa, *H. c. gigas* from Angola, the Congo Basin, West Africa and Tanzania, *H. c. niangarae* from a portion of the Congo Basin, and *H. c. thomensis* from Sao Tome.

On the basis of morphological and bioacoustical evidence, only a portion of which was published, Simmons (2005) modified previous taxonomic views and recognized the *H. commersoni* species group as composed of *H. commersoni* on Madagascar, *H. gigas* (including the form *niangarae*) and *H. vittatus* (Peters, 1852) (including the form *marungensis*) of sub-Saharan Africa, and *H. thomensis* on Sao Tome. While this is the classification followed herein, it has been noted in the literature that the species limits and known distribution of the African forms of the *commersoni* group is in need of further resolution, particularly proper diagnoses of *H. gigas* and *H. vittatus* (Monadjem *et al*., 2010; Happold, 2013a, 2013b).

Recent work on the molecular genetics of *H. commersoni* from different areas of Madagascar, particularly the western half of the island, has found this species to be paraphyletic, with one clade notably divergent from the balance of animals on the island (Rakotoarivelo *et al*., 2015). Further, based on craniodental morphometrics (Ranivo & Goodman, 2007) and bioacoustics (Ramasindrazana *et al*., 2015), there have been previous indications that either this species shows considerable variation across its range or a possible cryptic species exists on the island.

In her study of subfossil bat bones recovered from Anjohibe Cave (Fig. 1), northeast of Mahajanga, Samonds (2007) conducted a detailed analysis of the *Hipposideros* remains, the oldest of which were deposited about 86,000 years ago based on Uranium-series (230Th/234U) dating techniques on the flowstone intercalated with the bone-bearing breccia deposits. Amongst these specimens, which showed considerable variation in size, she identified and named an extinct species, *H. besaoka*, distinguished from the temporally sympatric *H. commersoni* based on its larger mandibular size and broader upper molars. Further, from cave deposits at Tsimanampetsotsa, extreme southwest (Fig. 1), tentatively dated to the Pliocene-

Pleistocene, bat bone remains were identified to *Hipposideros* sp., which were slightly smaller than those named *H. commersoni* (Sabatier & Legendre, 1985).

On the basis of morphology and bioacoustic datasets (Ranivo & Goodman, 2007; Ramasindrazana *et al.*, 2015), it is unclear if *H. commersoni* as currently defined represents a highly variable taxon or a non-monophyletic group. The purpose of this paper, using external and craniodental measurements and characters of *H. commersoni* overlaid on phylogenetic data, is to determine how many species of *Hipposideros* currently occur on the island. Further, if cryptic species are identified, can subfossil remains of *H. besaoka* be confidently assigned based on craniodental morphology to one of these extant clades? In this case, this would indicate that this presumed extinct taxon is extant.

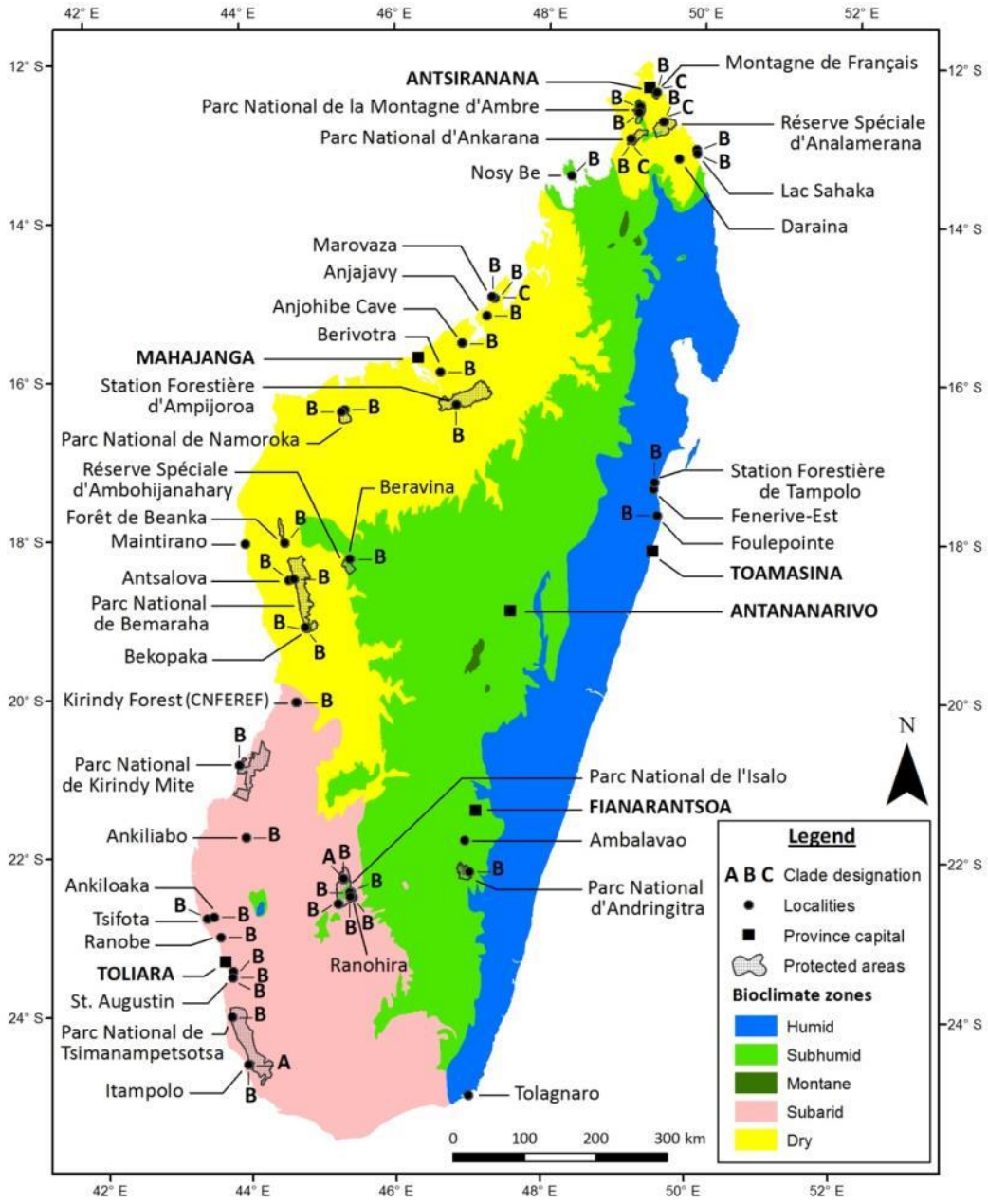

Figure 1. Map of Madagascar showing different sampling localities of Hipposideros used in the morphological and molecular portions of this study and the different clade representation. The map also shows other localities mentioned in the text. An overlay is used of the simplified bioclimatic regions of the island (Cornet, 1974).

1

2

MATERIALS AND METHODS

SPECIMENS

Animals were captured, manipulated and dispatched with thoracic pressure following guidelines accepted by different Malagasy governmental authorities and the international scientific community for the handling of wild animals (Sikes, Gannon, and the Animal Care and Use Committee of the American Society of Mammalogists, 2011). Material for the morphological and molecular genetic analyses presented herein are housed in the following museums: FMNH—Field Museum of Natural History, Chicago; MNHN—Muséum national d'Histoire naturelle, Paris; UADBA—Département de Biologie Animale, Université d'Antananarivo, Antananarivo; UADPAB—Département de Paleontologie et Anthropologie Biologique, Université d'Antananarivo, Antananarivo; and USNM—The National Museum of Natural History (formerly The United States National Museum), Washington, D.C.

ACCESS TO TYPE SPECIMENS AND SERIES

In the description of *Rhinolophus commersoni* by Geoffroy St. Hilaire (1813), a species that would subsequently be placed in the genus *Hipposideros*, he explicitly mentioned that this new taxon was based on illustrations and notes made by Philibert Commerson during his travels to Madagascar (p. 263, "J'ai trouvé cette espèce parmi les dessins et manuscrits de Commerson, avec la désignation et les caractères suivants") based on animals captured near "fort Dauphin" now also known as Tolagnaro (Fig. 1). As the name *H. commersoni* is not associated with a designated holotype, and such a namebearing type is needed for clarifying the taxonomic status of this species in the context of this paper, we follow article 75 of the International Code of Zoological Nomenclature and designate a neotype herein.

Through the courtesy of Dr. Karen Samonds, we have been able to examine and measure a portion of the type series of the subfossil taxon *H. besaoka* obtained at Anjohibe Cave, and housed in the UADPAB collection (Table S1).

MORPHOLOGICAL STUDY

Using a plastic ruler to an accuracy of 1.0 mm, standard external measurements were taken in the field from *Hipposideros commersoni* specimens before preparation; these variables include: total length (TL), tail length (TaL), hind foot length (HF, not including claw), ear length (EL) and forearm length (FA). Mass was taken with a spring balance to the nearest 0.5 g. Associated data for these measurements were obtained from field catalogues. The majority of recent specimens used in this study were collected by SMG and the external measurements of these

animals were consistently taken; these data are not combined herein with measurements taken by other field collectors.

Ten cranial or mandibular and 18 tooth measurements were taken using a digital calliper to the nearest 0.1 mm, except those variables with acronyms in **bold**, associated with differentiation of subfossil *H. besaoka* and accurate to the nearest 0.01 mm. Many of the landmarks used to define these different measurements can be found in Freeman (1981). Tooth abbreviations include: I = incisor, C = canine, P = premolar and M = molar. Upper case abbreviations are for upper teeth and lower case abbreviations for lower teeth. We consider the first upper premolar, which is greatly reduced, as P2 and the next premolar as P4 and the same numeration system is used for the lower premolars.

CRANIAL AND MANDIBULAR MEASUREMENTS include: greatest skull length (GSKL), from posterior-most part of occipital to anterior-most point of upper canines; condylocanine length (CCL), from occipital condyles to anterior-most point of upper canines; greatest zygomatic breadth (ZYGO), width taken across zygomatic arches at the widest point; postorbital breadth (POB), dorsal width at most constricted part of skull; mastoid breadth (MAST), maximum width of skull across mastoid processes; mandible length (MAND), from the posterior-most portion of the condyles to anteriormedial most point of upper incisors; and moment arm of the temporal (MOMARM), length from mandibular condyle to tip of coronoid process; depth of mandibular base at level of canine (**DMB c**), taken perpendicular along the buccal surface from the dorsal edge of the cingulum to edge of the base; depth of mandibular base at level of 1st lower molar (m_1) (**DMB $\mathbf{m_1}$**), taken perpendicular along the buccal surface from the anteriormost portion of the cingulum to edge of the base; depth of mandibular base at level of 3rd lower molar (m3) (**DMB $\mathbf{m_3}$**), taken perpendicular along the buccal surface from the anteriormost portion of the cingulum to edge of the base.

The DENTAL MEASUREMENTS associated with the cranial portion: complete cranial toothrow ($C\text{-}M^3$), length from anterior alveolar border of canine to posterior alveolar border of 3rd molar; complete molariform toothrow ($PM^4\text{-}M^3$), length from anterior alveolar border of 2nd premolar (PM^4) to posterior alveolar border of 3rd molar; width across upper canines ($C^1\text{-}C^1$), taken across the outer alveolar borders of the canines; width across 3rd upper molars ($M^3\text{-}M^3$), taken across the outer alveolar borders of the 3rd molars; mesiodistal length of 2nd upper molar (**MD $\mathbf{M^2}$**), taken in line to the toothrow at the level of the buccal cingulum; buccolingual length of 2nd upper molar (**BL$\mathbf{M^2}$**), taken perpendicular to the toothrow at the widest point; buccolingual length of 3rd upper molar (**BL $\mathbf{M^3}$**), taken perpendicular to the toothrow at the widest point.

The DENTAL MEASUREMENTS associated with the mandibular portion: mesiodistal length of complete mandibular toothrow (i_1-m_3), length from anterior alveolar border of incisors to posterior alveolar border of 3rd molar; complete canine-molar mandibular toothrow (c-m_3), length from anterior alveolar border of canine to posterior alveolar border of 3rd molar; mesiodistal length of 1st lower molar (m_1) (**MD m_1**), taken in line to the toothrow at the level of the buccal cingulum; mesiodistal length of 3rd lower molar (**MD m_3**), taken in line to the toothrow at the widest point; buccolingual length of 1st lower molar (**BL m_1**), taken perpendicular to the toothrow at the widest point; buccolingual length of 3rd lower molar (m_3) (**BL m_3**), taken perpendicular to the toothrow at the widest point; total length of lower canine (**TL c_1**), taken along the vertical axis of the tooth from buccal cingulum to distal tip; total length of 1st lower molar (**TLm_1**), taken along the vertical axis of the tooth from buccal cingulum to distal tip; and total length of 3rd lower molar (**TL m_3**), taken along the vertical axis of the tooth from buccal cingulum to distal tip.

External and craniodental measurements are only reported for adults, which are defined by the presence of a fully erupted permanent dentition and fused basisphenoid-basioccipital suture. As members of the *H. commersoni* species group are known to exhibit considerable sexual dimorphism (Ranivo & Goodman, 2007; Monajem *et al.*, 2010), males and females are separated in all morphometric comparisons.

STATISTICAL APPLICATIONS

To investigate morphological segregation among the *H. commersoni* lineages revealed by the DNA analyses, we performed principal component analysis (PCA) on external (TL, TaL, HF, EL and FA), cranial (GSKL, CCL, ZYGO, POB, MAST and MOMARM) and dental (C-M^3, PM^4-M^3, C^1-C^1, M^3-M^3, i_1–m_3 and c–m_3) measurements in SPSS (v. 22.0, IBM SPSS Statistics for Windows, Armonk, NY). As mentioned earlier, as *H.commersoni* exhibits significant sexual dimorphism, and males were available only for clade B, PCAs were limited to females.

To determine whether the craniodental morphology of subfossil *H. besaoka* could be distinguished from those of the extant *H. commersoni* lineages, we performed separate PCAs on two different datasets of subfossil dental measurements, the first named herein"lower teeth" included: MD m1, MD m3, BL m1, BL m3 and total lengths of c1, m1 and m3; and the second referred to as "upper teeth" included: MD M2, BL M2 and BL M3. As all of the available material of *H. besaoka* is fragmentary, we used the greatest number of specimens for the lower teeth dataset for statistical analyses, which was from the right side, and in the case of the upper teeth dataset, only material was available from the left side (Table S1). For comparisons to

subfossils, we included in the PCAs both modern male and female specimens to verify that sexual dimorphism did not confound any interpretations.

DNA ISOLATION AND SEQUENCING

Tissues from 148 *H. commersoni* measured in the morphological portion of the study were used in the molecular analyses (Table S2). Two African species *H. gigas* and *H. vittatus* were included as out-group taxa and used to root the phylogenetic trees. Total genomic DNA was extracted using the NucleoSpin Tissue kit (Macherey-Nagel), following the manufacturers standard protocol. The cytochrome *b* (*Cyt b*, 705 bp) mitochondrial gene was amplified using primers L14724AG (5'–ATG ATA TGA AAA ACC ATC GTT G–3'; Guillen-Servent & Francis, 2006), H15915 (5'–TCT CCA TTT CTG GTT TAC AAG AC–3'; Irwin, Kocher & Wilson, 1991), JorF (5'-GAC CTT CCA ACT CCC TCA AGC AT-3'; Rakotoarivelo *et al*., 2015) and H15553 (5'–TAG GCA AAT AGG AAA TAT CAT TCT GGT–3'; Irwin *et al*., 1991). PCR reactions included a negative control to check for possible contamination. Cycle sequencing was performed using the BigDye Chemistry, v3.1 and sequencing products were analyzed on an Applied Biosystems 3730xl Genetic Analyzer (Applied Biosystematics, Perkin Elmer). All raw sequence data were viewed and edited in BioEdit v7.1.11 (Hall, 1999). The edited sequences were aligned using the ClustalW application in BioEdit, with the final alignment checked manually to ensure homology. We deposited all new sequences in GenBank (Table S2).

MOLECULAR STUDY AND TREE BUILDING

Maximum-likelihood analysis was performed using the GTRGAMMAI model (assuggested by AIC in jModelTest v.2.1; Darriba *et al.*, 2012) implemented in the program RAxML (Stamatakis, 2014). Branch support was assessed using 1,000 bootstrap iterations. RAxML was also used to calculate pairwise genetic distances. Bayesian analysis was conducted using MrBayes 3.2 (Ronquist *et al*., 2012). Priors were set to nst = 6, invariant sites and gamma. Two independent runs were performed, each consisting of four Markov chain Monte Carlo (MCMC) and run for 30 million generations (trees sampled every 1000th generation). Stationarity of log-likelihood tree scores was assessed using Tracer 1.5 (Rambaut & Drummond, 2007). Effective sample size (ESS) values of all parameters exceeded 700. A 50% majority rule consensus tree was constructed using the CONSENSE module in PHYLIP (Felsenstein, 2005), after the first 20% of generations were discarded as burn-in.

RESULTS

MOLECULAR GENETICS

Maximum likelihood and Bayesian analyses produced consistent topologies. The increased taxonomic sampling used in this study confirms the paraphyly of *H. commersoni* as suggested by Rakotoarivelo *et al.* (2015). Three well-supported monophyletic clades are recovered amongst animals classically considered *H.commersoni* (Fig. 2): clade A (ML bootstrap, 100; Bayes' PP, 1.0), clade B (ML bootstrap, 64; Bayes' PP, 1.0) and clade C (ML bootstrap, 75; Bayes' PP, 1.0). Clade A contains two individuals (FMNH 175970 and FMNH 184173) and is strongly associated (ML bootstrap, 100; Bayes' PP, 1.0) with the out-group taxa *H. gigas* and *H. vittatus.* To ensure sequencing consistency, we re-extracted and re-amplified the specimens belonging to clade A, the sequences recovered were identical. The remaining *H. commersoni* specimens form a monophyletic group (ML bootstrap, 75; Bayes' PP, 1.0), containing two distinct clades (Fig. 2). Clade B is the most genetically diverse (average within clade sequence divergence = 0.3; Table 1) and geographically widespread clade, with individuals belonging to this group collected from different portions of Madagascar. Clade C consists of specimens restricted to the extreme north of Madagascar (Fig. 1).

The average genetic distance (Table 1) between clade A and other *H. commersoni* clades (clade B = 0.11; clade C = 0.09) were comparable to that observed between thetwo out-group taxa *H. gigas* and *H. vittatus* (0.11) and it is clear that clade A represents adistinct evolutionary lineage separate from other *H. commersoni* (clade B and C).

1

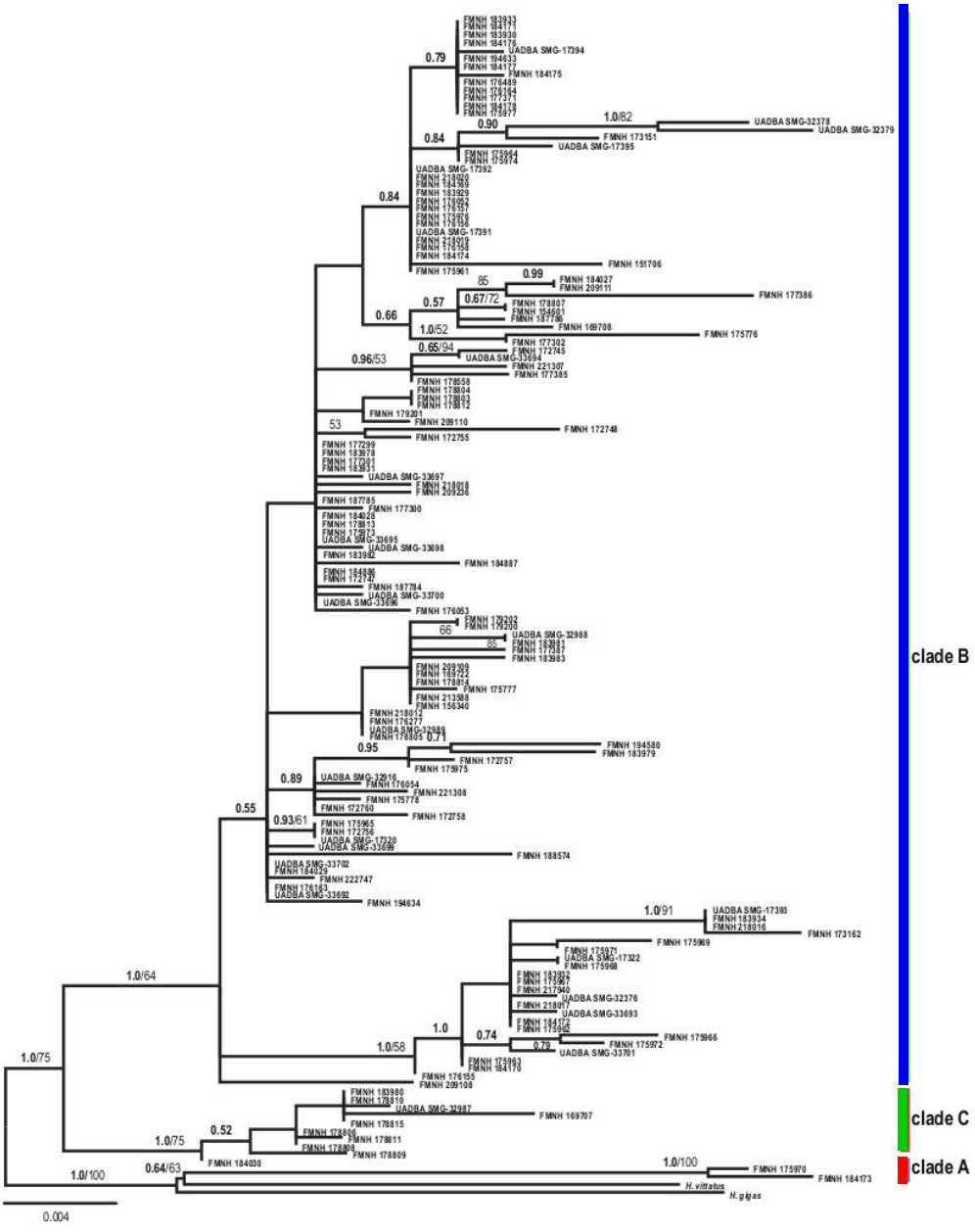

Figure 2. Maximum likelihood phylogeny inferred from analysis of *Hipposideros commersoniCyt b* data. Bayesian posterior probability (bold) and maximum likelihood bootstrap values are provided and only values greater than 0.50 and 50, respectively, are shown. For further details on the sequenced specimens, see Table S2.

Table 1. Average pairwise sequence distances among the *Hipposideros* outgroup taxa and the major lineages of the ingroup, estimated using the GTR+I+G substitution model and *Cyt b* data. Average within lineage pairwise sequence distances are given in bold on the diagonal.

	Clade A	Clade B	Clade C	*H. gigas*
Clade A	**0.01**			
Clade B	0.11	**0.03**		
Clade C	0.09	0.06	**0.01**	
H. gigas	0.12	0.10	0.09	
H. vittatus	0.10	0.10	0.09	0.11

MORPHOLOGICAL CHARACTERS SEPARATING CLADES A, B & C

Even though most of the individuals used in the molecular analyses were also measured and incorporated into the morphological comparisons (Table S2), other than aspects of size, no clear difference was found in external or craniodental morphological characters to distinguish individual bats allocated to the three clades delineated in the previous section. This includes aspects of gross anatomy, such as noseleaf structure, and craniodental aspects known to vary amongst related species of African *Hipposideros* (Happold, 2013c). On the basis of external (Table 2), cranial (Table 3) and dental (Table 4) measurements, bats allocated to clade C were generally larger than clade A, while clade B showed some overlap with clade C and on average waslarger than clade A.

MULTIVARIATE COMPARISONS OF CLADE GROUPS AND CRANIODENTAL MORPHOLOGY

The PCAs for separated cranial and dental variables show the same general patterns as the combined cranial and dental variables described below (Fig. S1; Table S3).

The first three components of the combined craniodental PCA explain >89% of the variation, with PC1 accounting for >77%; all of these variables load high (>0.8) on PC1 with the exception of POB (Table 5). Only POB loads high on PC2. These patterns suggest that PC1 is a measure of size, and bats that load high on PC1 (e.g. individuals from clade C) have

relatively larger skulls than bats that load low on PC1 (e.g. individuals from clade A). PC2 is a measure of skull width and individuals that load high on PC2 have a broader POB than those that load low on PC2.

The first three components of the external morphology PCA explain >83% of the variation, with PC1 accounting for ~47% (Table 5). All the variables load high on PC1 (>0.7), except HF, which is the only variable that loads high on PC2 (Table 5). Similar to the craniodental patterns, this suggests that PC1 is a proxy for size - small-sized bats (e.g. from clade A) load low and larger-sized individuals (from clades B and C) load high along this axis. PC2 is a measure of HF; individuals of clades A and C exhibit intermediate HF length whereas individuals from clade B display a large range of HF. Projections of PC1 vs. PC2 (Fig. 3A, B) show a distinct overlap in morphological space of clades B and C, and individuals from these clades occur in sympatry in northwestern Madagascar (see Discussion). Individuals from clade A show no or little overlap with individuals from clade C and are allopatric in distribution, yet they exhibit overlap with clade B, particularly with smaller-sized clade B individuals, and these clades occur in sympatry at Isalo and Itampolo (Fig. 1). Both the holotype of the species described below, *H. cryptovalorona* sp. nov. (FMNH 175970) and the neotype of *H. commersoni* (FMNH 175972) were obtained at the same locality and during the same night of capture. While these two individuals show some separation in craniodental and external measurements, other individuals referred to clade B and captured with FMNH 175970 & 175972 span nearly the complete spread of points in the PCAs (Fig. 3A,B), emphasizing the lack of correlation between clade affinity and size associated with craniodental and external measurements. The paratype of *H. cryptovalorona* is amongst the smallest individuals of any of the three clades.

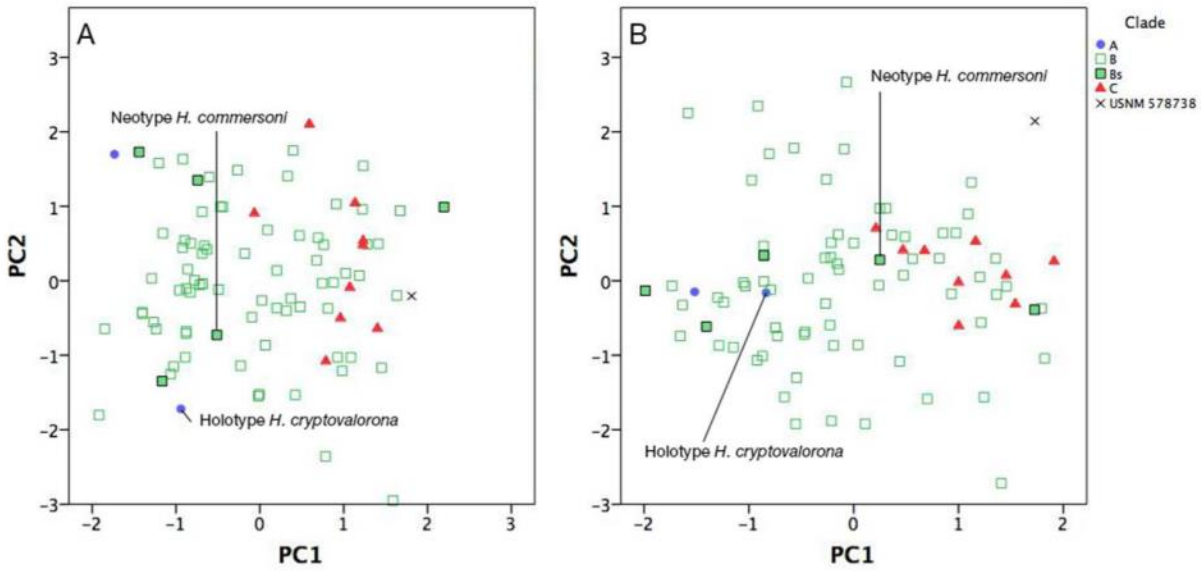

Figure 3. Principal Component Analysis plots of A. 12 craniodental measurements and B. five external measurements for genotyped Malagasy *Hipposideros* female specimens. Clade B specimens from Sahanafa are shown as shaded squares with black outline (clade Bs). Holotype of *H. cryptovalorona* (clade A, FMNH 175970) and neotype of *H. commersoni* (clade B, FMNH 175972), both obtained from Sahanafa, are labeled accordingly. Information on component loadings is presented in Table 5.

IS THE SUBFOSSIL HIPPOSIDEROS BESAOKA*A VALID SPECIES?*

On the basis of gross comparisons, *H. besaoka* has a distinctly more robust mandible and lower teeth than extant animals referred to *H. cryptovalorona* and *H. commersoni* (Fig. 4). The first three components of the subfossil dental PCAs explain > 84% of the variation, with PC1 accounting for ~60% in the lower teeth dataset, and ~ 83% in the upper teeth dataset (Table 7). Associated with PC1, all the variables are positively correlated, with the exception of BL m3 in the lower teeth dataset (Table 7). This variable loads high on PC2, whereas in the upper teeth dataset both MD M2 and BL M2 load high on PC2. Projections of PC1 vs. PC2 derived from the lower teeth dataset (Fig. 5A) provide a distinct separation of *H. besaoka* from adult females of the three extant *Hipposideros* clades and a nearly complete separation from adult males of clade B, specifically along the PC1 axis, indicating that *H. besoaka* is significantly larger than extant *Hipposideros* taxa (Table 6). Similarly, plotting PC1 vs. PC2 from the upper teeth dataset (Fig. 5B) clearly separates *H. besaoka* from adult extant *Hipposideros* clades along the PC1 axis, yet along the PC2 axis there is considerable overlap among *H.besaoka* and extant adult

Hipposideros individuals. A manner to test this conclusion would be to isolate, amplify, and sequence ancient DNA from animals allocated to *H.besaoka*, specifically from tooth dentine, which has been successful for a variety of Malagasy subfossil mammals (e.g., Karanth *et al.*, 2005) to determine if this taxon is genetically distinct from clades A, B, and C identified herein.

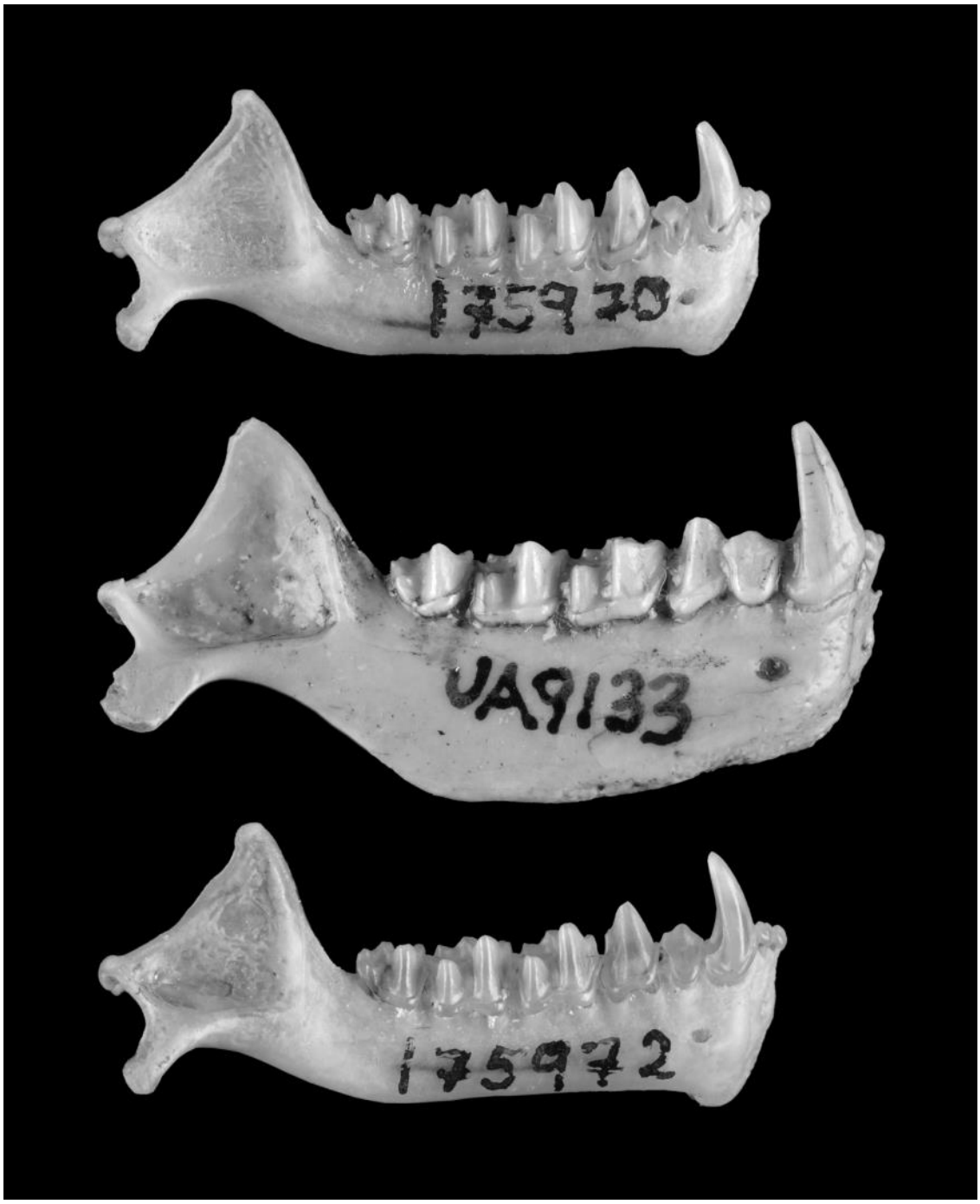

Figure 4. Views of mandibles belonging to three different species of *Hipposideros* that occurred on Madagascar since the Late Pleistocene (from top to bottom): extant *H. cryptovalorona* (holotype, FMNH

175970, female), extinct *H. besaoka* (UADPAB 9133, sex unknown but perhaps male), and extant *H. commersoni* (neotype, FMNH 175972, female). (Photograph taken by J. Weinstein, Field Museum image number Z95243_01d.)

1

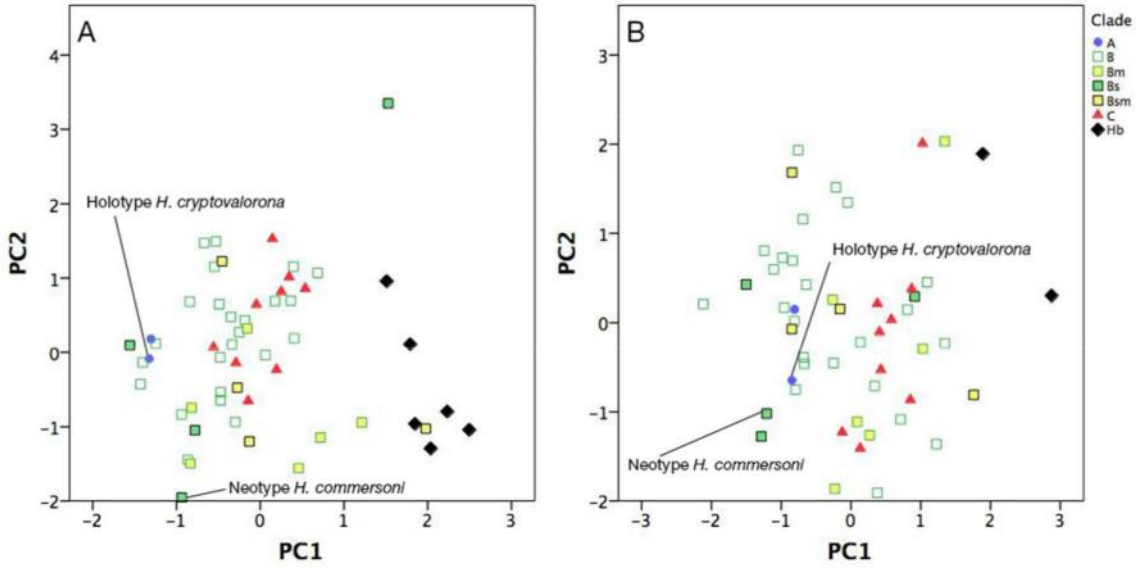

Figure 5. Principal Component Analysis plots of A. seven subfossil dental measurements (lower teeth dataset) and B. three subfossil dental measurements (upper teeth dataset) for extant Malagasy *Hipposideros* specimens and *H. besaoka* specimens. Clade B females = B, clade B females from Sahanafa = Bs, Clade B males = Bm, Clade B males from Sahanafa = Bsm, clade C females = C, and *H. besaoka* = Hb. Holotype of *H. cryptovalorona* (clade A, FMNH 175970) and neotype of *H. commersoni* (clade B, FMNH 175972), both obtained from Sahanafa, are labelled accordingly. Information on component loadings is presented in Table 6.

2

3

4

TAXONOMIC CONCLUSIONS

In following with the results of the molecular study, we consider clades B and C to represent the same taxon, *Hipposideros commersoni* sensu stricto, and clade A to represent an undescribed species, which is described in a subsequent section.

NEOTYPE OF*HIPPOSIDEROS COMMERSONI (FIG. 6)*

As mentioned earlier, a holotype was not designated by Geoffroy St. Hilaire (1813) in his description of *Rhinolophus* (*Hipposideros*) *commersoni*, which was based on illustrations and different notes made by Philibert Commerson. Following the rules of The International Code of Zoological Nomenclature we designate a neotype here. The collections of the MNHN (Paris), where a potential type would have been deposited by Geoffroy St. Hilaire was searched to no avail for a specimen from Madagascar that predates the description of this species. Hence, we have chosen a specimen that was measured and sequenced in the context of this study as the neotype of *H. commersoni*.

Neotype of Hipposideros commersoni

Adult female, FMNH 175972, collected 9 December 2002 by S. M. Goodman (field number SMG 13401). The specimen was conserved in 12% formaldehyde and subsequently transferred to 70% ethanol. Before preservation, the skull was removed via small incisions on both sides of the mouth, conserved in 60% ethanol, and then cleaned by dermestid beetles. The skull is in excellent condition. Samples of pectoral muscle were collected and saved in lysis buffer. The specimen, with a full adult dentition and the basisphenoid–basioccipital suture completely fused, had large mammae, and an enlarged embryo (crown-rump length of 41 mm). External measurements include total length 133 mm, tail length 34 mm, hindfoot length (without claws) 16 mm, ear length 29 mm, forearm length 82 mm and body mass 63 g (including 14.5 g embryo) (Table 2). Information associated with the specimen includes “Netted over Sahanafa River in gallery forest.”

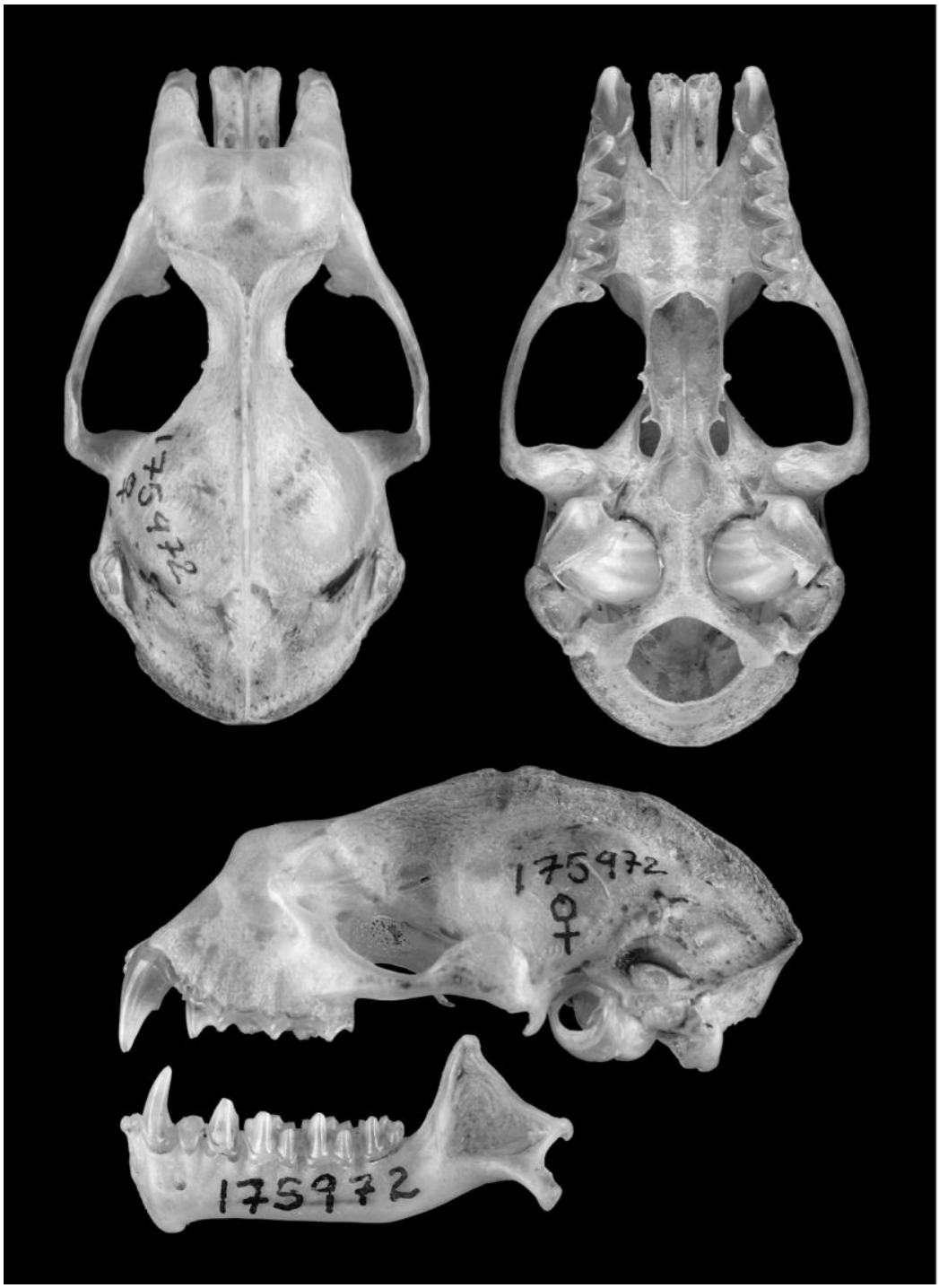

Figure 6. Different views of skull and mandible of neotype of *Hipposideros commersoni* (FMNH 175972, female) from Province de Fianarantsoa, Parc National de l'Isalo, along Sahanafa River. Pictures include dorsal view of cranium (upper row, left), ventral view of cranium (upper row, right), and lateral view of cranium and mandible (lower row). (Photograph taken by J. Weinstein, Field Museum image number Z95239_007d.)

Type locality

Madagascar: Province de Fianarantsoa, Parc National de l'Isalo, along Sahanafa River, near foot of Bevato, 28 km SE Berenty-Betsileo, 22°19.0'S, 45°17.6'E, 550 m asl.

Original diagnosis and type locality

Geoffroy St. Hilaire (1813) provided the following diagnosis of his *Rhinolophus Commersonii*: simple nasal leaf with a rounded terminal edge: without rostrum structure: the tail is half the length of the leg and occurs on Madagascar ["Feuille nasale simple abord terminal arrondi: sans bourse sur la front: la queue de la moitie moins longue de la jambe…Habite Madagascar"]. The neotype designated here fits these same charactersand was obtained on Madagascar.

It was specifically mentioned that Commerson's original description was based on an animal from near "fort Dauphin" [=Tolagnaro] (Fig. 1). In the context of this current study, only a single adult female was measured from this locality (USNM 578738), for which no fresh tissue was available. On the basis of the PCA analyses of cranial-dental and external characters, USNM 578738 is relatively large, yet it overlaps with other large-sized specimen referred to clades B and C (Figs. 3A, B). It also has a relatively large HF, similar to some smaller and medium-sized specimens from clade B (Fig. 3B). We prefer to designate a sequenced animal as the neotype of *H. commersoni*, in this case from Isalo, rather than the individual from Tolagnaro.

Note on spelling of species name

In the original description of this taxon, Geoffroy St. Hilaire (1813) proposed the name "*Rhinolophus Commersonii*". Over the past nearly 200 years, the species name for this bat, with few exceptions, has been presented as *commersoni*. Following the International Code of Zoological Nomenclature, article 33.3.1 concerning "Incorrect subsequent spellings", "when an incorrect subsequent spelling is in prevailing usage and is attributed to the publication of the original spelling, the subsequent spelling and attribution are to be preserved and the spelling is deemed to be a correct original spelling." Hence, we maintain the spelling *H. commersoni*.

Morphological characters

Amongst *Hipposideros commersoni*, without exception, females of clade C are on average larger than those of clade B for external (Table 2), cranial (Table 3) and dental (Table 4) measurements. As *H. cryptovalorona* sp. nov., named below, is morphologically similar to *H. commersoni*, different characters are presented within the new species diagnosis and description, rather than being repeated here.

Molecular variation and phylogeny

Phylogenetic analyses confirmed the paraphyly of what was previously considered *H. commersoni*. Two well-supported, independently evolving lineages were recovered. The first lineage (clade A) is genetically distinct from the other *H. commersoni* lineage; the latter is further subdivided into two geographically correlated clades (clade B and C). Clade A is morphologically similar to *H. commersoni* individuals in clades B and C, but based on genetic data, this lineage can be recognised as a distinct species under the Evolutionary Species Concept (Simpson, 1961; Wiley, 1981; Templeton, 1989), Phylogenetic Sspecies Concept (Eldredge & Cracraft, 1980; Cracraft, 1983) and the Genetic Species Concept (Bradley & Baker, 2001). The *Cyt b* sequence variation observed between clade A and *H. commersoni* (clade B and C) exceeds that recorded for other Afro-Malagasy bats. For example, *Cyt b* sequence divergence separating *Chaerephon pusillus* and *C. leucogaster* from congeners ranges from only 1.3-2.3% (Goodman *et al.*, 2010), and species belonging to *Rhinolophus hildebrandtii* complex differ by 7.7-9.0% (Taylor *et al.*, 2012). The 9-11% average sequence divergence separating clade A from clade B and C is thus strong evidence for clade A representing a distinct species. The 6% sequence variation between clade B and C is also not trivial and highlights the need for further fine-scale phylogeographic study to clearly identify and understand the processes underpinning the evolution of these cryptic taxa.

HIPPOSIDEROS CRYPTOVALORONA SP. NOV (FIGS. 2 & 7)

syn. *Hipposideros c. commersoni* Hill, 1963, in part

syn. *Hipposideros commersoni* Peterson *et al*., 1995, in part

syn. *Hipposideros commersoni* Simmons, 2003, in part

syn. *Hipposideros commersoni* Goodman, 2011, in part

Holotype

Adult female, FMNH 175970, collected 9 December 2002 by S. M. Goodman (field number SMG 13399). The specimen was conserved in 12% formaldehyde and subsequently transferred to 70% ethanol. Before preservation, the skull was removed via small incisions on both sides of the mouth, conserved in 60% ethanol, and then cleaned by dermestid beetles. The skull is in good condition, with the exception of the medial portion of the left upper canine is cracked. Samples of pectoral muscle were collected and saved in lysis buffer. The specimen, with a full

adult dentition and the basisphenoid–basioccipital suture completely fused, had large mammae, an enlarged embryo (crownrump length of 43 mm) and enlarged pubic nipples (see Simmons, 1993). External measurements include total length 123 mm, tail length 34 mm, hindfoot length (without claws) 15 mm, ear length 27 mm, forearm length 80 mm and body mass 55 g (including 12.5 g embryo) (Table 2). Information associated with the specimen includes “Netted over Sahanafa River in gallery forest.”

Type locality

Madagascar: Province de Fianarantsoa, Parc National de l’Isalo, along Sahanafa River, near foot of Bevato, 28 km SE Berenty-Betsileo, 22°19.0’S, 45°17.6’E, 550 m asl. This is the same site as the neotype of *H. commersoni* (clade B, FMNH 175972).

Paratype

The only other individual amongst the sequenced animals that grouped with clade A, *H. cryptovalorona*, is FMNH 184173 (field number SMG 14582). This animal was obtainedat Madagascar: Province de Toliara, Grotte d’Androimpano, 4.2 km NE Itampolo(village), on old road to Ejeda, 24°39.012'S, 43°57.797'E, 110 m asl. This specimen wasobtained “In disturbed spiny bush along western escarpment of Mahafaly Plateau.Captured at rim of sink hole.”

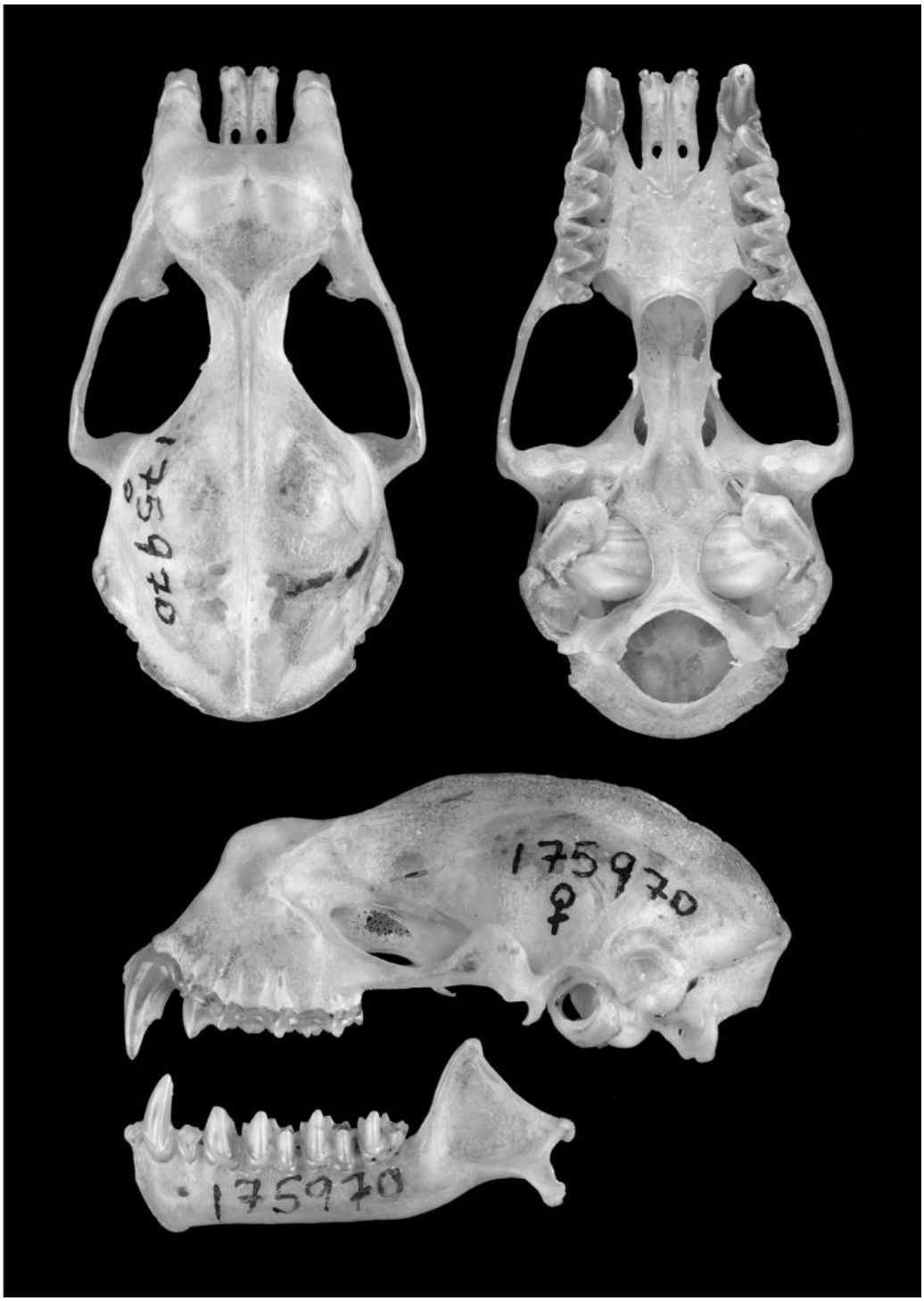

Figure 7. Different views of skull and mandible of *Hipposideros cryptovalorona* sp. nov. (FMNH 175970, female), holotype from Province de Fianarantsoa, Parc National de l'Isalo, along Sahanafa River. Pictures include dorsal view of cranium (upper row, left), ventral view of cranium (upper row, right), and lateral view of cranium and mandible (lower row). (Photograph taken by J. Weinstein, Field Museum image number Z95238_06d.)

Etymology

The name *cryptovalorona* is derived from the Greek '*kryptos*', meaning hidden or concealed and from the Sakalava dialect of Malagasy '*valorona*', which is the local vernacular name of *Hipposideros* and refers to its distinct nasal structure, and can be translated as "eight nose", referring to the complicated and multiple layers of the nose structure.

Diagnosis and description

This is a large-bodied hipposiderid bat known from two specimens, the holotype (FMNH 175970) and paratype (FMNH 184173), both of which are female and with a forearm length of 80-81 mm (Table 2). On the basis of external characters, this species is either smaller than or towards the minimum range values for *H. commersoni* (clades B & C).

The non-attached ears have pointed and rounded tips and are narrow at the base, similar to *H. commersoni*. In *H. cryptovalorona* a small section of tail (3-4 mm) protrudes from the uropatagium. Noseleaf is large and not particularly elaborate compared to other African and Asian members of the genus. It has a small internarial septum and three lateral leaflets, the innermost with median emargination. Anterior portion of noseleaf with three cells separate by two distinct septa and without thickened emargination or lateral process; in all cases these characters are similar to the neotype of *H. commersoni* (FMNH 175972).

Pelage in holotype is relatively dense and short, with the dorsum having a slightly shaggy appearance. The back fur is a medium light brown with the mid-doral portion showing a slightly grizzled coloration, and ventrum slightly lighter and tending towards tan-brown. The paratype is distinctly darker in coloration than the holotype, particularly the dorsum with certain fur having a dark brown appearance. Both specimens have distinct white fur patches on the shoulders. The wing and tail membranes in FMNH 175970 are pale brown and FMNH 184173 distinctly dark brown. The neotype of *H. commersoni* cannot be differentiated in plumage coloration and texture from the holotype of *H. cryptovalorona.*

Skull in *H. cryptovalorona* is large, with prominent lambdoid and sagittal crests and with a greatest skull length of 26.5-27.4 (Table 3); these measurements show some overlap with the minimum values of clade B and are smaller than clade C of *H. commersoni* (Table 3). The same pattern exists in the other cranial measurements between *H. cryptovalorona* and *H. commersoni*, although with the exception of postorbital breadth there is no overlap between the new species and clade C (Table 3). The greatest zygomatic breadth is wider than the mastoid breath. The jugal has a well-developed dorsal projection. The rostrum of *H. cryptovalorona* has a distinct frontal depression and the anterior portion laterally inflated.

The different dental measurements of *H. cryptovalorona* presented in Table 4 show broad overlap with *H. commersoni* but tend to be smaller and falling within the range of lower values of clade B and showing no overlap with clade C. Upper incisors widely separated. Upper canines with a groove running the anterolateral length of the tooth and with a prominent posterior cusp positioned at approximately half the tooth length. The first upper premolar (P2) is greatly reduced and is in direct contact with the canine and the next premolar (P4).

Common name

We propose for this new species the English vernacular name Madagascar Cryptic Leafnosed Bat and the French vernacular name La Phyllorhine cryptique de Madagascar.

Molecular genetics

The independently evolving *H. cryptovalorona* lineage is diagnosable primarily using molecular data. The average *Cyt b* GTR+I+G genetic distance between clade A and other *H. commersoni* (clade B and C) is 9-11%. The results from this study also suggest that clade A is not closely related to the other Madagascar *Hipposideros*, with the phylogenetic analysis placing clade A in close association with the African taxa *H. gigas* and *H. vittatus*. Further analysis will need to be conducted to determine the phylogenetic position of this new species within the genus.

Table 2. External measurements (in millimetres) and mass (in grams) of adults (sexes separated) of different clades of *Hipposideros commersoni* based on the results of the MtDNA analyses. Clade A is referable to ***Hipposideros cryptovalorona* sp. nov.** and clades B and C to *H. commersoni*. Measurements all taken by the same field collector (SMG) and presented as mean ± standard deviation, minimum and maximum measurements and number of specimens. The considerable variance in body mass is associated with seasonal accumulation of body fat.

	Total length	Tail length	Hindfoot length	Ear length	Forearm length	Body mass
***H. cryptovalorona* sp. nov.**						
Clade A						
Holotype						
FMNH 175970 (♀)	123	34	15	27	80	42.5*
Paratype						
FMNH 184173 (♀)	119	30	14	26	81	26
H. commersoni						
Clade B						
Neotype						
FMNH 175972 (♀)	133	34	16	29	82	48.5*
Clade B						
♂♂	137.6 ± 7.23 125-156, n = 27	36.0 ± 3.38 28-42, n = 27	16.5 ± 1.34 14-18, n = 27	29.6 ± 1.41 27-32, n = 27	90.7 ± 4.17 84-97, n = 27	56.0 ± 15.19 33-92, n = 27
♀♀	127.1 ± 6.55 112-139, n = 74	33.2 ± 4.01 25-42, n = 75	14.8 ± 1.46 12-18, n = 76	28.8 ± 1.71 25-32, n = 76	82.9 ± 3.78 75-91, n = 76	43.8 ± 8.32 25.5-63.0, n = 76
Clade C						
♀♀	133.6 ± 4.50 125-138, n = 9	36.8 ± 2.91 31-41, n = 9	15.8 ± 0.44 15-16, n = 9	30.7 ± 0.71 30-32, n = 9	86.4 ± 2.88 82-91, n = 9	42.1 ± 5.07 30.0-46.5, n = 9

* Body mass excluding the weight of the embryo.

Table 3. Cranial measurements (in millimetres) of adults (sexes separated) of different clades of *Hipposideros commersoni* based on the results of the MtDNA analyses. Clade A is referable to ***Hipposideros cryptovalorona*** **sp. nov.** and clades B and C to *H. commersoni*. Measurements presented as mean ± standard deviation, minimum and maximum measurements and number of specimens. See Materials and Methods for an explanation of variable acronyms.

	GSKL	CCL	ZYGO	POB	MAST	MAND	MOMARM
H.cryptovalorona **sp. nov.**							
Clade A							
Holotype							
FMNH 175970 (♀)	27.4	24.2	14.6	2.6	12.7	17.9	5.8
Paratype	26.5	23.6	13.6	3.2	11.7	17.6	5.5
FMNH 184173 (♀)							
H. commersoni							
Clade B							
Neotype							
FMNH 175972 (♀)	28.5	24.7	15.3	2.8	13.2	18.5	6.0
♂♂	30.9 ± 1.42	27.3 ± 1.03	16.6 ± 0.87	3.0 ± 0.19	14.2 ± 0.89	20.5 ± 0.82	6.7 ± 0.33
(n = 34)	28.7-33.9	25.4-29.2	15.0-18.3	2.5-3.4	12.8-15.8	19.0-21.9	6.1-7.4
♀♀	28.5 ± 1.14	25.2 ± 1.09	15.1 ± 0.60	2.9 ± 0.18	13.1 ± 0.56	18.7 ± 0.89	6.0 ± 0.37
	26.6-31.3,	23.4-27.6,	14.0-16.6,	2.5-3.3,	12.2-14.3,	17.1-20.5,	5.0-7.1,
	n = 79	n = 79	n = 79	n = 79	n = 79	n = 78	n = 77
Clade C							
♀♀	29.7 ± 0.63	26.3 ± 0.59	15.6 ± 0.56	3.1 ± 0.18	13.7 ± 0.48	19.6 ± 0.45	6.2 ± 0.20
(n = 9)	28.2-30.5	25.1-27.1	15.0-16.8	2.8-3.4	12.9-14.4	18.5-20.0	6.0-6.6

GSKL, greatest skull length, from posterior-most part of occipital to anterior-most point of upper canines; CCL, condylocanine length, from occipital condyles to anterior-most point of upper canines; ZYGO, greatest zygomatic breadth, width taken across zygomatic arches at the widest point; POB, postorbital breadth, dorsal width at most constricted part of skull; MAST, mastoid breadth, maximum width of skull across mastoid processes; MAND, mandible length, from the posteriormost portion of the condyles to anterior-medial-most point of upper incisors; MOMARM, moment arm of the temporal, length from mandibular condyle to tip of coronoid process.

Table 4. Dental measurements (in millimetres) of adults (sexes separated) of different clades of *Hipposideros commersoni* based on the results of the MtDNA analyses. Clade A is referable to ***Hipposideros cryptovalorona*** **sp. nov.** and clades B and C to *H. commersoni*. Measurements presented as mean ± standard deviation, minimum and maximum measurements and number of specimens. See Materials and Methods for an explanation of variable acronyms.

	C^1-M^3	P^4-M^3	C^1-C^1	M^3-M^3	i_1-m_3	c-m_3
H. cryptovalorona **sp. nov.**						
Clade A						
Holotype						
FMNH 175970 (♀)	9.6	7.3	7.2	10.0	11.9 10.9	
Paratype						
FMNH 184173 (♀)	9.3	7.4	6.6	9.7	11.6	10.5
H. commersoni						
Neotype						
FMNH 175972 (♀)	9.6	7.3	7.1	10.0	11.9	10.9
Clade B	10.7 ± 0.64	7.9 ± 0.38	8.3 ± 0.44	10.9 ± 0.43	13.3 ± 0.65	12.2 ± 0.63
♂♂	9.7-12.8	7.2-8.8	7.5-9.1	10.1-12.0	11.9-14.5	11.0-13.6
(n = 34)						
♀♀	10.0 ±0.52	7.5 ± 0.37	7.5 ± 0.47	10.3 ± 0.49	12.4 ± 0.61	11.3 ± 0.58
	9.2-11.8,	6.7-8.4,	6.5-8.7,	9.2-11.9,	11.1-13.7,	10.2-12.4,
	n = 79	n = 78	n = 79	n = 78	n = 78	n = 78
Clade C	10.5 ± 0.25	7.9 ± 0.17	8.1 ± 0.52	10.8 ± 0.23	13.0 ± 0.28	11.8 ± 0.30
♀♀	10.0-10.8	7.6-8.2	7.3-8.7	10.4-11.7	12.5-13.3	11.4-12.2
(n = 9)						

C–M^3, complete cranial toothrow, length from anterior alveolar border of canine to posterior alveolar border of third molar; PM^4–M^3, complete molariform toothrow, length from anterior alveolar border of second premolar (PM^4) to posterior alveolar border of third molar; C^1–C^1, width across upper canines, taken across the outer alveolar borders of the canines; M^3–M^3, width across third molars, taken across the outer alveolar borders of the third molars; i_1–m_3, mesiodistal length of complete mandibular toothrow, length from anterior alveolar border of incisors to posterior alveolar border of third molar; c–m_3, complete canine–molar mandibular toothrow, length from anterior alveolar border of canine to posterior alveolar border of third molar.

Table 5. Principal components loadings, eigenvalues and cumulative variance for 13 craniodental and five external variables.

Craniodental	PC1	PC2	PC3	External	PC1	PC2	PC3
GSKL	0.972	-0.070	0.048	TL	0.796	-0.240	0.316
CCL	0.971	-0.098	-0.007	TaL	0.705	-0.495	0.323
ZYGO	0.85	-0.001	0.452	HF	0.338	0.822	0.447
POB	0.226	0.969	-0.004	Ear	0.766	0.170	-0.516
MAST	0.915	-0.023	0.212	FA	0.844	0.156	-0.279
MAND	0.956	-0.101	0.033	Eigenvalue	2.541	1.031	0.75
MOMARM	0.831	0.053	0.142	Proportion of variance	50.8	20.6	15.0
C^1-M^3	0.929	-0.077	-0.242	Cumulative variance (%)	50.8	71.4	86.4
PM^4-M^3	0.868	0.042	-0.414				
C^1-C^1	0.886	-0.062	0.189				
M^3-M^3	0.882	0.158	0.064				
i_1-m_3	0.947	-0.011	-0.233				
c-m_3	0.940	-0.027	-0.204				
Eigenvalue	10.07	1.01	0.64				
Proportion of variance	77.4	7.7	4.9				
Cumulative variance (%)	77.4	85.2	90.1				

GSKL, greatest skull length, from posterior-most part of occipital to anterior-most point of upper canines; CCL, condylocanine length, from occipital condyles to anterior-most point of upper canines; ZYGO, greatest zygomatic breadth, width taken across zygomatic arches at the widest point; POB, postorbital breadth, dorsal width at most constricted part of skull; MAST, mastoid breadth, maximum width of skull across mastoid processes; MAND, mandible length, from the posteriormost portion of the condyles to anterior-medial-most point of upper incisors; MOMARM, moment arm of the temporal, length from mandibular condyle to tip of coronoid process; C–M^3, complete cranial toothrow, length from anterior alveolar border of canine to posterior alveolar border of third upper molar; PM^4–M^3, complete molariform toothrow, length from anterior alveolar border of second premolar (PM^4) to posterior alveolar border of third molar; C^1–C^1, width across upper canines, taken across the outer alveolar borders of the canines; M^3–M^3, width across third upper molars, taken across the outer alveolar borders of the third molars; i_1–m_3, mesiodistal length of complete mandibular toothrow, length from anterior alveolar border of incisors to posterior alveolar border of third molar; c–m_3, complete canine–molar mandibular toothrow, length from anterior alveolar border of canine to posterior alveolar border of third molar; TL, total length; TaL, tail length; HF, hind foot length (not including claw); FA, forearm length.

Table 6. Principal components loadings, eigenvalues and cumulative variance for two datasets of subfossil dental variables

Lower teeth	PC1	PC2	PC3	Upper teeth	PC1	PC2	PC3
MD m_1	0.73	0.207	-0.517	MD M^2	0.901	-0.386	0.199
BL m_1	0.82	0.131	-0.274	BL M^2	0.897	0.407	0.173
MD m_3	0.791	0.226	-0.145	BL M^3	0.934	-0.019	-0.358
BL m_3	0.413	0.775	0.461	Eigenvalue	2.488	0.314	0.197
TL c_1	0.778	-0.298	0.253	Proportion of variance	82.9	10.5	6.6
TL m_1	0.897	-0.254	0.218	Cumulative variance (%)	82.9	93.4	100
TL m_3	0.886	-0.337	0.151				
Eigenvalue	4.195	0.979	0.711				
Proportion of variance	59.9	14.0	10.2				
Cumulative variance (%)	59.9	73.9	84.1				

MD m_1, mesiodistal length of first lower molar (m_1), taken in line with the toothrow at the level of the buccal cingulum; BL m_1, buccolingual length of first lower molar, taken perpendicular to the toothrow at the widest point; MD m_3, mesiodistal length of third lower molar, taken in line with the toothrow at the widest point; BL m_3, buccolingual length of third lower molar (m_3), taken perpendicular to the toothrow at the widest point; TL c_1, total length of lower canine, taken along the vertical axis of the tooth from buccal cingulum to distal tip; TL m_1, total length of first lower molar, taken along the vertical axis of the tooth from buccal cingulum to distal tip; TL m_3, total length of third lower molar, taken along the vertical axis of the tooth from buccal cingulum to distal tip; MD M^2, mesiodistal length of second upper molar, taken in line with the toothrow at the level of the buccal cingulum; BL M^2, buccolingual length of second upper molar, taken perpendicular to the toothrow at the widest point; BL M^3, buccolingual length of third upper molar, taken perpendicular to the toothrow at the widest point.

Table 7. Craniodental measurements (in millimetres) of subfossils used in the original description of *Hipposideros besaoka* and adults (sexes separated) of different clades of *H. commersoni* based on the results of the MtDNA analyses. Measurements presented as mean ± standard deviation, minimum and maximum measurements and number of specimens.

	MD M^2	BL M^2	BL M^3	MD m_1	BL m_1	MD m_3	BL m_3	DMB c	DMB m_1	DMB m_3
H. besaoka										
Left mandible				2.26 ± 0.177 2.08-2.50, n = 4	1.48 ± 0.70 1.41-1.57, n = 4	2.32, 2.41 n = 2	1.33, 1.36 n = 2	4.00 ± 0.293 3.73-4.31, n = 4	4.01 ± 0.586 3.18-4.57, n = 4	4.56 n = 1
Right mandible				2.27 ± 0.111 2.09-2.44, n = 9	1.48 ± 0.061 1.40-1.58, n = 9	2.25 ± 0.070 2.14-2.36, n = 7	1.27 ± 0.042 1.24-1.35, n = 7	3.99 ± 0.341 3.55-4.34, n = 5	3.82 ± 0.445 3.13 ± 4.47, n = 9	3.77 ± 0.267 3.05-4.56, n = 8
Left cranial fragment	2.47 ± 0.117 2.36-2.63, n = 4	2.76 ± 0.252 2.47-2.92, n = 3	2.28, 2.55, n = 2							
Hipposideros cryptovalorona sp. nov.										
Clade A										
♀♀ (n = 2)	2.15, 2.21	2.08, 2.14	2.01, 2.04	1.88, 1.95	1.26, 1.29	1.87, 1.87	1.27, 1.28	2.93, 3.01	1.79, 2.09	2.12, 2.22
H. commersoni										
Clade B										
♂♂ (n = 10)	2.31 ± 0.136 2.05-2.52	2.32 ± 0.222 2.08-2.84	2.15 ± 0.139 1.95-2.42	2.12 ± 0.138 1.94-2.32	1.34 ± 0.092 1.22-1.50	2.10 ± 0.135 1.97-2.38	1.21 ± 0.072 1.11-1.36	3.40 ± 0.351 2.86-3.87	2.80 ± 0.684 2.08-3.85	2.96 ± 0.717 2.21-4.22
♀♀ (n = 28)	2.23 ± 0.142 2.02-2.52	2.23 ± 0.165 1.91-2.55	2.08 ± 0.126 1.85-2.32	2.12 ± 0.120 1.93-2.44	1.31 ± 0.092 1.17-1.62	2.08 ± 0.113 1.87-2.29	1.25 ± 0.106 1.11-1.55	3.19 ± 0.329 2.52-3.69	2.16 ± 0.185 1.87-2.46	2.36 ± 0.197 2.04-2.69
Clade C										
♀♀ (n = 9)	2.35 ± 0.364 2.28-2.40	2.36 ± 0.158 2.14-2.68	2.19 ± 0.083 2.03-2.29	2.14 ± 0.153 1.88-2.40	1.34 ± 0.050 1.27-1.42	2.18 ± 0.089 2.01-2.30	1.27 ± 0.098 1.15-1.45	3.25 ± 0.364 2.67-3.87	2.41 ± 0.321 1.92-3.02	2.54 ± 0.268 2.26-3.00

MD M^2, mesiodistal length of second upper molar, taken in line with the toothrow at the level of the buccal cingulum; BL M^2, buccolingual length of second upper molar, taken perpendicular to the toothrow at the widest point; BL M^3, buccolingual length of third upper molar, taken perpendicular to the toothrow at the widest point. MD m_1, mesiodistal length of first lower molar (m_1), taken in line with the toothrow at the level of the buccal cingulum; BL m_1, buccolingual length of first lower molar, taken perpendicular to the toothrow at the widest point; MD m_3, mesiodistal length of third lower molar, taken in line with the toothrow at the widest point; BL m_3, buccolingual length of third lower molar (m_3), taken perpendicular to the toothrow at the widest point; DMB c, depth of mandibular base at level of canine, taken perpendicular along the buccal surface from the dorsal edge of the cingulum to edge of the base; DMB m_1, depth of mandibular base at level of first lower molar (m_1), taken perpendicular along the buccal surface from the anterior-most portion of the cingulum to edge of the base; DMB m_3, depth of mandibular base at level of third lower molar (m_3), taken perpendicular along the buccal surface from the anterior-most portion of the cingulum to edge of the base.

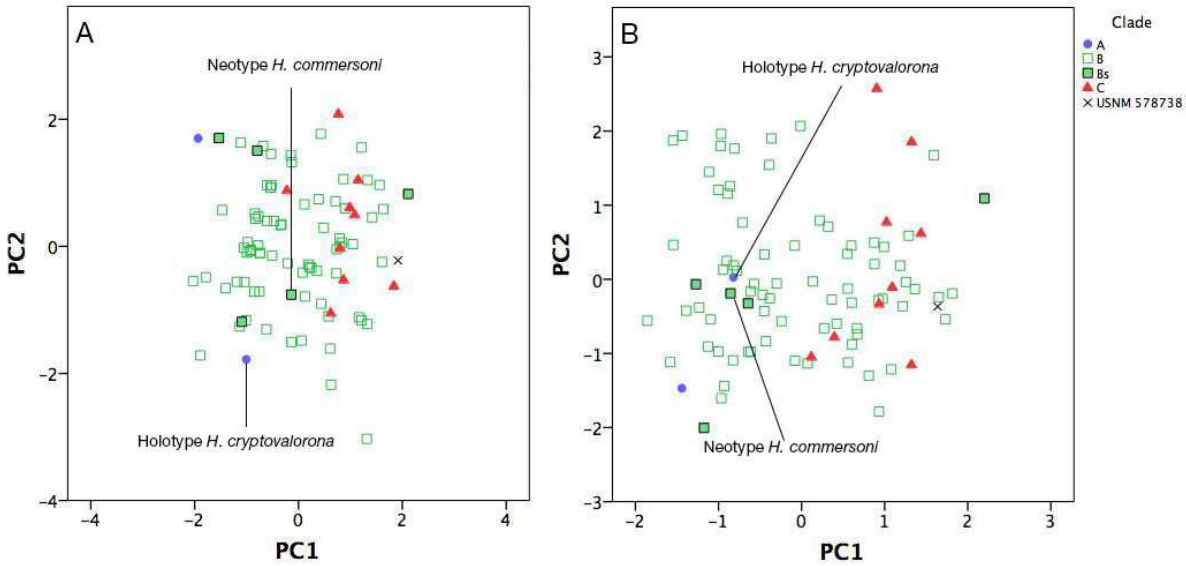

Fig. S1 Principal component analysis plots of a) seven cranial measurements and b) six dental measurements for genotyped Malagasy *Hipposideros*female specimens.

DISCUSSION

Herein using a molecular analysis of Malagasy and certain African populations of *Hipposideros* belonging to the *commersoni* group overlaid on morphology, we assess the question if a cryptic species of this genus exists on Madagascar. Based largely on the molecular data, we found one well-differentiated mitochondrial clade (A) was notably divergent from other individuals of Malagasy *H. commersoni* (clades B and C); clade A is described herein as new to science, *H. cryptovalorona*. This new species is known from two sites in the south: within the Parc National de l'Isalo and near Itampolo (Fig. 1). It is smaller on average than *H. commersoni* for a few external and craniodental measurements (Tables 2-4). In order to advance on this systematic revision of the Malagasy *H.commersoni* complex, it was necessary to name a neotype for *H. commersoni* (sensu Geoffroy St. Hilaire, 1813). Further, we evaluate using craniodental morphology, if a late Pleistocene taxon, *H. besaoka*, described from subfossils collected in Anjohibe Cave, northwestern Madagascar, is a valid species and the possibility that it is still extant. We conclude that it is probably a bona fide taxon and most importantly in the context of the work presented herein, morphologically distinct from *H. cryptovalorona*.

Based on single locus or multilocus molecular data and/or morphological differences, several cases of previously undetected cryptic diversity in *Hipposideros* taxa were recently found in Southeast Asian species (Esselstyn *et al.*, 2012; Murray *et al.*, 2012; Lavery *et al.*, 2014) and African species (Vallo *et al.*, 2008, 2011). For example, *H. khaokhouaensis* from Laos is very similar in general body size and shape to its sister species *H. rotalis*, but differs in the size of the noseleaf, rostral chambers, skull structures related to sound emission or reception, frontal skull width, and echolocation frequency (Guillen-Servent & Francis, 2006). By contrast, genetic divergence and sympatric occurrence suggest that two forms of Senegalese *H. ruber* might represent cryptic species, despite being morphologically indistinguishable (Vallo *et al.*, 2011). However, absence of nuclear gene flow between them is yet to be investigated to demonstrate their reproductive isolation.

Although the field of taxonomy increasingly accepts 'molecular' species descriptions in the absence of other reliable characters (Cook *et al.*, 2010), there are many arguments against the practice of molecular species descriptions; for example DNA sequencing is expensive, requires great expertise, is less accessible for developing nations, and presents various pitfalls in acquiring and analysing sequence data. However, when properly applied, molecular species delineation can provide reliable, replicable characters for cryptic species complexes (e.g., Vogler & Monaghan, 2007; Jorger & Schrodl, 2013). Indeed, keeping discovered taxa formally undescribed does not solve the taxonomic challenges but adds to them by creating parallel

species lists comprising, for example, numbered Operational Taxonomic Units or candidate species (Jorger & Schrodl, 2013). This weakens accurate and precise knowledge of biodiversity, and in turn does not help to advance conservation policy.

Nonetheless, species descriptions based on data from a single maternally-inherited locus might contain errors in the form of incorrectly assumed apomorphies, especially when working with sparsely sampled groups such as the *H. commersoni* species complex. Further, putative molecular apomorphies of described species may become plesiomorphies when new species with the same characteristics are added to analyses, or they may vanish based on intraspecific variation. Given that species descriptions are hypotheses, newly described taxa need to be re-evaluated (i.e., confirmed, falsified or modified)when new data, material or analytical methods become available.

At both the Isalo and Itampolo sites from where *H. cryptovalorona* is known, it occurs in strict sympatry with *H. commersoni* representatives of clade B. One of the reasons an individual from Isalo was chosen as the neotype of *H. commersoni* was to emphasize that these two species overlap in their distribution. On the night of 9 December 2002, mist nets were set up in several areas crossing the Sahanafa River within the Parc National de l'Isalo, and individuals of *H. commersoni* and *H. cryptovalorona* were captured. These included the female holotype (FMNH 175970) of *H.cryptovalorona*, as well as five females, including the neotype, and four males of *H. commersoni* (FMNH 175968-969 and 175971-977). The day roost locality (localities) of these individuals was (were) almost certainly in crevices and caves in the sandstone cliffs surrounding the netting location, but it is unknown if these two species occur in the same colony.

In contrast, the paratype of *H. cryptovalorona* (FMNH 184173) from near Itampolo was captured along the rim of the sink hole leading to the Grotte d'Androimpano as bats were exiting their day roost site within the cave after dusk and seven females and two males of *H. commersoni* (FMNH 184169-172 and 184174-178) were also obtained. This would indicate that these two species occupy the same cave system, but not necessarily the same microhabitats within the cave.

At other localities on Madagascar individuals assigned to *H. commersoni* and falling within clades B and C have been captured at the same sites (Fig. 1): 4.2 km SE Marovaza, in cave, clade B (FMNH 184029, female) and clade C (FMNH 184030, female); Montagne de Francais, Foret d'Ampitiliantsambo, clade B (FMNH 183981, female) and clade C (FMNH 183980, female); Reserve Speciale d'Analamerana, Grotte de Bazaribe, 3.6 km SE Menagisy, clade B (FMNH 178803-805, 178807, 178812-814, females) and clade C (FMNH 178806,

178808-811, 178815, females); and Parc National d'Ankarana, 2.6 km E Andrafiabe, in forest near Andrafiabe Cave, clade B (UADBA 32988-989, FMNH 221307-308, females) and clade C (UADBA 32987, female). These data further indicate the sympatric occurrence of distinct haplotypes of *H. commersoni*.

There have been previous indications, based on morphology and bioacoustics, of either considerable variation within *H. commersoni* or a possible cryptic species of *Hipposideros* on Madagascar (Ranivo & Goodman, 2007). The recognition herein of an undescribed cryptic species of *Hipposideros* on Madagascar based on molecular genetics helps to reconcile several points. The considerable size variation in animals previously referred to as *H. commersoni* was inferred to be associated with possible fixed phenotypic and genetic patterns in certain populations and cryptic species occurring in sympatry. Specifically, *H. cryptovalorona* appears to be relatively small-bodied and sympatric with *H. commersoni* individuals from clade B that exhibit the full small to large range of body size among bats measured in this study. All individuals assigned to clade C are relatively large and allopatric with *H. cryptovalorona*, yet they were sympatric with both larger and smaller individuals assigned to clade B. Another explanation offered for considerable differences in body size at certain sites on the island is fixed differences in regional populations and certain population being seasonally migratory; specifically large northern animals moving to the south during the non-breeding season (Ranivo & Goodman, 2007). Such patterns are known from continental populations of the *H.commersoni* complex and apparently related to seasonal reduction in food resources (Vaughan, 1977; McWilliam, 1982; Cotterill & Fergusson, 1999). While apparent migratory movements of *H. commersoni* have been observed north of the Kirindy Forest (Fig. 1) (Ramasindrazana *et al*., 2015), there seems to be a problem in the inherent logic of migratory direction. The northern portion of Madagascar has more stable environmental conditions and a less pronounced dry season as compared to the south (Cornet, 1974), and one would presume that if such migratory movements took place, it would be from the south to the north, rather than vice-versa. A detailed phylogeographic study of *H. commersoni* is needed to better understand the spatial pattern of genetic and morphological structure observed in clade B and C.

A recent study on the phylogenetic relationships of the bat families Hipposideridae and Rhinolophidae found the genus *Hipposideros* to be paraphyletic (Foley *et al.*, 2015). Members of the *H. commersoni* group fell outside and in a basal position relative to the other members of this genus; hence the generic placement of *commersoni* is called into question. A recent analysis by Rakotoarivelo *et al.* (2015) included a wider taxonomic sampling of *Hipposideros* and *Rhinolophus*. In the latter study *H. cryptovalorona* was placed basal relative to *H.commersoni*

(clades B and C) with the African forms, *H. gigas* and *H. vittatus*, separating the different Malagasy clades. This indicates several interesting possibilities in the evolutionary and dispersal history of members of the *commersoni* species complex. One possible scenario is that their origin is on Madagascar and the ancestor of *H. cryptovalorona* crossed the Mozambique Channel and colonized Africa, giving rise to the forms *H. gigas* and *H. vittatus*, and presumably *H. thomensis*. Subsequently, there was a reversed event and subsequent return to the island of an ancestor that gave rise to *H. commersoni* as represented herein as clades B and C. This would explain the two divergent clades on Madagascar recovered in this current study, *H. cryptovalorona* and *H. commersoni*, with the African taxa having an intermediate position. A parallel scenario has been proposed for members of the Rhinonycteridae, a family closely related to Hipposideridae, with bi-directional colonization events between Madagascar and Africa (Russell, Goodman & Cox, 2008; Foley *et al.*, 2015).

Now that the phylogenetic relationships of the *H. commersoni* group on Madagascar are clearer, the next step in addressing the evolutionary and dispersal history of the different members of this Afro-Malagasy complex is resolution of the species relationships of the African forms, particularly *H. vittatus* and *H. gigas*. Samples across a broad geographic area of sub-Saharan Africa and using a combination of molecular markers, bioacoustics, karyology and morphology would be valuable to resolve these issues.

REFERENCES

Bates PJJ, Rossiter SJ, Suyanto A, Kingston T. 2007. A new species of *Hipposideros* (Chiroptera: Hipposideridae) from Sulawesi. *Acta Chiropterologica* **9:** 13–26.

Bradley RD, Baker RJ. 2001. A test of the genetic species concept: cytochrome-b sequences and mammals. *Journal of Mammalogy* **82:** 960–973.

Cook LG, Edwards RD, Crisp MD, Hardy NB. 2010. Need morphology always be required for new species descriptions? *Invertebrate Systematics* **24**: 322.

Cornet A. 1974. *Essai de cartographie bioclimatique à Madagascar*. Note explicative n°55. ORSTOM, Paris.

Cotterill FPD, Fergusson RA. 1999. Reproductive ecology of Commerson's leaf-nosed bats *Hipposideros commersoni* (Chiroptera: Hipposideridae) in south-central Africa: interactions between seasonality and large body size; and implications for conservation. *South African Journal of Zoology* **34**: 53–63.

Cracraft J. 1983. Species concepts and speciation analysis. In: Johnston RF, ed. *Current ornithology. Vol. I.* New York: Plenum Press, 159–187.

Darriba D, Taboada GL, Doallo R, Posada D. 2012. JModelTest 2: more models, new heuristics and parallel computing. *Nature Methods* **9**: 772.

Douangboubpha B, Bumrungsri S, Satasook C, Soisook P, Si Si Hla Bu, Aul B, Harrison DL, Pearch M, Thomas NM, Bates PJJ. 2011. A new species ofsmall *Hipposideros* (Chiroptera: Hipposideridae) from Myanmar and a revaluation ofthe taxon *H. nicobarulae* Miller, 1902 from the Nicobar Islands. *ActaChiropterologica* **13:** 61–78.

Eldredge N, Cracraft J. 1980. Phylogenetic patterns and the evolutionary process. New York: Columbio University Press.

Esselstyn JA, Evans BJ, Sedlock JL, Anwarali Kahn FA, Heaney LR. 2012. Singlelocus species delimitation: a test of the mixed yule-coalescent model, with an empirical application to Philippine round-leaf bats. *Proceedings of the Royal Society B: Biological Sciences* **279**: 3678–-3686.

Fahr J, Kalko EKV. 2011. Biome transitions as centres of diversity: habitat heterogeneity and diversity patterns of West African bat assemblages across spatial scales. *Ecography* **34:** 177–195.

Felsenstein J. 2005. *PHYLIP (Phylogeny Inference Package)*. Distributed by the author. Seattle: Department of Genome Sciences, University of Washington.

Foley NM, Thong VD., Soisook P, Goodman SM, Armstrong KN, Jacobs DS, Puechmaille SJ, Teeling EC. 2015. How and why overcome the impediments toresolution: lessons from rhinolophid and hipposiderid bats. *Molecular Biology and Evolution* **32:** 313–333.

Francis CM, Kock D, Habersetzer J. 1999. Sibling species of *Hipposideros ridleyi* (Mammalia, Chiroptera, Hipposideridae). *Senckenbergiana Biologica* **79:** 255–270.

Freeman PW. 1981. A multivariate study of the family Molossidae (Mammalia, Chiroptera): morphology, ecology, evolution. *Fieldiana: Zoology*, new series **7:** 1–171.

Geoffroy Saint-Hilaire E. 1813. Sur un genre des chauves-souris, sous le nom de Rhinolophes. *Annales du Musée d'Histoire naturelle de Paris* **20:** 254–266.

Goodman SM, Ramasindrazana B. 2013. Bats or the order Chiroptera. In: Goodman SM, Raherilalao MJ, eds. *Atlas of selected land vertebrates of Madagascar*. Antananarivo: Association Vahatra, 169–209.

Goodman SM, Buccas W, Naidoo T, Ratrimomanarivo F, Taylor PJ, Lamb J. 2010. Patterns of morphological and genetic variation in western Indian Ocean members of the *Chaerephon* '*pumilus'* complex (Chiroptera: Molossidae), with the description of a new species from Madagascar. *Zootaxa* **2551:** 1–36.

Guillen-Servent A, Francis CM. 2006. A new species of bat of the *Hipposideros bicolor* group (Chiroptera: Hipposideridae) from Central Laos, with evidence of convergent evolution with Sundaic taxa. *Acta Chiropterologica* **8:** 39–61.

Hall TA. 1999. BioEdit: a user-friendly biological sequence alignment editor andanalysis program for Windows 95/98/NT. *Nucleic Acids Symposium Series* **41**: 95–98.

Happold M. 2013a. *Hipposideros gigas* giant leaf-nosed bat. In: Happold M, Happold DCD, eds. *Mammals of Africa. Volume IV*. London: Bloomsbury Publishing, 385–387.

Happold M. 2013b. *Hipposideros vittatus* striped leaf-nosed bat. In: Happold M, Happold DCD, eds. *Mammals of Africa. Volume IV*. London: Bloomsbury Publishing, 395–398.

Happold M. 2013c. Genus *Hipposideros*, Old World Leaf-nosed bats. In: Happold M, Happold DCD, eds. *Mammals of Africa. Volume IV*. London: Bloomsbury Publishing, 367–371.

Hill JE. 1963. A revision of the genus *Hipposideros*. *Bulletin of the British Museum (Natural History), Zoology* **11:** 1–129.

Irwin DM, Kocher TD, Wilson AC. 1991. Evolution of the cytochrome *b* gene of mammals. *Journal of Molecular Ecology* **32**: 128–144.

Jones G, Barlow KE. 2004. Cryptic species of echolocating bats. In: Thomas JA, Moss CF, Vater M, eds. Echolocation in bats and dolphins. Chicago: University of Chicago Press, 345–349.

Jorger KM, Schrodl M. 2013. How to describe a cryptic species? Practical challenges of molecular taxonomy. *Frontiers in Zoology* **10:** 59.

Karanth KP, Delefosse T, Rakotosamimanana B, Parsons TJ, Yoder AD. 2005. Ancient DNA from giant extinct lemurs confirms single origin of Malagasy primates.*Proceedings of the National Academy of Sciences*, USA **102**: 5090-5095.

Kingston T, Lara MC, Jones G, Zubaid A, Kunz TH, Schneider CJ. 2001. Acousticdivergence in two cryptic *Hipposideros* species: a role for social selection? *Proceedings of the Royal Society of London Series B, Biological Sciences* **268:** 1381–1386.

Koopman KF. 1994. Chiroptera: systematics. In: Niethammer J, Schliemann H, Starck D, eds. *Handbuch der Zoologie*, Vol. VII. Berlin: Walter de Gruyter, 100–109.

Koubinova D, Sreepada KS, Koubek P, Zima J. 2010. Karyotypic variation in rhinolophid and hipposiderid bats (Chiroptera: Rhinolophidae, Hipposideridae). *Acta Chiropterologica* **12:** 393–400.

Lavery TH, Leung LK-P, Seddon JM. 2014. Molecular phylogeny of hipposiderid bats (Chiroptera: Hipposideridae) from Solomon Islands and Cape York Peninsula, Australia. *Zoologica Scripta* **43**: 429–442.

McWilliam AN. 1982. *Adaptive responses to seasonality in four species of insectivorous bats in coastal Kenya.* PhD thesis, University of Aberdeen.

Monadjem A, Taylor PJ, Cotterill FPD, Schoeman MC. 2010. *Bats of southern and central Africa: a biogeographic and taxonomic synthesis.* Johannesburg: Wits University Press: Johannesburg.

Monadjem A, Richards L, Taylor PJ, Denys C, Dower A, Stoffberg S. 2013. Diversity of Hipposideridae in the Mount Nimba massif, West Africa, and thetaxonomic status of *Hipposideros lamottei*. *Acta Chiropterologica* **15:** 341–352.

Murray SW, Campbell P, Kingston T, Zubaid A, Francis CM, Kunz TH. 2012. Molecular phylogeny of hipposiderid bats from southeast Asia and evidence ofcryptic diversity. *Molecular Phylogenetics and Evolution* **62:** 597–611.

Peterson RL, Eger JL, Mitchell L. 1995. *Chiroptères*. *Vol. 84. Faune de Madagascar.* Paris: Muséum national d'Histoire naturelle.

Pye JD. 1972. Bimodal distribution of constant frequencies in some hipposiderid bats (Mammalia: Hipposideridae). *Journal of Zoology* **166:** 323–335.

Rakotoarivelo A, Willows-Munro S, Schoeman MC, Lamb JM, Goodman SM. 2015. Cryptic diversity in *Hipposideros commersoni* sensu stricto (Chiroptera: Hipposideridae) in western portion of Madagascar. *BMC Evolutionary Biology* **15:** 235–253.

Ramasindrazana B, Rakotondramanana CF, Schoeman MC, Goodman SM. 2015. Evidence of echolocation call divergence in *Hipposideros commersoni* sensu stricto (E. Geoffroy, 1803) from Madagascar and correlation with body size. *Acta Chiropterologica* **17:** 85–94.

Rambaut A, Drummond AJ. 2007. Molecular evolution, phylogenetics and epidemiology, Tracer v.1.5. 2007 [12 December 2014]. Available from: http://tree.bio.ed.ac.uk/software/tracer/.

Ranivo J, Goodman SM. 2007. Variation geographique de *Hipposideros commersoni* de la zone seche de Madagascar (Mammalia, Chiroptera, Hipposideridae). *Verhandlungen des naturwissenschaftlichen Vereins Hamburg* **43:** 35–56.

Ronquist F, Teslenko M, van der Mark P, Ayres DL, Darling A, Hohna S, Larget B, Liu L, Suchard MA, Huelsenbeck JP. 2012. MrBayes 3.2: Efficient Bayesian phylogenetic inference and model choice across a large model space. *SystematicBiology* **61**: 539-542.

Russell A., Goodman SM, Cox MP. 2008. Coalescent analyses support multiple mainland-to-island dispersals in the evolution of Malagasy *Triaenops* bats (Chiroptera: Hipposideridae). *Journal of Biogeography* **35**: 995–1003.

Sabatier M, Legendre S. 1985. Une faune a rongeurs et chiropteres Plio-Pleistocenes de Madagascar. *Actes du 110ème Congrès national des Sociétés savantes, Montpellier, Section des Sciences* **6**: 21-28.

Samonds KE. 2007. Late Pleistocene bat fossils from Anjohibe Cave, northwestern Madagascar. *Acta Chiropterologica* **9:** 39–65.

Sikes RS, Gannon WL, American Society of Mammalogists. 2011. Guidelines of the American Society of Mammalogists for the use of wild mammals in research. *Journal of Mammalogy* **92:** 235–253.

Simmons NB. 1993. Morphology, function, and phylogenetic significance of pubic nipples in bats (Mammalia, Chiroptera). *American Museum Novitates* **3077:** 1–37.

Simmons NB. 2005. Order Chiroptera. In: Wilson DE, Reeder DM, eds. *Mammal species of the World: a taxonomic and geographic reference,* 3rd edition. Baltimore: Johns Hopkins University Press, 312–529.

Simpson GG. 1961. *Principles of animal taxonomy*. New York: Columbia University Press.

Stamatakis A. 2014. RAxML version 8: a tool for phylogenetic analysis and postanalysis of large phylogenies. *Bioinformatics* **30:**1312–1313.

Taylor PJ, Stoffberg S, Monadjem A, Schoeman MC, Bayliss J, Cotterill FP. 2012. Four new bat species (*Rhinolophus hildebrandtii* complex) reflect Plio-Pleistocenedivergence of dwarfs and giants across an Afromontane archipelago. *PloS One* **7**:e41744.

Templeton AR. 1989. The meaning of species and speciation: A genetic perspective. In: Otte D, Endler JA, eds. *Speciation and its consequences*, Sunderland, MA: Sinauer, 3-27.

Thabah A, Rossiter SJ, Kingston T, Zhang S, Parsons S, Mya Mya K, Zubaid A, Jones G. 2006. Genetic divergence and echolocation call frequency in cryptic species of *Hipposideros larvatus* s.l. (Chiroptera: Hipposideridae) from the Indo-Malayan region. *Biological Journal of the Linnean Society* **88:** 119-130

Thong VD, Puechmaille SJ, Denzinger A, Bates PJJ, Dietz C, Csorba G, Soisook P, Teeling EC, Matsumura S, Furey NM, Schnitler H.-U. 2012a. Systematics of the *Hipposideros turpis* complex and a description of a new subspecies from Vietnam. *Mammal Review* **42:** 166–192.

Thong VD, Puechmaille SJ, Denzinger A, Dietz C, Csorba G, Bates PJJ, Teeling EC, Schnitzler H-U. 2012b. A new species of *Hipposideros* (Chiroptera: Hipposideridae) from Vietnam. *Journal of Mammalogy* **93:** 1–11.

Vallo P, Guillen-Servent A, Benda P, Pires BD, Koubek P. 2008. Variation of mitochondrial DNA in the *Hipposideros caffer* complex (Chiroptera: Hipposideridae) and its taxonomic implications. *Acta Chiropterologica* **10**: 193–206.

Vallo P, Benda P, Martinkova N, Kaňuch P, Kalko EKV, Červeny J, Koubek P. 2011. Morphologically uniform bats *Hipposideros* aff. *ruber* (Hipposideridae) exhibit high mitochondrial genetic diversity in southeastern Senegal. *Acta Chiropterologica***13:** 79–88.

Vaughan TA. 1977. Foraging behaviour of the giant leaf-nosed bat (*Hipposideros commersoni*). *East African Wildlife Journal* **15**: 237–249.

Vogler A, Monaghan M. 2007. Recent advances in DNA taxonomy. *Journal of Zoological Systematics and Evolutionary Research* **45**: 1–10.

Wiley EO. 1981. Remarks on Willis' species concept. *Systematic Zoology* **30:** 86-87.

SUPLEMENTARY MATERIALS

Table S1. Listing of subfossil material of *Hipposideros besaoka* from Anjohibe Cave used in the morphological analyses. All specimens are housed in the UADPAB and several are uncatalogued.

Left cranial fragment: 9086, 9087, 9088, 9092; left mandible: 9051, 9056, 9116, 9132; right mandible: 9039, 9044, 9090, 9133, 9140, uncatalogued L23, L35, L36, L38.

Table S2. List of specimens segregated by clade, associated binomial name and collection locality used in the morphological (specimen numbers in bold) and molecular analyses (specimen numbers in italics), as well as Genbank accession numbers. PN = Parc National, RS = Réserve Spéciale, SF = Station Forestière. FMNH = Field Museum of Natural History, UADBA = Université d'Antananarivo, Département de Biologie Animale, USNM = National Museum of Natural History. Certain specimens deposited in UADBA have yet to be catalogued and are referred to by field numbers.

Species	**Museum number**	**Province/Locality**	**GenBank numbers**	**Clade**
H. cryptovalorona	FMNH *175970*	Fianarantsoa/PN de l'Isalo, along Sahanafa River, 28 km SE Berenty-Betsileo		A
H. cryptovalorona	FMNH *184173*	Toliara/Grotte d'Androimpano, 4.2 km NE Itampolo (village), on old road to Ejeda		A
H. commersoni	FMNH *156340*	Antsiranana/PN de la Montagne d'Ambre, Grande Lac, 12 km SW Joffreville		B
H. commersoni	FMNH *169722*	Antsiranana/PN d'Ankarana, 2.6 km E Andrafiabe, near Andrafiabe Cave		B
H. commersoni	FMNH *154601*	Antsiranana/PN de la Montagne d'Ambre, 5.5 km SW Joffreville		B
H. commersoni	FMNH *169708*	Antsiranana/PN d'Ankarana, 2.6 km E Andrafiabe, near Andrafiabe Cave		B
H. commersoni	FMNH *176277*	Antsiranana/PN d'Ankarana, 3.5 km SE Andrafiabe (village)		B
H. commersoni	FMNH *178803*	Antsiranana/RS d'Analamerana, Grotte de Bazaribe, 3.6 km SE Menagisy		B
H. commersoni	FMNH *178804*	Antsiranana/RS d'Analamerana, Grotte de Bazaribe, 3.6 km SE Menagisy		B

H. commersoni	FMNH *178805*	Antsiranana/RS d'Analamerana, Grotte de Bazaribe, 3.6 km SE Menagisy	B
H. commersoni	FMNH *178807*	Antsiranana/RS d'Analamerana, Grotte de Bazaribe, 3.6 km SE Menagisy	B
H. commersoni	FMNH *178812*	Antsiranana/RS d'Analamerana, Grotte de Bazaribe, 3.6 km SE Menagisy	B
H. commersoni	FMNH *178813*	Antsiranana/RS d'Analamerana, Grotte de Bazaribe, 3.6 km SE Menagisy	B
H. commersoni	FMNH *178814*	Antsiranana/RS d'Analamerana, Grotte de Bazaribe, 3.6 km SE Menagisy	B
H. commersoni	FMNH *188574*	Antsiranana/Nosy Be, Centre National de Recherches Océanographiques, 1.5 km E Hell-ville	B
H. commersoni	FMNH *213588*	Antsiranana/PN d'Ankarana, 2.6 km E Andrafiabe, near Andrafiabe Cave	B
H. commersoni	FMNH *177385*	Antsiranana/PN d'Ankarana, 3.5 km ESE Andrafiabe, Grotte d'Andrafiabe	B
H. commersoni	FMNH *177386*	Antsiranana/PN d'Ankarana, 3.5 km ESE Andrafiabe, Grotte d'Andrafiabe	B
H. commersoni	FMNH *177387*	Antsiranana/PN d'Ankarana, 3.5 km ESE Andrafiabe, Grotte d'Andrafiabe	B
H. commersoni	FMNH *183978*	Antsiranana/Lac Sahaka, Foret d'Analabe	B
H. commersoni	FMNH *183979*	Antsiranana/Lac Sahaka, Foret d'Analabe	B
H. commersoni	FMNH *183981*	Antsiranana/Montagne de Français, Foret d'Ampitiliantsambo	B
H. commersoni	UADBA *32988*	Antsiranana/PN d'Ankarana, 2,6 km E Andrafiabe, in forest near Andrafiabe Cave	B
H. commersoni	UADBA *32989*	Antsiranana/PN d'Ankarana, 2,6 km E Andrafiabe, in forest near Andrafiabe	B

		Cave	
	FMNH *221307*	Antsiranana/PN d'Ankarana, 2,6 km E Andrafiabe, in forest near Andrafiabe	
H. commersoni		Cave	B
	FMNH *221308*	Antsiranana/PN d'Ankarana, 2,6 km E Andrafiabe, in forest near Andrafiabe	
H. commersoni		Cave	B
H. commersoni	FMNH *151706*	Fianarantsoa/Ambalavao, 43 km S, Andringitra Reserve	B
H. commersoni	FMNH *175961*	Fianarantsoa/PN de l'Isalo, Canyon des Singes (Andranokova), 2 km W Ranohira bas	B
H. commersoni	FMNH *175962*	Fianarantsoa/just outside PN de l'Isalo, along Menamaty River, 8 km N Ranohira (RN7)	B
H. commersoni	FMNH *175963*	Fianarantsoa/just outside PN de l'Isalo, along Menamaty River, 8 km N Ranohira (RN7)	B
H. commersoni	FMNH *175964*	Fianarantsoa/just outside PN de l'Isalo, along Menamaty River, 8 km N Ranohira (RN7)	B
H. commersoni	FMNH *175965*	Fianarantsoa/just outside PN de l'Isalo, along Menamaty River, 8 km N Ranohira (RN7)	B
H. commersoni	FMNH *175966*	Fianarantsoa/just outside PN de l'Isalo, along Menamaty River, 8 km N Ranohira (RN7)	B
H. commersoni	FMNH *175967*	Fianarantsoa/just outside PN de l'Isalo, along Menamaty River, 8 km N Ranohira (RN7)	B
H. commersoni	FMNH *175968*	Fianarantsoa/PN de l'Isalo, along Sahanafa River, 28 km SE Berenty-Betsileo	B
H. commersoni	FMNH *175969*	Fianarantsoa/PN de l'Isalo, along Sahanafa River, 28 km SE Berenty-Betsileo	B
H. commersoni	FMNH *175971*	Fianarantsoa/PN de l'Isalo, along Sahanafa River, 28 km SE Berenty-Betsileo	B

H. commersoni	FMNH *175972*	Fianarantsoa/PN de l'Isalo, along Sahanafa River, 28 km SE Berenty-Betsileo	B
H. commersoni	FMNH *175973*	Fianarantsoa/PN de l'Isalo, along Sahanafa River, 28 km SE Berenty-Betsileo	B
H. commersoni	FMNH *175974*	Fianarantsoa/PN de l'Isalo, along Sahanafa River, 28 km SE Berenty-Betsileo	B
H. commersoni	FMNH *175975*	Fianarantsoa/PN de l'Isalo, along Sahanafa River, 28 km SE Berenty-Betsileo	B
H. commersoni	FMNH *175976*	Fianarantsoa/PN de l'Isalo, along Sahanafa River, 28 km SE Berenty-Betsileo	B
H. commersoni	FMNH *175977*	Fianarantsoa/PN de l'Isalo, along Sahanafa River, 28 km SE Berenty-Betsileo	B
H. commersoni	FMNH *217940*	Fianarantsoa/PN de l'Isalo, 10,5 km SW Ranohira, Hotel Jardin du Roi	B
H. commersoni	UADBA SMG-*17320*	Fianarantsoa/PN de l'Isalo, 3,8 km NW Ranohira along Namaza River	B
H. commersoni	FMNH *218012*	Fianarantsoa/PN de l'Isalo, 3,8 km NW Ranohira along Namaza River	B
H. commersoni	UADBA SMG-*17322*	Fianarantsoa/PN de l'Isalo, 3,8 km NW Ranohira along Namaza River	B
H. commersoni	UADBA SMG-*17391*	Fianarantsoa/PN de l'Isalo, Grotte de Bekapity	B
H. commersoni	UADBA SMG-*17392*	Fianarantsoa/PN de l'Isalo, Grotte de Bekapity	B

H. commersoni	UADBA SMG-*17393*	Fianarantsoa/PN de l'Isalo, Grotte de Bekapity	B
H. commersoni	UADBA SMG-*17394*	Fianarantsoa/PN de l'Isalo, Grotte de Bekapity	B
H. commersoni	UADBA SMG-*17395*	Fianarantsoa/PN de l'Isalo, Grotte de Bekapity	B
H. commersoni	FMNH *218016*	Fianarantsoa/PN de l'Isalo, Grotte de Bekapity	B
H. commersoni	FMNH *218017*	Fianarantsoa/PN de l'Isalo, Grotte de Bekapity	B
H. commersoni	FMNH *218018*	Fianarantsoa/PN de l'Isalo, Grotte de Bekapity	B
H. commersoni	FMNH *218019*	Fianarantsoa/PN de l'Isalo, Grotte de Bekapity	B
H. commersoni	FMNH *218020*	Fianarantsoa/PN de l'Isalo, Grotte de Bekapity	B
H. commersoni	FMNH *175776*	Mahajanga/PN du Tsingy de Namoroka, near source of Mandevy River, 32 km NW Andranomavo	B
H. commersoni	FMNH *175777*	Mahajanga/PN du Tsingy de Namoroka, near source of Mandevy River, 32 km NW Andranomavo	B
H. commersoni	FMNH *175778*	Mahajanga/PN du Tsingy de Namoroka, near source of Mandevy River, 32 km NW Andranomavo	B

H. commersoni	FMNH *177299*	Mahajanga/SF d'Ampirojoa	B
H. commersoni	FMNH *177300*	Mahajanga/SF d'Ampirojoa	B
H. commersoni	FMNH *177301*	Mahajanga/SF d'Ampirojoa	B
H. commersoni	FMNH *177302*	Mahajanga/SF d'Ampirojoa	B
H. commersoni	FMNH *178558*	Mahajanga/PN du Tsingy de Namoroka, Site Andriabe, 2 km SE Namoroka village	B
H. commersoni	FMNH *184027*	Mahajanga/Grotte d'Ankelimahogo, 18.5 km S Anjajavy village	B
H. commersoni	FMNH *184028*	Mahajanga/Marovaza	B
H. commersoni	FMNH *184029*	Mahajanga/4.2 km SE Marovaza, in cave	B
H. commersoni	FMNH *209108*	Mahajanga/Grotte d'Anjohibe, 3.7 km NE Antanamarina	B
H. commersoni	FMNH *209109*	Mahajanga/Grotte d'Anjohibe, 3.7 km NE Antanamarina	B
H. commersoni	FMNH *209110*	Mahajanga/Grotte d'Anjohibe, 3.7 km NE Antanamarina	B
H. commersoni	FMNH *209111*	Mahajanga/Grotte d'Anjohibe, 3.7 km NE Antanamarina	B
H. commersoni	FMNH *209236*	Mahajanga/Forêt de Beanka, cave along Kimanambolo River	B
H. commersoni	FMNH *184886*	Mahajanga/Berivotra, village	B
H. commersoni	FMNH *184887*	Mahajanga/Berivotra, village	B

H. commersoni	FMNH *187784*	Mahajanga/Forêt de Mamakibetro, 18.3 km NNE Ansalova	B
H. commersoni	FMNH *187785*	Mahajanga/Forêt de Mamakibetro, 18.3 km NNE Ansalova	B
H. commersoni	FMNH *187786*	Mahajanga/Forêt d'Ampidirabe, 16.3 km N Antsalova	B
H. commersoni	FMNH *194580*	Mahajanga/RS d'Ambohijanahary, Mahajeby Forest, 21.8 km ESE de Beravina	B
H. commersoni	UADBA *32916*	Mahajanga/Grotte d'Anjohibe, 3.7 km NE Antanamarina	B
H. commersoni	FMNH *179200*	Toamasina/SF de Tampolo, 10 km NW Fenerive-Est	B
H. commersoni	FMNH *179201*	Toamasina/SF de Tampolo, 10 km NW Fenerive-Est	B
H. commersoni	FMNH *179202*	Toamasina/SF de Tampolo, 10 km NW Fenerive-Est	B
H. commersoni	FMNH *183982*	Toamasina/Foulepointe, Forêt d'Analalava	B
H. commersoni	FMNH *183983*	Toamasina/Foulepointe, Forêt d'Analalava	B
H. commersoni	FMNH *172745*	Toliara/PN du Tsingy de Bemaraha, Ankidrodroa, 2.5 km NE Bekopaka	B
H. commersoni	FMNH *172747*	Toliara/PN du Tsingy de Bemaraha, Ankidrodroa, 2.5 km NE Bekopaka	B
H. commersoni	FMNH *172748*	Toliara/PN du Tsingy de Bemaraha, Ankidrodroa, 2.5 km NE Bekopaka	B
H. commersoni	FMNH *172755*	Toliara/PN du Tsingy de Bemaraha, Ankidrodroa, 2.5 km NE Bekopaka	B
H. commersoni	FMNH *172756*	Toliara/PN du Tsingy de Bemaraha, Ankidrodroa, 2.5 km NE Bekopaka	B

H. commersoni	FMNH *172757*	Toliara/PN du Tsingy de Bemaraha, Ankidrodroa, 2.5 km NE Bekopaka	B
H. commersoni	FMNH *172758*	Toliara/PN du Tsingy de Bemaraha, Ankidrodroa, 2.5 km NE Bekopaka	B
H. commersoni	FMNH *172760*	Toliara/PN du Tsingy de Bemaraha, 3.5 km E Bekopaka	B
H. commersoni	FMNH *173151*	Toliara/PN de Tsimanampetsotsa, 6.5 km NE Efoetse, near Mitoho Cave	B
H. commersoni	FMNH *173162*	Toliara/PN de Tsimanampetsotsa, 6.5 km NE Efoetse, near Mitoho Cave	B
H. commersoni	FMNH *176052*	Toliara/PN de Kirindy Mite, 0.75 km SW Manahy	B
H. commersoni	FMNH *176053*	Toliara/PN de Kirindy Mite, 0.75 km SW Manahy	B
H. commersoni	FMNH *176054*	Toliara/PN de Kirindy Mite, 0.75 km SW Manahy	B
H. commersoni	FMNH *176155*	Toliara/Forêt des Mikea, 9.5 km W Ankiloaka	B
H. commersoni	FMNH *176164*	Toliara/Forêt des Mikea, 7.5 km NE Tsifota	B
H. commersoni	FMNH *176163*	Toliara/Forêt des Mikea, 7.5 km NE Tsifota	B
H. commersoni	FMNH *183929*	Toliara/PN de Tsimanampetsotsa, 6.5 km NE Efoetse, near Mitoho Cave	B
H. commersoni	FMNH *183930*	Toliara/PN de Tsimanampetsotsa, 6.5 km NE Efoetse, near Mitoho Cave	B
H. commersoni	FMNH *183931*	Toliara/PN de Tsimanampetsotsa, 6.5 km NE Efoetse, near Mitoho Cave	B
H. commersoni	FMNH *183932*	Toliara/PN de Tsimanampetsotsa, 6.5 km NE Efoetse, near Mitoho Cave	B

H. commersoni	FMNH *183933*	Toliara/PN de Tsimanampetsotsa, 6.5 km NE Efoetse, near Mitoho Cave	B
H. commersoni	FMNH *183934*	Toliara/PN de Tsimanampetsotsa, 6.5 km NE Efoetse, near Mitoho Cave	B
H. commersoni	FMNH *184169*	Toliara/Grotte d'Androimpano, 4.2 km NE Itampolo (village), on old road to Ejeda	B
H. commersoni	FMNH *184170*	Toliara/Grotte d'Androimpano, 4.2 km NE Itampolo (village), on old road to Ejeda	B
H. commersoni	FMNH *184171*	Toliara/Grotte d'Androimpano, 4.2 km NE Itampolo (village), on old road to Ejeda	B
H. commersoni	FMNH *184172*	Toliara/Grotte d'Androimpano, 4.2 km NE Itampolo (village), on old road to Ejeda	B
H. commersoni	FMNH *184174*	Toliara/Grotte d'Androimpano, 4.2 km NE Itampolo (village), on old road to Ejeda	B
H. commersoni	FMNH *184175*	Toliara/Grotte d'Androimpano, 4.2 km NE Itampolo (village), on old road to Ejeda	B
H. commersoni	FMNH *184176*	Toliara/Grotte d'Androimpano, 4.2 km NE Itampolo (village), on old road to Ejeda	B
H. commersoni	FMNH *184177*	Toliara/Grotte d'Androimpano, 4.2 km NE Itampolo (village), on old road to Ejeda	B
H. commersoni	FMNH *184178*	Toliara/Grotte d'Androimpano, 4.2 km NE Itampolo (village), on old road to Ejeda	B
H. commersoni	FMNH *176489*	Toliara/Fiherenana	B
H. commersoni	FMNH *177371*	Toliara/Ranobe	B
H. commersoni	FMNH *176156*	Toliara/Forêt des Mikea, 16 km W Vorehy	B
H. commersoni	FMNH *176157*	Toliara/Forêt des Mikea, 16 km W Vorehy	B

H. commersoni	FMNH *176158*	Toliara/Forêt des Mikea, 8.4 km SSE Befandefa	B
H. commersoni	FMNH *194633*	Toliara/District de Manja, Beronto Forest, 11 km SSE Ankiliabo	B
H. commersoni	FMNH *194634*	Toliara/District de Manja, Beronto Forest, 11 km SSE Ankiliabo	B
H. commersoni	UADBA *32376*	Toliara/Mikea, Grotte de Maki near Hôtel La Mangrove	B
H. commersoni	UADBA *32378*	Toliara/Grotte de Tanambao, 0.75 km E St. Augustin	B
H. commersoni	UADBA *32379*	Toliara/Grotte de Tanambao, 0.75 km E St. Augustin	B
H. commersoni	UADBA *33692*	Toliara/Kirindy Forest (CNFEREF)	B
H. commersoni	UADBA *33693*	Toliara/Kirindy Forest (CNFEREF)	B
H. commersoni	UADBA *33694*	Toliara/Kirindy Forest (CNFEREF)	B
H. commersoni	UADBA *33695*	Toliara/Kirindy Forest (CNFEREF)	B
H. commersoni	UADBA CFR-*301*	Toliara/Kirindy Forest (CNFEREF)	B
H. commersoni	UADBA *33697*	Toliara/Kirindy Forest (CNFEREF)	B
H. commersoni	UADBA *33698*	Toliara/Kirindy Forest (CNFEREF)	B
H. commersoni	UADBA CFR-*306*	Toliara/Kirindy Forest (CNFEREF)	B

H. commersoni	UADBA *33700*	Toliara/Kirindy Forest (CNFEREF)	B
H. commersoni	UADBA *33701*	Toliara/Kirindy Forest (CNFEREF)	B
H. commersoni	UADBA *33702*	Toliara/Kirindy Forest (CNFEREF)	B
H. commersoni	FMNH *222747*	Toliara/Kirindy Forest (CNFEREF)	B
H. commersoni	FMNH *169707*	Antsiranana/PN d'Ankarana, 2.6 km E Andrafiabe, near Andrafiabe Cave	C
H. commersoni	FMNH *178806*	Antsiranana/RS d'Analamerana, Grotte de Bazaribe, 3.6 km SE Menagisy	C
H. commersoni	FMNH *178808*	Antsiranana/RS d'Analamerana, Grotte de Bazaribe, 3.6 km SE Menagisy	C
H. commersoni	FMNH *178809*	Antsiranana/RS d'Analamerana, Grotte de Bazaribe, 3.6 km SE Menagisy	C
H. commersoni	FMNH *178810*	Antsiranana/RS d'Analamerana, Grotte de Bazaribe, 3.6 km SE Menagisy	C
H. commersoni	FMNH *178811*	Antsiranana/RS d'Analamerana, Grotte de Bazaribe, 3.6 km SE Menagisy	C
H. commersoni	FMNH *178815*	Antsiranana/RS d'Analamerana, Grotte de Bazaribe, 3.6 km SE Menagisy	C
H. commersoni	FMNH *183980*	Antsiranana/Montagne de Français, Foret d'Ampitiliantsambo	C
H. commersoni	UADBA *32987*	Antsiranana/PN d'Ankarana, 2.6 km E Andrafiabe, in forest near Andrafiabe Cave	C
H. commersoni	FMNH *184030*	Mahajanga/4.2 km SE Marovaza, in cave	C
H. commersoni	UADBA 48666	Antsiranana/PN de la Montagne d'Ambre, 5.5 km SW Joffreville	

H. commersoni	UADBA 48642	Antsiranana/PN de la Montagne d'Ambre, 5.5 km SW Joffreville
H. commersoni	UADBA 48661	Antsiranana/PN de la Montagne d'Ambre, 5.5 km SW Joffreville
H. commersoni	USNM 578738	Toliara/Ste. Luce Forest, 2.3 km NW Manafiafy

Table S3. Principal component loadings, eigenvalues and cumulative variance for seven cranial and six dental variables.

Cranial	PC1	PC2	PC3	Dental	PC1	PC2	PC3
GSKL	0.976	-0.070	0.018	$C\text{-}M^3$	0.953	-0.139	0.320
CCL	0.966	-0.093	-0.049	$PM^4\text{-}M^3$	0.913	-0.298	0.331
ZYGO	0.896	-0.007	0.315	$C^1\text{-}C^1$	0.876	0.402	0.442
POB	0.224	0.972	0.024	$M^3\text{-}M^3$	0.893	0.302	-0.456
MAST	0.936	-0.027	0.237	$i_1\text{-}m_3$	0.965	-0.119	-0.287
MAND	0.965	-0.093	-0.122	$c\text{-}m_3$	0.960	-0.106	0.698
MOMARM	0.868	0.071	-0.416	Eigenvalue	5.180	0.378	0.184
Eigenvalue	5.32	0.972	0.338	Proportion of variance	86.3	6.3	3.1
Proportion of variance	76.0	13.9	4.8	Cumulative variance (%)	86.3	92.6	95.7
Cumulative variance (%)	76.0	89.9	94.7				

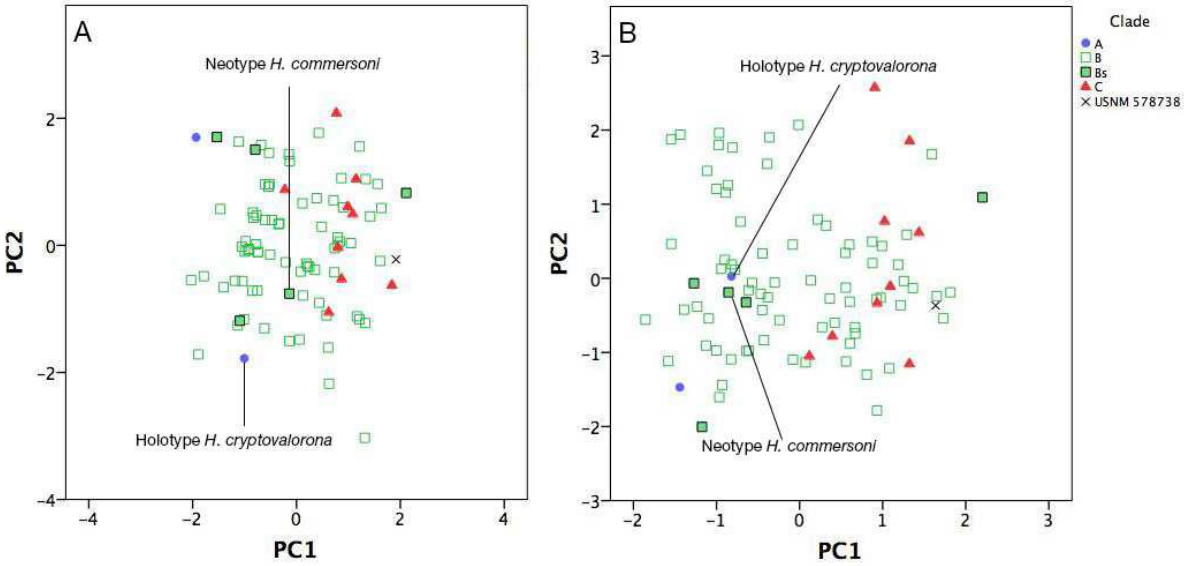

Fig. S1 Principal component analysis plots of a) seven cranial measurements and b) sixdental measurements for genotyped Malagasy *Hipposideros* female specimens.

CHAPTER THREE

Phylogeography and population genetics of *Hipposideros commersoni* s.s. (Chiroptera: Hipposideridae), an endemic Malagasy bat

ABSTRACT

Hipposideros commersoni (Hipposideridae), a bat species endemic to Madagascar, is widespread across the island, utilising open woodland, degraded habitats, and forested areas from sea level to 1325 m. We investigated the fine-scale phylogeographic history and relationships of populations occurring in the western half of the island using sequence data from two mitochondrial DNA regions and extensive geographical sampling. Bayesian clustering analysis implemented in BAPS revealed four main *H. commersoni* lineages: B1, B2, B3, and C. The most recent common ancestor of *H. commersoni* was dated to 3.33 million years ago (mid-Pliocene). Population expansion events were inferred for groups B1, B2, and B3 from approximately 127,600 (group B1) to 6,870 years BP (group B2). Conflicting results were obtained from Bayesian clustering and AMOVA analyses; strong population genetic structure was obtained from the former but not the latter. Sequence data indicated that genetic subdivisions do not support an isolation-by-distance model. Lineage dispersal, genetic divergence, and expansion events of *H. commersoni* were likely to be associated with Plio-Pleistocene climate fluctuations. Our data suggested that the northern and the central western regions of Madagascar may have acted as refugia for this species during periods of cooler and drier climate conditions associated with the Plio-Pleistocene.

Keywords: bioclimate, diversification, geographical structure, *Hipposideros*, Madagascar.

1. Introduction

The biota of Madagascar, with its numerous higher-level endemic taxonomic groups, as well as a large number of endemic genera and species (Myers et al., 2000), have been isolated from those of other continental landmasses for over 120 million years (Ali and Aitchison, 2008). The mechanisms driving this diversity are varied. Excluding vicariance, which can be applied to some living vertebrate lineages (Noonan and Chippindale 2006; Yoder and Nowak, 2006), different abiotic (e.g., ocean current direction or prevailing winds) and biotic (e.g. dispersal ability) filters have been in place over geological time limiting or promoting the colonization of the island by continental vertebrates (Ali and Huber, 2010; Samonds et al., 2012, 2013).

Given Madagascar's topographical, meteorological, and geological complexity, after successful colonization of this mini-continent by different ancestral forms, in many cases subsequent diversification took place, leading to endemic species as well as some of the most extraordinary adaptive radiations known in the world. Examples of such patterns of extensive speciation and morphological variation in volant vertebrates include birds of the families Vangidae and Bernieridae (Cibois et al., 2001; Jønsson et al., 2012; Reddy et al., 2012). In contrast, other adaptive radiations found on the island show distinctly less morphological differentiation and these groups contain numerous cryptic species, for example, bats of the genus *Miniopterus* (Christidis et al., 2014; Schoeman et al., 2015). Further, there are cases of presumed congenerics colonizing the island independently of one another, such as amongst bats of the families Molossidae (Lamb et al., 2011) and Rhinonycteridae (Foley et al., 2015; Russell et al., 2007). Regardless, the discerned periods of rapid cladogenesis amongst these different groups are not coincidental, yet no single unifying explanation can be presented to explain successful colonization and subsequent diversification patterns amongst extant volant vertebrates (Samonds et al., 2012, 2013).

Factors that may mediate colonization success include the period of initial colonization, ranging from the Mesozoic through the Cenozoic (Holocene), and life-history traits (e.g. large organisms with fast and efficient flight are more likely to colonize than small and slow flying organisms). Subsequent biogeographic and phylogeographic patterns of species are driven in part by the landscape and climatic heterogeneity of the island (Pearson and Raxworthy, 2009; Vences et al., 2009; Wilmé et al., 2006). Additionally, differences in modes of dispersal and habitat requirements amongst flying Malagasy vertebrates result in different biogeographic and phylogeographic patterns (e.g., for birds see Cruaud et al., 2011; Fuchs et al., 2007, 2013; for bats

see Chan et al., 2011; Goodman et al., 2010a, 2010b, 2016; Lamb et al., 2012; Ratrimomanarivo et al., 2007, 2008, 2009a, 2009b; Russell, 2007, 2008a, 2008b; Weyeneth et al., 2011). These different factors make Madagascar an excellent model system for testing and contrasting the process of species diversification and fine-scale spatial patterning across different lineages.

Hipposideros commersoni (Family Hipposideridae), which feeds predominantly on Coleoptera, is widespread across Madagascar and utilizes open woodland, degraded habitats, and forested areas from sea level to 1325 m (Goodman and Ramasindrazana, 2013; Rakotoarivelo et al., 2009). It occupies day roosts in caves found in areas of eroded sedimentary rock, often forming colonies of several thousand individuals; individuals also roost under vegetation in areas of relatively non-degraded or heavily degraded forest vegetation (Goodman, 2006; Raharinantenaina et al., 2008). There is evidence that *H. commersoni* exhibits morphological and bioacoustic variation across its geographical range; this includes sexual dimorphism, where males are significantly larger than females; both of these parameters show a clinal pattern correlated with latitude (Ranivo and Goodman, 2007; Ramasindrazana et al., 2015). For details on the complex taxonomic history of *H. commersoni* sensu lato, which previously included some African populations, see Goodman et al. (2016). Herein, we consider this species endemic to Madagascar.

Examination of Quaternary fossils from Madagascar found in cave deposits at Anjohibe (Fig. 1) revealed that a species referable to *Hipposideros*, *H. besaoka*, morphologically similar to *H. commersoni*, went extinct in the Late Pleistocene or Holocene (Samonds, 2007); these two species probably occurred sympatrically at Anjohibe. One particularly striking aspect of the fossil record of the genus *Hipposideros* is that specimens dating from the second half of the Eocene of France (Sigé, 1988), the Miocene of Australia (Hand, 1993, 1997), and the Pliocene of Ethiopia (Wesselman, 1984) show remarkably consistent craniodental structure across tens of million years and are notably similar to living members of this genus. Given this conservative morphological pattern, it is assumed that molecular genetics will provide an important signal to the evolutionary history of members of this genus, and there are probably numerous unrecognized cryptic species.

Recent work on the molecular genetics of animals referred to as *H. commersoni* from different areas of Madagascar, particularly the western half of the island, has found the presence of several independently evolving lineages, some geographically structured (Rakotoarivelo et al., 2015). On the basis of these results, a cryptic endemic species (clade A in Rakotoarivelo et al., 2015) was identified, and subsequently named as *H. cryptovalorona* (Goodman et al., 2016).

Rakotoarivelo et al. (2015) found *H. commersoni* sensu stricto (clades B and C therein) to be sister to African *H. vittatus* and *H. gigas*, with *H. cryptovalorona* basal to this grouping. On the basis of molecular clock estimates, clade A diverged from clades B and C during the Miocene, approximately 5.81 MYA and clades B and C last shared a common ancestor about 3.38 MYA. This indicates that large-bodied *Hipposideros* experienced two possible colonization events hypotheses. First, Clade A and Clade B-C could have originated from two independent eastward dispersals from Africa. The second hypothesis involves multiple, bidirectional dispersal; an early eastward dispersal to Madagascar, followed by a later back-dispersal to Africa.

Herein we focus on intra-population variability within *H. commersoni* sensu stricto, specifically clades B and C of Rakotoarivelo et al. (2015). Using sequence data from two mitochondrial genes and increased geographical sampling, we investigate the fine-scale phylogeographic history and relationships of populations occurring in the western half of the island.

1

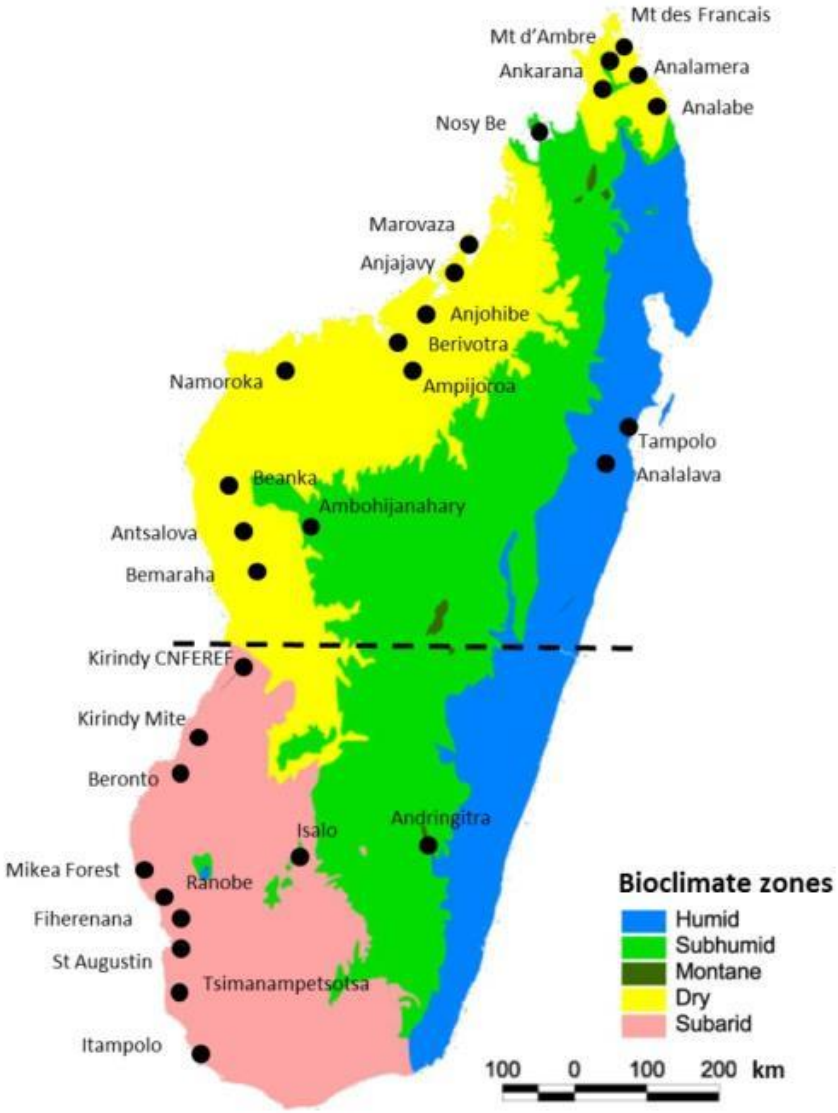

Fig. 1. Map of the different collection localities of specimens of *Hipposideros commersoni* used in this study. The map overlay is the simplified bioclimatic zones classification proposed by Cornet (1974). The stippled line separates the "northern group" from the "southern group"

2

3

2. Materials and methods

2.1. Taxon sampling

All of the tissue samples used herein were associated with specimens deposited in museums (Table S1) and no individual was specifically collected for this study. In total, 146 specimens of *Hipposideros commersoni* falling within clades B and C of Rakotoarivelo et al. (2015) and from 29 localities were included: the majority spanning much of the latitudinal breadth and known distribution of the species in the western half of the island, including 140 specimens from the dry and subarid bioclimatic zones, five specimens from the humid or subhumid bioclimatic zones (Montagne d'Ambre, Nosy Be, Tampolo, Analalava, Andringitra), and one specimen from the mid-western Central Highlands at the limit of the subhumid zone (Ambohijanahary) (Fig. 1; Table S1, Supporting information). Two African species, *H. gigas* and *H. vittatus*, were included as out-group taxa and used to root the phylogenetic trees. We did not include genetic data of *H. cryptovalorona*, which is basal to *H. commersoni* s.s., *H. gigas* and *H. vittatus*, and is presumed to represent a separate colonization event of members of the *H. commersoni* group on Madagascar (Goodman et al., 2016).

2.2. DNA amplification and sequencing

Genomic DNA was isolated using the NucleoSpin® Tissue kit (Macherey-Nagel, Germany), following the manufacturer's protocol for tissue samples. Two mitochondrial (mtDNA) markers were amplified: hypervariable control region (CR, 481 bp) using the primers P/E (Wilkinson and Chapman, 1991) and cytochrome *b* (*Cyt b*, 705 bp) using the primers JorF/H15553 (Irwin et al., 1991; Rakotoarivelo et al., 2015). PCR amplifications consisted of: ~20-150 ng template DNA, 2.5 µl 10 x KAPA buffer, 1 U KAPA Taq DNA polymerase, 200 µM dNTPs, 0.2 µM of each primer and 18.4 µl dH_2O to give a final reaction volume of 25 µl. The PCR cycle parameters for CR and *Cyt b* included an initial denaturation step at 95 °C for 3 min followed by 30 cycles at 95°C for 30 s, 50-55°C for 30 s, 72°C for 30 s, with a final extension step at 72°C for 5 min. PCR reactions included a negative control to check for possible contamination. PCR products were sent to the Central Analytical Facility at Stellenbosch University South Africa, for sequencing. Cycle sequencing was performed using the BigDye Chemistry, v3.1 and sequencing products were analyzed on an Applied Biosystems 3730xl Genetic Analyzer (Applied Biosystematics, Perkin

Elmer). All sequences were first aligned using ClustalW (Thompson et al., 1997) as implemented in BioEdit (Hall, 1999), and thereafter manually optimized. All new sequences were deposited in GenBank (Table S1).

2.3. Phylogenetic analyses

The two markers (CR, *Cyt b*) were analyzed separately and then combined into a single data set. The number of variable sites, number of parsimony informative sites and nucleotide frequencies were estimated for each data matrix in MEGA 6 (Tamura et al., 2013).

Phylogenetic reconstruction was performed using both maximum likelihood (ML) and Bayesian (Bayes) approaches using the programmes Garli 2.0 (Zwickl, 2006) and MrBayes 3.2 (Ronquist et al., 2012), respectively. The most appropriate substitution model for each gene (CR - GTR+I+G, *Cyt b* - TrN+I+G; Fig. 2) was selected using the Akaike information criterion (AIC) as implemented in jModelTest (Darriba et al., 2012; Posada and Crandall, 1998). For the concatenated data set, partitioned analyses were conducted, with data partitioned by gene. The parameters of nucleotide substitution models were unlinked across partitions. Each ML analysis was initiated from a random starting tree, with nodal support assessed using 1000 bootstrap replicates. Two independent Bayes runs of 5 million generations each were performed; each run consisted of four Monte Carlo Markov chains (MCMC), with topologies sampled every 250 generations. The program Tracer 1.6 (Rambaut et al., 2014) was used to determine that the effective sample size (ESS) had reached > 200 for all parameters. A 50% majority rule consensus tree was constructed using the CONSENSE program in the PHYLIP package (Felsenstein, 2005). In each simulation, the first 20% of generations were discarded as burn-in, after a pilot run to determine that this was sufficient to achieve stationarity.

We built haplotype networks for visualization of the two mitochondrial markers (CR, *Cyt b*) genealogies by converting MP tree estimates with Haploviewer (http://www.cibiv.at/~greg/haploviewer; Salzburger et al., 2011).

2.4. Population structure analyses

To examine the fine-scale population structure of *H. commersoni*, without making *a priori* assumptions about the partitioning of local populations, a Bayesian model-based approach to

inferring hidden genetic population structures was implemented in the program BAPS 6 (Bayesian analysis of population structure; Cheng et al., 2013; Corander and Marttinen, 2006). BAPS potentially offers insight into the historical genetic connectivity of populations. Analyses were first performed on the entire data (including all sequenced individuals from across the latitudinal range of *H. commersoni*) and then repeated on subsections of the data, including only individuals assigned to the "northern group" and the "southern group". In each independent run the number of proposed clusters (K) ranged from 1 to 10. In each case, analyses were conducted using the concatenated mtDNA.

A Mantel test was used to determine the relationship between genetic and geographic distance across distribution of *H. commersoni* and significance was assessed by 1000 permutations using Alleles In Space (AIS) program (Miller, 2005).

The geographical pattern of genetic differentiation was evaluated using analysis of molecular variance (AMOVA) with Arlequin 3.5 (Excoffier and Lischer, 2010). We assessed population structure at three hierarchical levels of subdivision (among regions, among populations within regions, and within populations). Two separate regions have been defined, at least in part based on the transition between the subarid and dry bioclimatic zones (Fig. 1): "northern group" includes all animals obtained in the latitudinal swath to the north of Kirindy (CNFEREF) and "southern group" including those to the south of Kirindy (CNFEREF). To evaluate possible correlations of genetic differentiation with climatological aspects of Madagascar, we also used AMOVA to test significant genetic differentiation among four bioclimatic zones, following the classification of Cornet (1974): "Dry1" includes sites from Nosy Be to the northern most locality; "Dry2" from Marovaza to Bemaraha; "Subarid"; and "Humid-Subhumid" as delineated in Fig. 1.

2.5. Demographic analysis, molecular clock dating, and Bayesian phylogeographic reconstruction

The time of most recent common ancestor of major evolution lineages was assessed using BEAST (Drummond and Rambaut, 2007) with a strict molecular clock, a coalescent prior (appropriate for intraspecific radiations), and the GTR + I + G model. A *Cyt b* mutation rate of 0.0088 substitutions site^{-1} MY^{-1} (6% divergence over 3.38 MY between clades B and C; table 2) was applied as a fixed mean substitution rate. Several preliminary short runs were performed to adjust the prior

parameters, including models and MCMC length, and to ensure sufficient mixing of chains. Tracer 1.6 was used to assess the convergence of the trace files (Rambaut et al., 2014). We ran three independent runs of 20 million generations, with sampling every 1,000 generations, and a burn-in of the first 10% of generations. Results were combined using Tracer 1.6 (Rambaut et al., 2014); effective sample size (ESS) values exceed 200 for all parameters. An additional molecular clock analysis was conducted using a faster mutation rate for *Cyt b* of 0.013 substitutions site^{-1} MY^{-1} (Thong et al., 2012; Lin et al., 2014) for comparison purposes. This analysis was performed using the strict molecular clock model in BEAST. All other parameters were the same as in previous analysis.

Population genetic and demographic analyses were performed separately for four *H. commersoni* clades (clades B1, B2, B3, and C see Results) using the concatenated sequence data (CR+*Cyt b*). Following Rogers and Harpending (1992) and Russell et al. (2005), we used haplotype (*Hd*) and nucleotide (*p*) diversity values, neutrality tests (Fs, Fu, 1997, and D* and F*, Fu and Li, 1993), and mismatch distribution analysis to estimate whether each population group was stationary or had undergone an historical population expansion or retraction. The following aspects are indicators of historical population expansion events (Russell et al., 2005): high *Hd* with low *p*, a unimodal pairwise difference distribution, significant Fs but non-significant D* and F*, and a high ratio of number of variable sites (*S*) to average number of nucleotide differences (*k*) (*S/k*). When evidence of population expansion was found, the associated timing in generations (*t*) was estimated from $\tau = 2ut$, where tau (τ) is a parameter of the time to expansion in units of mutations and *u* is the mutation rate per generation; *u* was calculated as the product of the mutation rate (μ: mutations per site per generation) and sequence length (703 bp); and *t* was the time (in generations) since expansion. We used a *Cyt b* mutation rate of $\mu = 1.78 \times 10^{-8}$ substitutions per site per generation, and the generation time was estimated to be two years. These analyses were carried out with DnaSP version 5.10 (Librado and Rozas, 2009). In the Bayesian skyline plot analysis, parameter settings and mutation rate (*Cyt b* mutation rate) were as described in the estimations of recent common ancestor amongst lineages. However, a Bayesian skyline coalescent was used as the tree prior and the MCMC search and this analysis was run for 20 million generations with the ESS value of each parameter > 200 for all parameters.

Bayesian Skyline plots were constructed using BEAST (Drummond and Rambaut, 2007) to estimate historical changes in population size over time of the two major lineages clades B (groups B1, B2, and B3) and C. This method assumes that sequences are sampled from a single panmitic

population, therefore the analysis considered all of the populations as a single group. This method uses Markov-Chain Monte Carlo sampling techniques to estimate the posterior distribution of effective population size given a set of aligned DNA sequences and a model of molecular evolution and takes into consideration uncertainty in the genealogical process (Drummond et al., 2005)

3. Results

3.1. Characteristics of molecular markers

The nucleotide composition and levels of variation of the two mitochondrial genes differed with CR having the highest number of variable characters (132 variable sites), while *Cyt b* was more conserved (76 variable sites). The CR partition contained the highest number of parsimony informative characters, whereas the mutational rate of *Cyt b* was more conservative, containing 52 parsimony informative characters (Table 1).

For the CR, after analyses with DNASP software, 92 unique haplotypes were identified. The haplotypic diversity for this dataset was high (Hd = 0.98), but the nucleotide diversity was low (p = 0.032). For the *Cyt b* gene, the same analysis identified 70 unique haplotypes, also with high haplotypic diversity (Hd = 0.98) and low nucleotide variability (π = 0.008).

Table 1

Characteristics of mtDNA datasets used in this study of *Hipposideros commersoni*. Patterns of sequence variability are presented for two mtDNA regions (CR and *Cyt b*) and the combined data matrix. The total number of nucleotide sites, variable and parsimony informative sites, as well as nucleotide frequencies are given for each partition and the combined data matrix

Gene	Total number of individuals	Total sites	Variable sites	Parsimony informative sites	Nucleotide frequencies			
					%A	%T	%C	%G
CR	146	481	132	91	32.90	27.00	25.80	14.34
Cyt b	146	703	76	52	26.90	27.36	30.57	15.18
Combined	146	1184	208	143	29.90	27.18	28.18	14.76

3.2. Phylogenetic analysis

Maximum likelihood and Bayesian analyses produced consistent topologies. There was no significant conflict between the CR and *Cyt b* topologies, although most clades in phylogenetic trees generated from the CR data had posterior probability bootstrap support values below 50% (Fig. S2). Consequently, the Bayesian phylogram constructed from the concatenated mtDNA data set is presented as Fig. 2. The ML and Bayesian analysis of the concatenated data matrix (CR + *Cyt b*; Fig. 2) recovered animals referred to as *H. commersoni* as a single monophyletic lineage, further supporting the conclusions of Rakotoarivelo et al. (2015). Two distinct clades were recovered: clade B (ML bootstrap, 59; Bayes' PP, 0.99) and clade C (ML bootstrap, 96; Bayes' PP, 1.0). Clade B is the most geographically widespread and genetically diverse clade (average within clade sequence divergence for *Cyt b* = 0.03; Table 2). The former major clade comprises a number of subclades or groups. Only one of these, (B2), is supported (ML bootstrap, 68; Bayes' PP, 0.99). Clade B1 is not supported and has a very shallow stem. The group labeled B3 was identified as a group based on the genetic mixture analysis in BAPS (Fig. 4), but does not form a monophyletic clade. The individuals belonging to this group were collected from regions throughout the island of Madagascar. Members of clade C were restricted to localities in the extreme north of Madagascar (Fig. 2), whereas members of clade B2 primarily were restricted to the south.

Haplotype network construction of *H. commersoni* implemented in HaploViewer yielded two connected haplotype sub-networks (clades B and C), similar to the topology described in the most concordant tree (Fig. 3). Clades B and C were distinguished by 13 mutational steps, whereas haplotype differences within clades are typically distinguished by only a few steps (Fig. 3).

Table 2

Average pairwise sequence distances among the *Hipposideros* outgroup taxa and the major lineages of the ingroup, estimated using the GTR+I+G substitution model and *Cyt b* data. Average within lineage pairwise sequence distances are given in bold on the diagonal.

	Clade B	Clade C	*H. gigas*
Clade B	**0.03**		
Clade C	0.06	**0.01**	
H. gigas	0.10	0.09	
H. vittatus	0.10	0.09	0.11

Table 3

Percentages from hierarchical analyses of molecular variance (AMOVA) for mtDNA control region of *Hipposideros commersoni* based on geographical groupings and bioclimatic zones.

Population groups	Among groups	Among populations within regions	Within populations
Northern/Southern	1.27***	2.32**	96.41***
Dry1/Dry2/Subarid/Humid-Subhumid	2.82***	2.56*	94.62***

Statistically significant results were indicated by asterisks: * $P < 0.05$;** $P < 0.01$; ***$P < 0.001$.

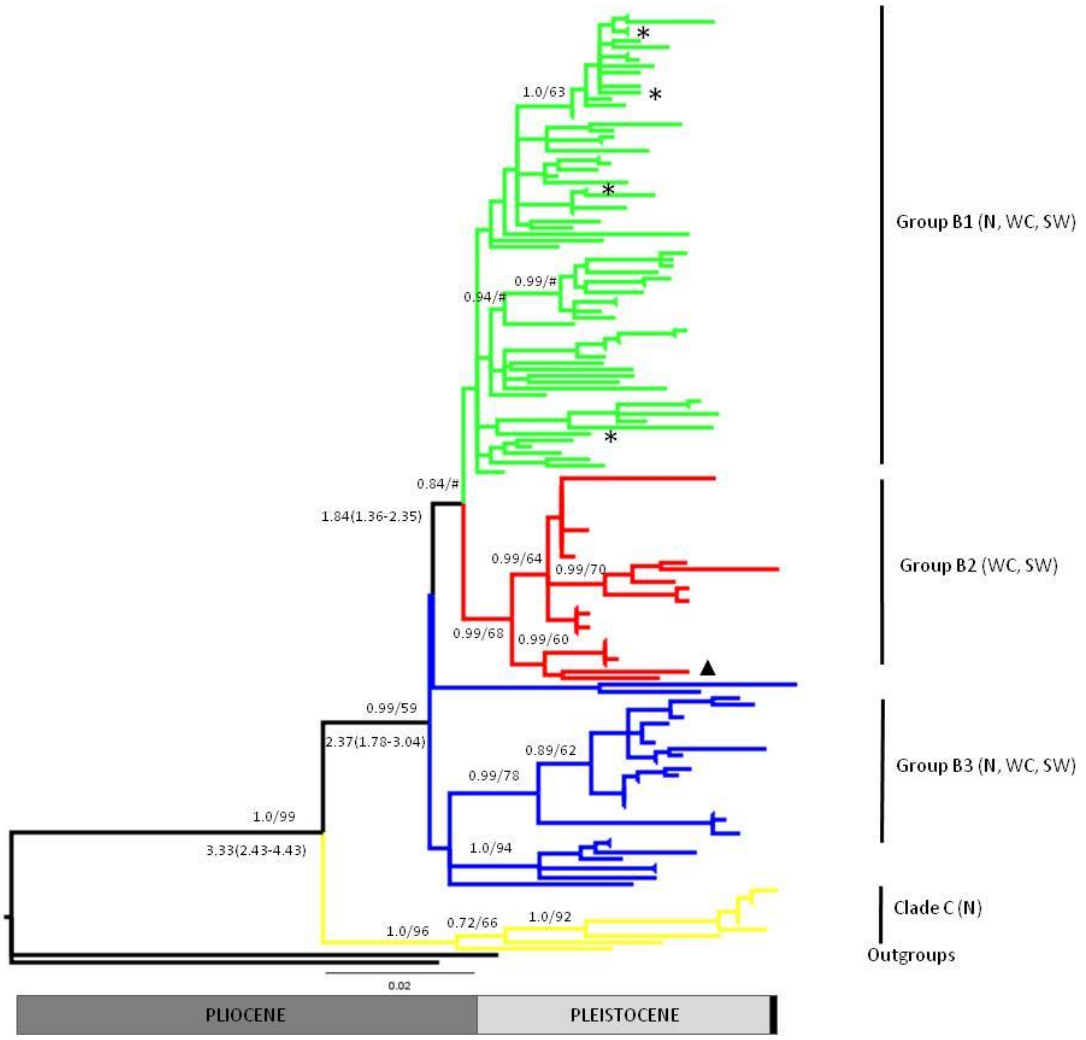

Fig. 2. Bayesian phylogram based on the combined analysis of mtDNA control region and Cytochrome b data drawn from 146 individual *Hipposideros commersoni*. Nodal support values are represented as Bayesian posterior probability/likelihood bootstrap percent (# = values ≥ 50); numbers below branches are times to the most recent common ancestor (in MY) with 95% highest posterior density. Groups B1, B2, B3 and C correspond to those identified by genetic mixture analysis in BAPS (Fig. 4) * = specimens from eastern Madagascar, specifically the sites of Analalava and Tampolo, ▲ = specimen from Andringitra, N = north, WC = west central, SW = southwest.

1

2

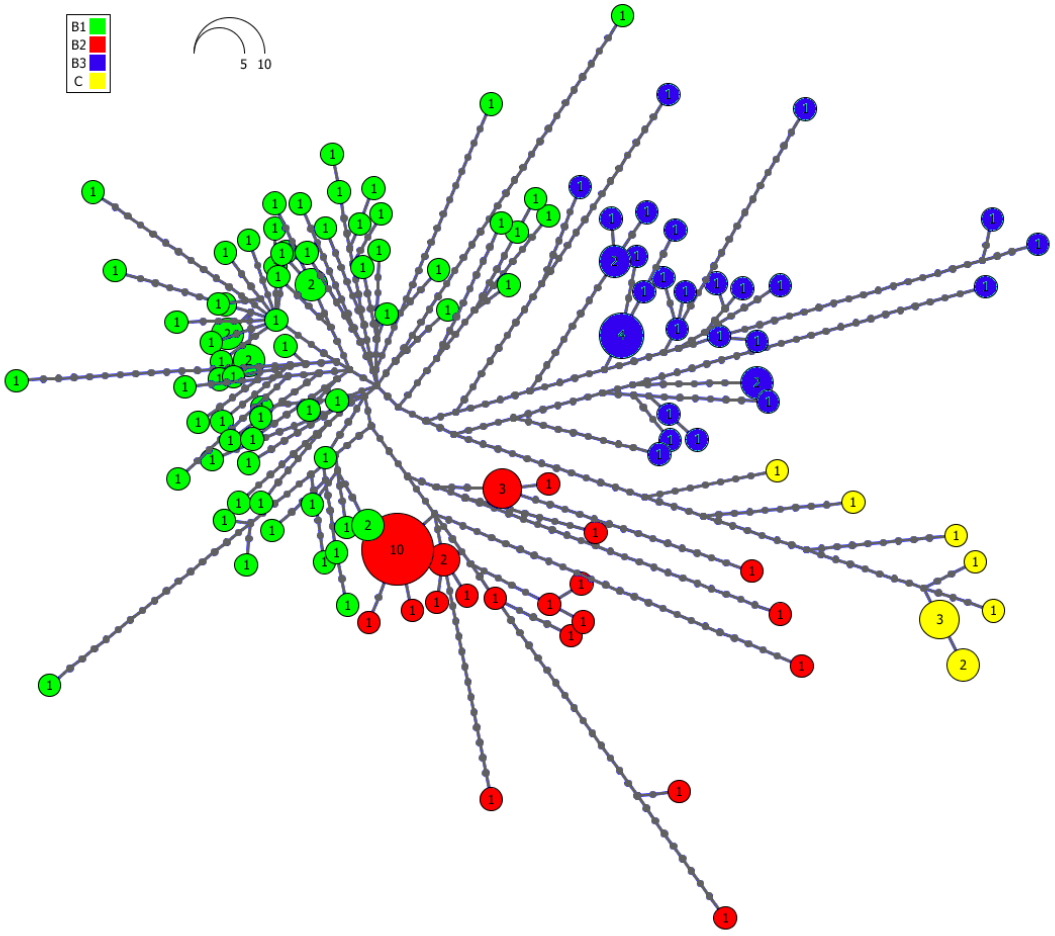

Fig. 3. Haplotype network of the combined of mtDNA control region and Cytochrome b data drawn from 146 individual *Hipposideros commersoni* built with HaploViewer. Clades and groups are color-coded based on the BAPS clustering results (as in Fig. 2). Numbers inside the proportionally sized circles represent the number of individuals sharing that particular haplotype.

3.3. Phylogeographical analyses

3.3.1. Bayesian clustering –historical population structure

The Bayesian clustering method of BAPS performed on the concatenated sequence data defined four genetically distinct clusters (P = 1, optimal partition, log likelihood = -5536.8; Fig. 4): two widespread clusters distributed throughout the range of *H. commersoni* (cluster 1 = group B1, and cluster 3 = group B3), the northern isolate (cluster 2 = clade C), and that restricted to largely the subarid bioclimate zone (cluster 4 = group B2).

Additional phylogeographical resolution was recovered through the independent analysis of the mtDNA of the southern and northern groups (Fig. 5). Four genetically distinct BAPS clusters were recovered within the southern group (P = 0.99, log likelihood of optimal partition = -2295.82), whereas within the northern group three distinct genetic clusters were recovered (P = 1, log likelihood of optimal partition = -2836.21). When all individuals were used, the Mantel test failed to support the isolation-by-distance (IBD) model (r = -0.009, $P > 0.05$).

Analysis of molecular variance (AMOVA) revealed that significant genetic variance was attributable to all three examined hierarchical levels (among regions, among populations within regions, and within populations). However, a large part of the total variation was found within populations (96.41% for geographical group and 94.62% for bioclimatic group, Table 3). The subarid bioclimatic region was the most differentiated region (Table 4). There was also differentiation between Dry1 and Dry2 but there was no differentiation between the dry regions (Dry1 and Dry2) and the humid-subhumid region (Table 4).

1

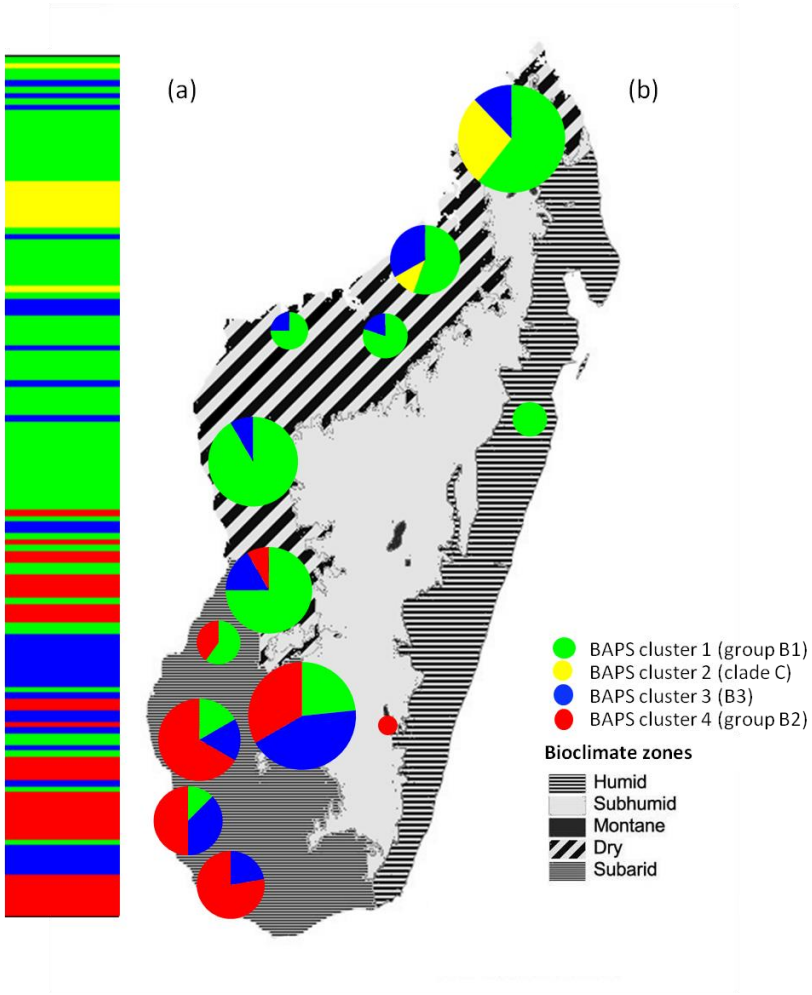

Fig. 4. Posterior mode clustering of *Hipposideros commersoni* concatenated mtDNA data using the individual based genetic mixture analysis in BAPS (a). The 146 specimens are clustered by specific locality or grouped neighbouring localities. (b) Distribution of estimated BAPS cluster frequency for the complete concatenated mtDNA sequence data. The simplified bioclimatic zone classifications of the island in which lineages are located are on the maps. Reference to clades and groups are associated with information in Fig. 2.

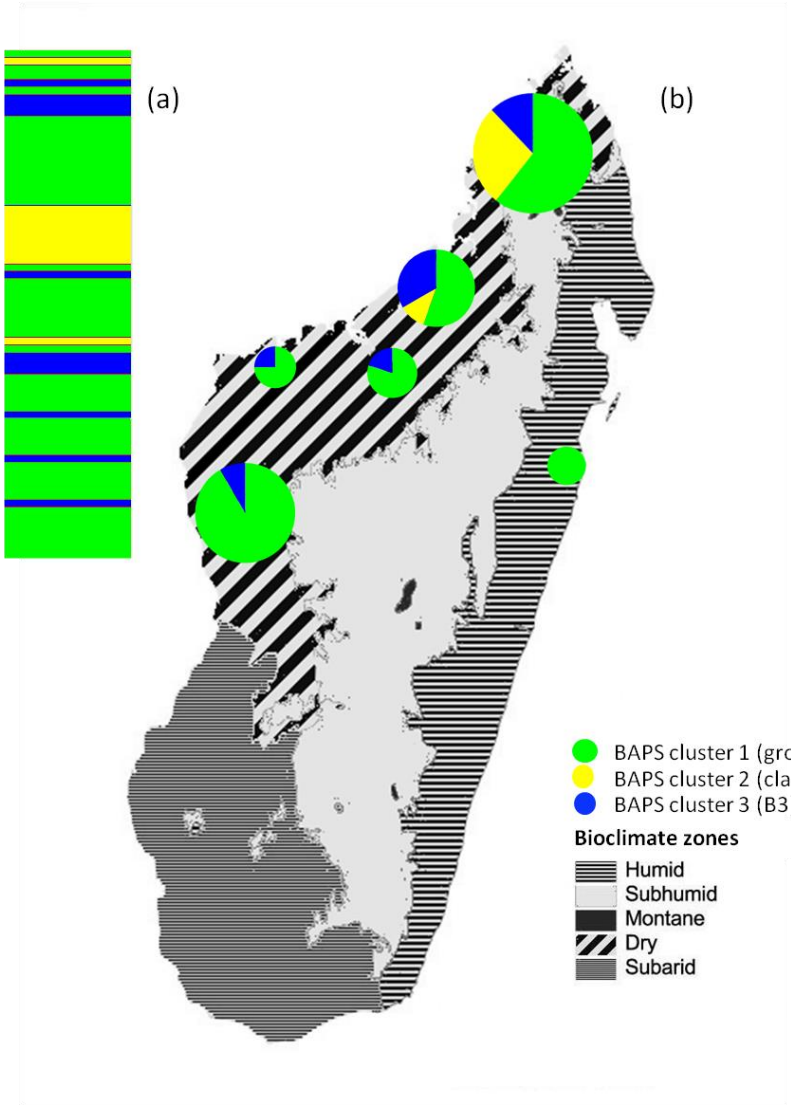
(a)
(b)
BAPS cluster 1 (group B1)
BAPS cluster 2 (clade C)
BAPS cluster 3 (B3)
Bioclimate zones
Humid
Subhumid
Montane
Dry
Subarid

1

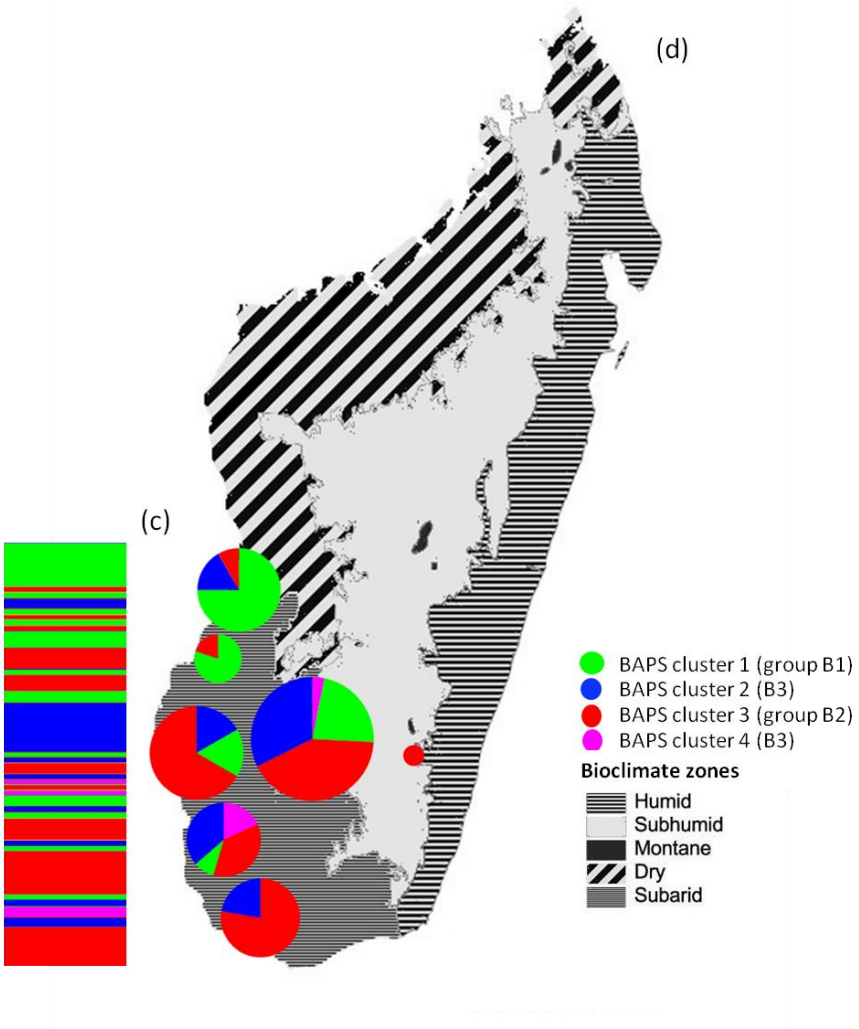

Fig. 5. Posterior mode clustering of (a) the northern group and (c) the southern group of *Hipposideros commersoni* using the genetic mixture analysis at the individual level in BAPS. The 69 individuals in the northern group and 77 individuals in the southern group are clustered by specific locality or grouped neighbouring localities. Distributions of the estimated BAPS cluster frequency for the mtDNA sequence data of (b) the northern group and (d) the southern group are shown. The simplified bioclimatic zone classification of the island in which lineages are located are on the maps.

3.3.2. Demographic history

With a mutation rate of 0.0088 substitutions site^{-1}MY^{-1}, the most recent common ancestor of *H. commersoni* studied herein could be traced back to 3.33 (95% highest posterior density (HPD); 2.43–4.43) MYA. The TMRCA of groups B1, B2, and B3 was dated to 2.37 (95% HPD; 1.78–3.04) MYA, and that of groups B1 and B2 to 1.84 (95% HPD; 1.36–2.35) MYA. Estimated TMRCA values for each clade or group (from C to B1) ranged from 1.46 (95% HPD: 1.14–1.86 MYA) to 2.03 (95% HPD: 1.46–2.67 MYA) (Fig. 2). The estimated divergence times using the faster substitution rate resulted in more recent divergence dates. For example, molecular clock estimates suggest that the two sister clades B and C shared their last common ancestor 2.09 MYA (95% HPD 1.75-2.71, Table 5). The TMRCA of groups B1 and B2 was dated to 1.13 (95% HPD; 0.87–1.43) MYA (Table 5). The 95% HPD intervals for divergence events from both analyses (calculated substitution rate and published substitution rate) were broad and did show overlap.

The Bayesian Skyline plot analysis indicated that all individuals herein assigned to groups B2 and B3 underwent a slow demographic expansion. On the other hand, B1 underwent a slow demographic expansion followed by two rapid expansion that started ~0.50 MYA_ago (10-fold increase). Furthermore, the group B1 experienced the second expansion ~0.20 MYA ago (6-fold increase), followed by stabe growth up to the present time, with no sign of population decline or genetic bottleneck during the evolutionary history of the clade. On the other hand, clade C remained stable up to the present time (Fig. 6).

Results of molecular diversity and neutrality tests for the major clades and groups (B1, B2, and C) are shown in Table 6. Groups B1 and B2, show evidence of an historical expansion, presenting unimodal mismatch distribution curves, as expected in cases of population expansion (Table ~~5~~6, Fig. 7). Further, neutrality tests were also in concordance with the above results. Fu's Fs statistic based on the *Cyt b* sequences revealed values significantly less than zero for groups B1 and B2, indicating a recent expansion. In addition, Tajima's D test was significantly negative for group B1, although negative and non-significant for group B2. In contrast with Groups B1 and B2, Group C showed less evidence of expansion. The mismatch distribution for group C was bimodal, and Fu's FS and Tajima's D values were negative but not significant. Lastly, the group B3 showed clearly multimodal mismatch distribution. Negative Fu's FS and Tajima's D values are usually interpreted as purifying selection, or as a signature of a recent population expansion. Fu (1997) interpreted the non-significant values in D* and F* tests combined with a significant Fs as evidence

of the absence of background selection, therefore supporting demographic expansion. Fu and Li's D* and F* tests supported significant deviation from neutrality for group B1. The population expansion tests conducted based on our estimated values of τ indicate that, the average time since the demographic expansion for *H. commersoni* ranged from approximately 63,732 (group B1) to 3,396 yr BP (group B2).

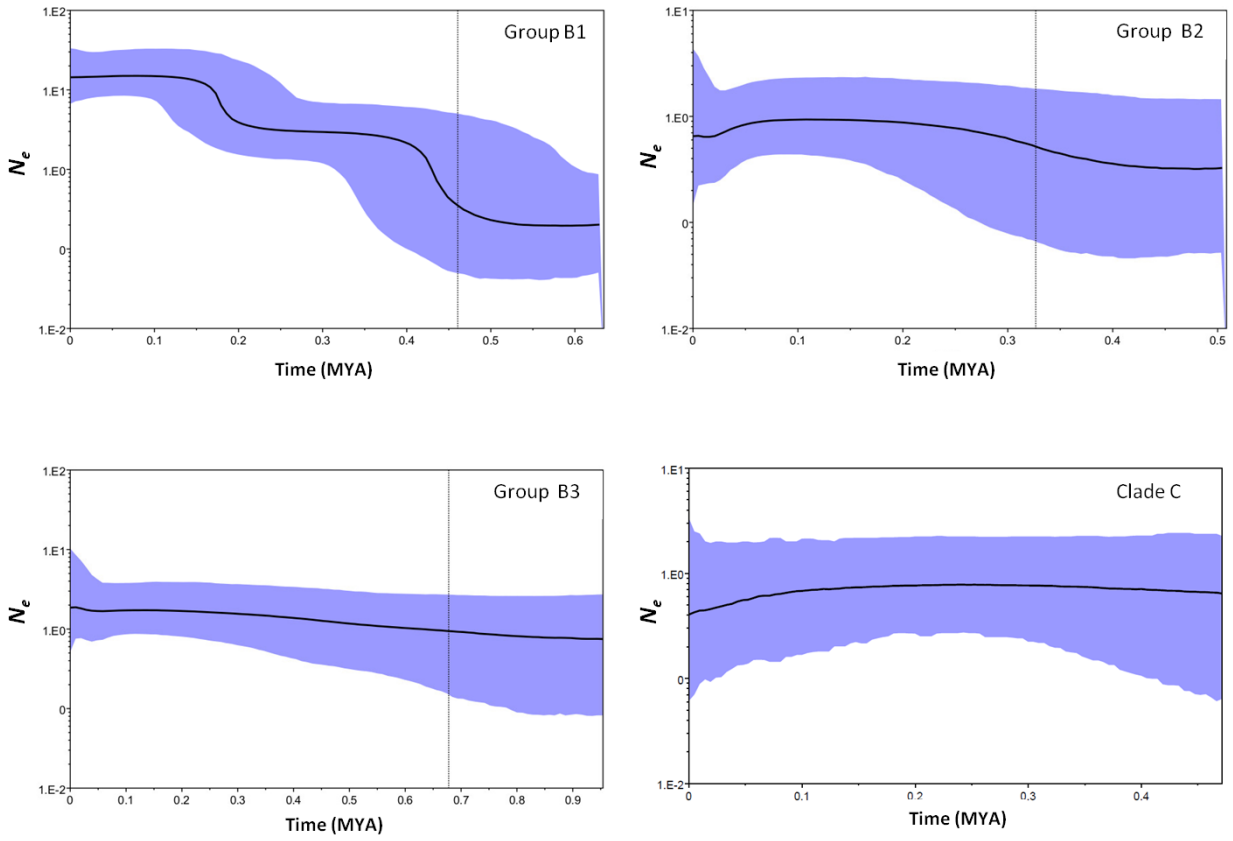

Fig. 6. Bayesian skyline plot for mtDNA with a strict clock and based on a generation time for *Hipposideros commersoni* of two years. The y-axis shows the effective number of individuals N_e. The thick solid line is the estimated median and the shaded area shows the 95% HPD limits. The x-axis is time scaled in million years ago (MYA).

1

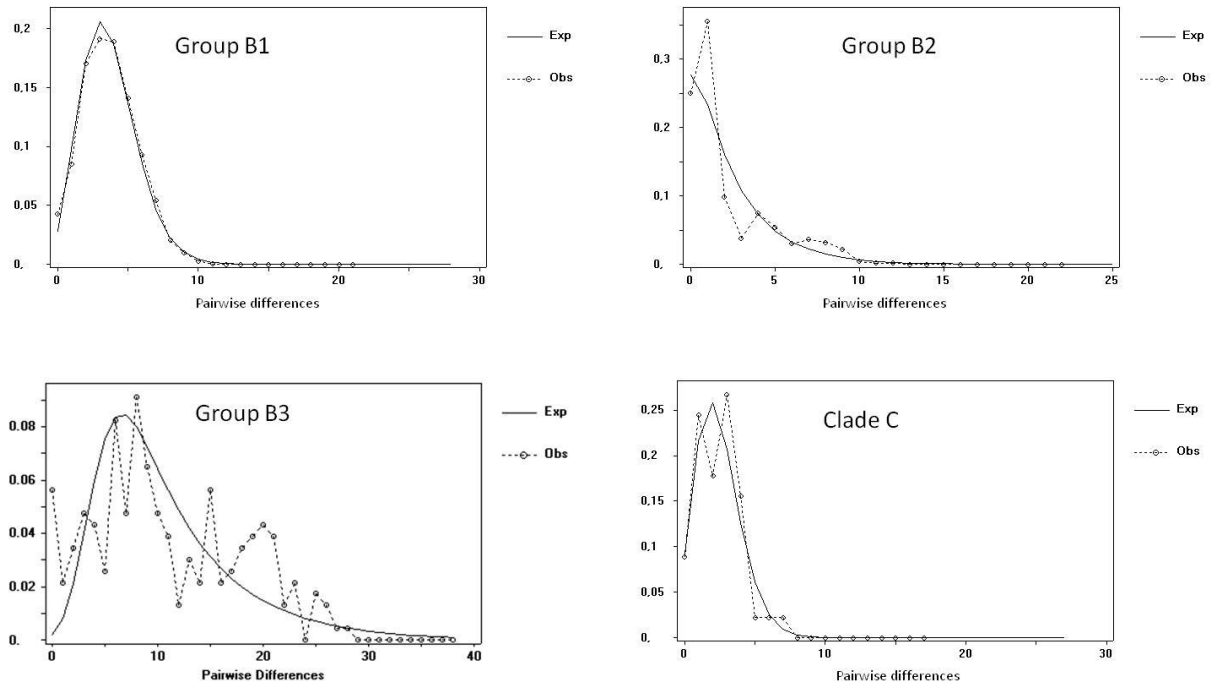

Fig. 7. Observed and expected mismatch distributions under population expansion model for groups B1, B2, B3, and clade C of *Hipposideros commersoni*.

2

3

4

5

6

Table 4

Pairwise ΦST values for mtDNA control region among populations of *Hipposideros commersoni*.

	Dry1	Dry2	Subarid	Humid-Subhumid
Dry1	-			
Dry2	0.064*	-		
Subarid	0.151*	0.069*	-	
Humid-Subhumid	0.050	0.0617	0.155*	-

Statistically significant results were indicated by asterisks: *$P < 0.001$.

Table 5

Hipposideros commersoni divergence dates (in MYA) from two molecular clock analyses: (A) strict clock with a mutation rate of 0.0088 substitutions site^{-1} MY^{-1}; (B) strict molecular clock model using a fixed mean substitution rate of 0.013 substitutions site^{-1} MY^{-1}. In bold are mean estimated values with 95% highest posterior density (HPD) ranges shown in brackets. See Figure 2 for the maximum clade probability tree corresponding to Scheme A.

Molecular clock scheme	Clade B and C	Clade B (B1, B2, and B3)	Group B1 and B2
A	**3.33** [2.43-4.43]	**2.37** [1.78–3.04]	**1.84** [1.36–2.35]
B	**2.09** [1.57-2.71]	**1.56** [1.19-1.97]	**1.13** [0.87–1.43]

Table 6

Neutrality statistics for three defined major clades and groups of *Hipposideros commersoni* based on *Cyt b* sequences.

	Group B1	Group B2	Group B3	Clade C
Nucleotide diversity (π)	0.005	0.003	0.009	0.003
Haplotype diversity (Hd)	0.957	0.750	0.944	0.911
Expansion coefficient (S/k)	12.771	8.108	3.761	3.719
Fu and Li's F*	-2.973 *	-2.143	0.165	-1.481
Fu and Li's D*	-2.973 *	-1.874	0.295	-1.407
Fu and Li's Fs	-45.655 ***	-2.518 *	-0.834	-2.671
Tajima's D	-2.037 *	-1.713	-0.295	-1.045
Raggedness (r)	0.0170	0.0615	0.0144	0.0672
Ramos-Onsins and Rozas (2002) (R2)	0.0351	0.0615	0.1240	0.1253
Mismatch distribution	Unimodal	Unimodal	Multimodal	Bimodal
Tau (τ)	3.199	0.170	4.676	2.189
Time since expansion (year BP)	63,732	3,396		-

Statistically significant results were indicated by asterisks: * $P < 0.05$, ** $P < 0.01$, *** $P < 0.001$.

4. Discussion

4.1. Phylogeography and demographic history

Paleoclimatic variation has played an important role in the distribution and speciation of organisms on continental landmasses and islands (Hewitt, 2000; Vences et al., 2009). Madagascar was cooler and drier during periods of late Tertiary-Quaternary glaciation, inducing habitat shifts that presumably forced certain taxa to retreat into refugia (Burney, 1995; Vences et al., 2009; Wilmé et al., 2006) such as the northern volcanic massif of Montagne d'Ambre or the central western massif of Isalo, from where they subsequently re-expanded during more favorable climatic periods.

We recovered some geographic genetic subdivision within *H. commersoni*, with Clade C located in the north of the island, and B2 in the south. Clades B and C appear to have diverged 3.33 MYA, in the mid-Pliocene. We suggest that initial intraspecific divergence within *H. commersoni* might be related to refugial isolation, with at least one of these refugia, having possibly harboured Clade C, located in the north of the island. The separation between the groups within clade B, which are distributed across the island, may have resulted from multi-directional dispersal during more favorable periods (see below). These findings suggest that divergence events within *H. commersoni* may have been associated with Plio-Pleistocene climatic fluctuations. Our results also reveal that genesis of the extant clades within Clade B commenced approximately 2.3 MYA. There is a scarcity of published divergence dates of bat taxa below the family level, and most dates are reliant on a sparse fossil record (Teeling et al., 2005). The uncertainty in the mutation rate of the concatenated dataset will affect the molecular clock dates presented here. These divergence dates should be considered preliminary until more precise calibration points can be added to the analyses.

At least three other Malagasy bat species, *Paratriaenops furculus* (Russell et al., 2007), *Chaerephon leucogaster* (Ratrimomanarivo et al., 2009), and *Myotis goudoti* (Weyeneth et al., 2011) show similar haplotypic segregation along a latitudinal gradient. However, the latitudinal distribution of different clades and the calculated expansion periods of the other species differ from late Pleistocene in *M. goudoti* to early Holocene in *C. leucogaster*, suggesting that no common historical process underlies the different demographic events between these taxa.

Based on demographic analysis, *H. commersoni* species forming the group B1 underwent two rapid five historical population expansion events: (1) slow demographic expansion between ~0.65 and ~0.50 MYA followed by (2) a first rapid expansion (10-fold increase) between ~0.50

MYA and ~0.40 MYA, after which (3) expansion continued at a slower rate until (4) the second rapid expansion event ~0.20 MYA ago (6-fold increase). Finally, (5) from ~0.15 MYA up to the present time, the group B1 presented stable growth. It is possible that these demographic shifts were associated with the optimality of climatic conditions for *H. commersoni*; the more favorable conditions are hypothesized to have contributed to more rapid population expansion and multi-directional dispersal associated with more suitable feeding habitats and abundant food resources.

The mismatch distribution analyses revealed a similar pattern of demographic expansion in groups, B1 and B2, as indicated by the significant negative Fu's Fs values and the unimodal mismatch distribution curves. The expansion of both is separated by ~60,000 years, with group B1 expanding 63,732 year BP and group B2 3,396 year BP.

Intriguingly, the extinct *H. besaoka* described from the late Pleistocene-Holocene of Anjohibe Cave, western lowland Madagascar was temporally sympatric with *H. commersoni* (Samonds, 2007). No clear hypothesis has been presented on the principal factor that led to the extinction of *H. besaoka*. Changes in vegetational types in lowland areas of the western half of the island in the late Pleistocene and Holocene of Madagascar saw a shift to drier climates and more arid natural vegetational types (Burney, 1997; Goodman and Jungers, 2014). These changes were most notable in the extreme southwestern portion of the island during the late Holocene with shift from forests and woodlands to drier wooded savanna (Burney, 1993; Goodman and Jungers, 2014). Similarly, northwestern Madagascar was the scene of vegetational changes from a mosaic of dry forest and wooded savanna from ~3500 years BP to a savanna formation from 1000-500 years BP (Matsumoto and Burney, 1994; Crowley and Samonds, 2013; Goodman and Jungers, 2014). What is unclear is why the factor(s) that led to the extinction of *H. besaoka* did not have the same impact on the presumed ecologically similar *H. commersoni*. Another possibility is competitive exclusion of the former by the latter.

Wesselman (1984) described fossil remains recovered from the Omo formation of Ethiopia and dated to the late Pliocene (2.08 MYA) as a distinct species, *H. kaumbului*. The author suggested that this taxon was morphologically similar to *H. commersoni*. From recent molecular research, it has been shown that different species included in the *H. commersoni* group (i.e. *H. gigas*, *H. vitattus*, *H. cryptovalorona*, and *H. commersoni*) are genetically distinct (Goodman et al., 2016; Rakotoarivelo et al., 2015). Apart from their size, these different species are morphologically similar to one another.

4.2. Population genetic structure

The Bayesian clustering analyses revealed four groups, consistent with a level of population genetic structure within the *H. commersoni* mtDNA data set. The haplotype network generated from mtDNA exhibited a split between the northern clade C and clade B, as did the phylogenetic analyses, in which clades B (moderately supported) and C (strongly supported) are reciprocally monophyletic. Based on a previous study (Rakotoarivelo et al., 2015), the lack of haplotype sharing in the OSTA5 gene for clades B and C supports the inferred genetic distinctness of these two lineages.

Although around 95% of the genetic variance occurred within populations, AMOVA revealed that a relatively low although highly significant proportion of the variance occurred among groups of *H. commersoni* based on latitude (north vs south) and climate (degree of humidity). Significant genetic differences were observed between populations from the dry region (Dry1 and Dry2) and subarid region (Table 4), possibly reflective of a lack of gene flow (Xu et al., 2010). Mantel tests failed to support the isolation-by-distance (IBD) model for *H. commersoni* across much of its distribution. This lack of relationship between genetic differentiation and geographic distance is in accordance with the high dispersal ability (Norberg and Rayner, 1987) of this species, which in turn may limit genetic differentiation among populations.

African members of the *H. commersoni* species complex, specifically *H. vittatus* and *H. gigas* undertake local seasonal movements associated with fluctuations in prey abundance (McWilliam, 1982; Vaughan, 1977). Large hipposiderid bats have high wing loading and low to medium aspect ratios (Norberg and Rayner, 1987), which may favor relatively quick, long-distance movements, allowing individuals to track food resources (Jones and Rayner, 1989; Bernard and Fenton, 2003).

On Madagascar, some apparent seasonal intra-island dispersal of *H. commersoni* has been documented at Kirindy (CNFEREF) (Fig. 1) (Rakotondramanana and Goodman, 2011; Ramasindrazana et al., 2015). This dispersal behaviour, particularly at a broad geographical scale, may explain shallow phylogeographic structure in this species. On the other hand, there is some evidence from the northwest, specifically the region of Anjohibe, that *H. commersoni* remains inactive in caves during times of resource shortage (A.R. Rakotoarivelo, unpublished results); this is the site where sequenced individuals falling within groups B1 and B3 have been identified.

Furthermore, no apparent physical barrier in the western half of the island, such as a high mountain range, divides the latitudinal distribution of *H. commersoni* (Fig. 1), and the members of the groups B1, B2, and B3 overlap in their distributions (Fig. 2). Bioclimatic features might have direct effect on habitat structure and prey availability of bats that show seasonal variation in their diet (Razakarivony et al., 2005; Rakotoarivelo et al., 2007), but these aspects do not explain the distributions of the different clades. Hence, based on the mitochondrial markers used herein, the best explanation for population genetic structure in this broadly distributed and apparently widely dispersing species, is that in the recent geological past populations were isolated in refugia and underwent some level of genetic differentiation. Subsequently, these populations - at least females - expanded and in many cases are now overlapping giving rise to the modern structure of the clades and groups presented herein. However, because the inferred evolutionary relationships in the current study are based mainly on information from mitochondrial genes, a more informative assessment of relationships between clades could be performed using microsatellites allowing the detection of nuclear gene flow between lineages.

4.3. Conservation implications

Hipposideros commersoni is a beetle specialist (Razakarivony et al., 2005; Rakotoarivelo et al., 2009) and due to its diet, may be susceptible to habitat destruction associated with diminished food resources. Besides habitat loss, a major threat to different Malagasy bat species, particularly those of larger body-size, is hunting for bush meat (Jenkins and Racey 2008). In western Madagascar, considerable numbers of *H. commersoni* are harvested for food at day roost sites (Goodman, 2006; Jenkins and Racey, 2008), including an estimate in the extreme southwest of 140,000 annually, particularly between January and March coinciding with the period of human food shortages (Goodman, 2006). This level of exploitation in certain areas of the island is certainly having a direct impact on the population dynamics of *H. commersoni*, reducing population size and presumably recruitment into the breeding population (Ramasindrazana and Goodman, 2012). Genetically divergent populations have been recognized in the literature as conservation priorities (Palsböll et al. 2007; Lu et al., 2013). Based on this and the results recovered in the current study, the populations of *H. commersoni* belonging to clade C of Analamera, Ankarana, Montagne d'Ambre, and Marovaza (Fig. 1) represent those of conservation importance.

5. Conclusions

Our research has indicated that several lineages of the endemic Malagasy bat *H. commersoni* sensu stricto, largely represented in our sequenced samples across most of western Madagascar, have a single common ancestor, which is dated to 3.33 MYA. Lineage dispersal, genetic divergence, and expansion events of *H. commersoni* (at least females) are likely associated with Plio-Pleistocene climate fluctuations. Our data indicate the northern region (Montagne d'Ambre and neighbouring areas) and the central western area of the Isalo Massif may have acted as refugia for this species during the Plio-Pleistocene, specifically periods of cooler and drier climate conditions. These are the areas where this species shows high levels of genetic diversity and overlap, and these zones should be the focus of conservation efforts.

Acknowledgements

The authors are grateful to the Département de Biologie Animale, Université d'Antananarivo; Madagascar National Parks (MNP); and the Ministère des Forêts et de l'Environnement, Direction générale des Forêts, Direction de la Conservation de la Biodiversité et du Système des Aires Protégées, all in Madagascar, for their administrative support. Funding was provided to A.R.R. by the IDP Foundation, Inc. associated with the Field Museum of Natural History African Training Fund, as well as the College of Agriculture, Engineering and Science, School of Life Sciences, University of KwaZulu-Natal. The molecular portion of this study was conducted in the Conservation Genetics Lab facilities, School of Life Sciences, University of KwaZulu-Natal (Ethics sub-committee clearance reference number: 119/14/animal). For access to tissue samples held in different museum, we acknowledge Julie Feinstein, American Museum of Natural History, and the late William Stanley, Field Museum of Natural History.

References

Ali, J.R., Aitchison, J.C., 2008. Gondwana to Asia: plate tectonics, paleogeography and the biological connectivity of the Indian sub-continent from the Middle Jurassic through latest Eocene (166–35 Ma). Earth Sci. Rev. 88, 145–166.

Ali, J.R., Huber, M., 2010. Mammalian biodiversity on Madagascar controlled by ocean currents. Nature 463, 653–656.

Bernard, E., Fenton, M.B., 2003. Bat mobility and roosts in a fragmented landscape in Central Amazonia, Brazil. Biotropica 35, 262–277.

Burney, D.A., 1993. Late Holocene environmental change in arid southwestern Madagascar. Quater. Res. 40, 98–106.

Burney, D.A., 1995. Climate change and fire ecology as factors in the Quaternary biogeography of Madagascar. In: Lourenço, W.R. (Ed.), Biogéographie de Madagascar. Editions ORSTOM, Paris.

Burney, D.A., 1997. Theories and facts regarding Holocene environmental change before and after human colonization. In: Goodman, S.M., Patterson B.D. (Eds.), Natural Change and Human Impact in Madagascar. Smithsonian Institution Press, Washington, DC.

Chan, L.M., Goodman, S.M., Nowak, M., Weisrock, D.W., Yoder, A.D., 2011. Increased population sampling confirms low genetic divergence among *Pteropus* (Chiroptera: Pteropodidae) fruit bats of Madagascar and other western Indian Ocean islands [Internet]. PLoS Currents: Tree of Life, doi: 10.1371/currents.RRN1226.

Cheng, L., Connor, T.R., Sirén, J., Aanensen, D.M., Corander, J., 2013. Hierarchical and spatially explicit clustering of DNA sequences with BAPS software. Mol. Biol. Evol. 30, 1224–1228.

Christidis, L., Goodman, S. M., Naughton, K., Appleton, B., 2014. Insights into the evolution of a cryptic radiation of bats: dispersal and ecological radiation of Malagasy *Miniopterus* (Chiroptera: Miniopteridae). PLoS One 9, e92440, doi:10.1371/journal.pone.0092440.

Cibois, A., Slikas, B., Schulenberg, T. S., Pasquet, E., 2001. An endemic radiation of Malagasy songbirds is revealed by mitochondrial DNA sequence data. Evol. 55, 1198–1206.

Corander, J., Marttinen, P., 2006. Bayesian identification of admixture events using multilocus molecular markers. Mol. Ecol. 15, 2833–2843.

Cornet, A., 1974. Essai de cartographie bioclimatique à Madagascar. Notice Explicative de l'ORSTOM 55, 1–28.

Crowley, B.E., Samonds, K.E., 2013. Stable carbon isotope values confirm a recent increase in grasslands in northwestern Madagascar. The Holocene 23, 1066–1073.

Cruaud, A., Raherilalao, M.J., Pasquet, E., Goodman, S.M., 2011. Phylogeography and systematics of the Malagasy rock-thrushes (Muscicapidae, *Monticola*). Zoolog. Scr. 40, 554–566.

Darriba, D., Taboada, G.L., Doallo, R., Posada, D., 2012. jModelTest 2: more models, new heuristics and parallel computing. Nature Methods 9(8), 772.

Drummond, A.J., Rambaut, A., 2007. BEAST: Bayesian evolutionary analysis by sampling trees. BMC Evol. Biol. 7, 214.

Excoffier, L., Lischer, H.E.L., 2010. Arlequin suite ver 3.5: a new series of programs to perform population genetics analyses under Linux and Windows. Mol. Ecol. Resour. 10, 564–567.

Felsenstein, J., 2005. PHYLIP: phylogeny inference package). Department of Genome Sciences, University of Washington, Seattle.

Foley, N.M., Thong, V.D., Soisook, P., Goodman, S.M., Armstrong, K.N., Jacobs, D.S., et al., 2015. How and why overcome the impediments to resolution: lessons from rhinolophid and hipposiderid bats. Mol. Biol. Evol.32, 313–333.

Fu, Y.X., 1997. Statistical tests of neutrality of mutations against population growth, hitchhiking and background selection. Genetics 147, 915–925.

Fu, Y.X., Li, W.H., 1993. Statistical tests on neutrality of mutations. Genetics 133, 693–709.

Fuchs, J., Pons, J.-M., Pasquet, E., Raherilalao M.J., Goodman, S.M., 2007. Geographical structure of the genetic variation in the Malagasy scops-owl (*Otus rutilus* s.l.) inferred from mitochondrial sequence data. The Condor 109, 409–418.

Fuchs, J., Parra, J. L., Goodman, S.M., Raherilalao, M.J., VanDerWal, J., Bowie, R.C.K., 2013. Extending species distribution models to the past 120,000 years corroborates the lack of phylogeographic structure in the crested drongo (*Dicrurus forficatus*) from Madagascar. Biological Journal of the Linnean Society108, 658–676.

Goodman, S.M., 2006. Hunting of Microchiroptera in extreme south-western Madagascar. Oryx, 40, 225–228.

Goodman, S.M., Jungers, W.L., 2014. Extinct Madagascar: Picturing the Island's Past. The University of Chicago Press, Chicago.

Goodman, S.M., Ramasindrazana, B., 2013. Bats or the order Chiroptera, in: Goodman, S.M., Raherilalao M.J. (Eds.), Atlas of Selected Land Vertebrates of Madagascar. Association Vahatra, Antananarivo, pp. 169–209.

Goodman, S.M., Chan, L.M., Nowak, M.D., Yoder, A.D., 2010a. Phylogeny and biogeography of western Indian Ocean *Rousettus* (Chiroptera: Pteropodidae). J. Mamm. 91, 593–606.

Goodman, S.M., Maminirina, C.P., Bradman, H.M., Christidis, L., Appleton, B., 2010b. Patterns of morphological and genetic variation in the endemic Malagasy bat *Miniopterus gleni* (Chiroptera: Miniopteridae), with the description of a new species, *M. griffithsi*. J. Zoolog. Syst. Evol. Res. 48, 75–86.

Goodman, S.M., Schoeman, M.C., Rakotoarivelo, A., Willows-Munro, S., 2016. How many species of *Hipposideros* have occurred on Madagascar since the Late Pleistocene? Zool. J. Linnean Soc. doi: 10.1111/zoj.12368

Hall, T.A., 1999. BioEdit: a user-friendly biological sequence alignment editor and analysis program for Windows 95/98/NT. Nucleic Acids Symp. Ser. 41, 95–98.

Hand, S.J., 1993. First skull of a species of *Hipposideros* (*Brachipposideros*) (Microchiroptera: Hipposideridae) from Australian Miocene sediments. Mem. Queensland Mus. 33,179–192.

Hand, S.J., 1997.*Hipposideros bernardsigei*, a new hipposiderid (Microchiroptera) from the Miocene of Australia and a reconsideration of the monophyly of related species groups. Münch. Geowiss. Abh. A34, 73–92.

Hewitt, G., 2000. The genetic legacy of the Quaternary ice ages. Nature 405, 907–913.

Irwin, D.M., Kocher, T.D., Wilson, A.C., 1991. Evolution of the cytochrome b gene of mammals. J. Mol. Evol. 32, 128–144.

Jenkins, R.K.B., Racey P.A., 2008. Bats as bushmeat in Madagascar. Madagascar Conservation & Development 3(1), 22–30.

Jones, G., Rayner, M.V., 1989. Optimal flight speed in pipistrelle bats, *Pipistrellus pipistrellus*. In: Hanák, V., Horáček, I., Gaisler, J. (Eds.), European bat research 1987. Charles University Press, Prague.

Jønsson, K.A., Fabre, P.-H., Fritz, S.A., Etienne, R.S., Ricklefs, R.E., Jørgensen, T.B., et al., 2012. Ecological and evolutionary determinants for the adaptive radiation of the Madagascan vangas. Proc. Natl. Acad. Sci. USA 109, 6620–6625.

Lamb, J.M., Ralph, T.M.C., Naidoo, T., Taylor, P.J., Ratrimomanarivo, F., Stanley, W.T., Goodman, S.M., 2011.Toward a molecular phylogeny for the Molossidae (Chiroptera) of Afro-Malagasy region. Acta Chiropterologica 13, 1–16.

Lamb, J.M., Naidoo, T., Taylor, P.J., Napier, M., Ratrimomanarivo, F., Goodman, S.M., 2012. Genetically and geographically isolated lineages of a tropical bat (Chiroptera, Molossidae) show demographic stability over the late Pleistocene. Biol. J. Linn. Soc. 106, 18–40.

Librado, P., Rozas, J., 2009. DnaSP ver. 5: a software for comprehensive analysis of DNA polymorphism data. Bioinformatics 25, 1451–1452.

Lin, A.-Q., Csorba, G., Li, L.-F., Jiang, T.-L., Lu, G.-J., Thong, V. D., Soisook, P., Sun, K.-P., Feng, J., 2014. Phylogeography of *Hipposideros armiger* (Chiroptera: Hipposideridae) in the Oriental Region: the contribution of multiple Pleistocene glacial refugia and intrinsic factors to contemporary population genetic structure. J. Biogeogr. 41, 317–327.

Lu, G., Lin, A., Luo, J., Blondel, D.V., Meiklejohn, K.A, Sun, K., et al. 2013. Phylogeography of the Ricketts big-footed bat, *Myotis pilosus* (Chiroptera: Vespertilionidae): a novel pattern of genetic structure of bats in China. BMC Evol. Biol. 13, 241.

Matsumoto, K., Burney, D.A., 1994. Late Holocene environments at lake Mitsinjo, northwestern Madagascar. The Holocene 4, 16–24.

McWilliam, A.N., 1982. Adaptive responses to seasonality in four species of insectivorous bats in coastal Kenya. Ph.D. Thesis. University of Aberdeen.

Miller, M.P., 2005. Alleles In Space (AIS): Computer Software for the Joint Analysis of Interindividual Spatial and Genetic Information. J. Hered. 96 (6), 722-724.

Myers, N., Mittermeier, R., Mittermeier, C., da Fonseca, G., Kent, J., 2000. Biodiversity hotspots for conservation priorities. Nature 403, 853–858.

Noonan, B., Chippindale, P.T., 2006. Vicariant origin of Malagasy reptiles supports late Cretaceous Antarctic land bridge. Am. Natur. 168, 730–741.

Norberg, U.M., Rayner, J.M.V., 1987. Ecological morphology and flight in bats (Mammalia: Chiroptera): wing adaptations, flight performance, foraging strategy and echolocation. Philos. Trans. R. Soc. Lond. B. Biol. Sci. 316, 335–427.

Palsböll, P.J., Berube, M., Allendorf, F.W., 2007. Identification of management units using population genetic data. Trends Ecol. Evol. 22(1), 11–16.

Pearson, R.G., Raxworthy, C.J., 2009. The evolution of local endemism in Madagascar: watershed versus climatic gradient hypotheses evaluated by null biogeographic models. Evol. 63, 959–967. doi: 10.1111/j.1558-5646.2008.00596.x

Posada, D., Crandall, K.A., 1998. Modeltest: testing the model of DNA substitution. Bioinformatics 14, 817–818.

Raharinantenaina, I.M.O., Kofoky, A.M., Mbohoahy, T., Andriafidison, D., Randrianandrianina, F., Ramilijaona, O.R., Jenkins, R.K.B., 2008. *Hipposideros commersoni* (E. Geoffory, 1813, Hipposideridae) roosting in trees in littoral forest, south-eastern Madagascar. African Bat Conservation News 15, 2–3.

Rakotoarivelo, A.R., Ranaivoson, N., Ramilijaona, O.R., Kofoky, A.F., Racey, P.A., Jenkins, R.K.B., 2007. Seasonal food habits of five sympatric forest microchiropterans in western Madagascar. J. Mamm. 88, 959–966.

Rakotoarivelo, A.R., Ralisata, M., Ramilijaona, O.R., Rakotomalala, M.R., Racey, P.A., Jenkins, R.K.B., 2009. The food habits of a Malagasy giant: *Hipposideros commersoni* (E. Geoffroy, 1813). Afr. J. Ecol. 47(3), 283–288.

Rakotoarivelo, A.R., Willows-Munro, S., Schoeman, M. C., Lamb, J.M., Goodman, S.M., 2015. Cryptic diversity in *Hipposideros commersoni* sensu stricto (Chiroptera: Hipposideridae) in the western portion of Madagascar. BMC Evol. Biol. 15, 235–253.

Rakotondramanana, C.F., Goodman, S.M., 2011. Inventaire de chauves-souris dans la concession forestiere de Kirindy CNFEREF, Morondava, Madagascar. Malagasy Nature 5, 109–120.

Ramasindrazana, B., Goodman, S.M., 2012. Bio-écologie des chauves-souris du Parc National de Tsimanampetsotsa. 1. Identification bioacoustique et habitat préférentiel. Malagasy Nature 6, 103–116.

Ramasindrazana, B., Rakotondramanana, C.F., Schoeman, M.C., Goodman, S.M., 2015. Evidence of echolocation call divergence in *Hipposideros commersoni* sensu stricto (E. Geoffroy, 1803) from Madagascar and correlation with body size. Acta Chiropterologica 17(1), 85–94.

Rambaut, A., Suchard, M.A., Xie, D., Drummond, A.J., 2014. Tracer v1.6 [computer program]. Available from: <http://beast.bio.ed.ac.uk/Tracer>.

Ramos-Onsins, S.E., Rozas, J., 2002.Statistical properties of new neutrality tests against population growth. Mol. Biol. Evol. 19, 2092–2100.

Ranivo, J., Goodman, S.M., 2007. Variation géographique de *Hipposideros commersoni* de la zone sèche de Madagascar (Mammalia, Chiroptera, Hipposideridae). Verh. Natwiss. Ver. Hambg. 43, 35–56.

Ratrimomanarivo, F., Vivian, J., Goodman, S.M., Lamb, J., 2007. Morphological and molecular assessment of the specific status of *Mops midas* (Chiroptera: Molossidae) from Madagascar and Africa. African Zoology 42, 237–253.

Ratrimomanarivo, F., Goodman, S.M., Hoosen, N., Taylor, P.J., Lamb, J., 2008. Morphological and molecular variation in *Mops leucostigma* (Chiroptera: Molossidae) of Madagascar and the Comoros: phylogeny, phylogeography and geographic variation. Mitt. Zool. Mus. Hambg. 105, 57–101.

Ratrimomanarivo, F.H., Goodman, S.M., Taylor, P.J., Melson, B., Lamb, J., 2009a. Morphological and genetic variation in *Mormopterus jugularis* (Chiroptera: Molossidae) in different bioclimatic regions of Madagascar with natural history notes. Mammalia 73, 110–129.

Ratrimomanarivo, F.H., Goodman, S.M., Stanley, W.T., Naidoo, T., Taylor, P.J., Lamb, J., 2009b. Geographic and phylogeographic variation in *Chaerephon leucogaster* (Chiroptera: Molossidae) of Madagascar and the western Indian Ocean islands of Mayotte and Pemba. Acta Chiropterologica 11, 25–52.

Razakarivony, V., Rajemison, B., Goodman, S.M., 2005. The diet of Malagasy Microchiroptera based on stomach contents. Mammal. Biol. 70, 312–316.

Reddy, S., Driskell, A., Rabosky, D.L., Hackett, S.J., Schulenberg, T.S., 2012. Diversification and the adaptive radiation of the vangas of Madagascar.Proc. R. Soc. Lond. B Biol. Sci. 279, 2062–2071.

Rogers, A.R., Harpending, H., 1992. Population growth makes waves in the distribution of pairwise genetic differences. Mol. Biol. Evol. 9 (3), 552–569.

Ronquist, F., Teslenko, M., Van der Mark, P., Ayres, D., Darling, A., Höhna, S., Larget, B., Liu, L., Suchard, M.A., Huelsenbeck, J.P., 2012. MrBayes 3.2: efficient Bayesian phylogenetic inference and model choice across a large model space. Syst. Biol. 61, 539–542.

Russell, A.L., Medellin, R.A., McCracken, G.F., 2005. Genetic variation and migration in the Mexican free-tailed bat (*Tadarida brasiliensis mexicana*). Mol. Ecol. 14, 2207–2222.

Russell, A.L., Ranivo, J., Palkovacs, E.P., Goodman, S.M., Yoder, A.D., 2007. Working at the interface of phylogenetics and population genetics: a biogeographical analysis of *Triaenops* spp. (Chiroptera: Hipposideridae). Mol. Ecol. 16, 839–851.

Russell, A.L., Goodman, S.M., Cox, M.P., 2008a. Coalescent analyses support multiple mainland-to-island dispersals in the evolution of Malagasy *Triaenops* bats (Chiroptera: Hipposideridae). J. Biogeog. 35, 995–1003.

Russell, A.L., Goodman, S.M., Fiorentino, I., Yoder, A.D., 2008b. Population genetic analysis of *Myzopoda* (Chiroptera: Myzopodidae) in Madagascar. J. Mammal. 89, 209–221.

Salzburger, W., Ewing, G.B., Von Haeseler, A. 2011.The performance of phylogenetic algorithms in estimating haplotype genealogies with migration. Mol. Ecol. 20, 1952–1963.

Samonds, K.E., 2007. Late Pleistocene bat fossils from Anjohibe Cave, northwestern Madagascar. Acta Chiropterologica 9, 39–65.

Samonds, K.E., Godfrey, L.R., Ali, J.R., Goodman, S.M., Vences, M., Sutherland, M.R., Irwin, M.T., Krause, D.W., 2012. Spatial and temporal arrival patterns of Madagascar's vertebrate fauna explained by distance, ocean currents, and ancestor type. Proc. Natl. Acad. Sci.USA 109, 5352–5357.www.pnas.org/cgi/doi/10.1073/pnas.1113993109.

Samonds, K.E., Godfrey, L.R., Ali, J.R., Goodman, S.M., Vences, M., Sutherland, M.R., Irwin, M.T., Krause, D.W., 2013. Imperfect isolation: factors and filters shaping Madagascar's extant vertebrate fauna. PLoS One 8(4): e62086. doi:10.1371/journal.pone.0062086.

Schoeman, M.C., Goodman, S.M., Ramasindrazana, B., Koubínová, D., 2015.Species interactions during diversification and community assembly in Malagasy *Miniopterus* bats. Evol. Ecol. 29, 17-47. doi: 10.1007/s10682-014-9745-4.

Sigé, B., 1988. Le gisement du Bretou (Phosphorites de Quercy, Tarn-et-Garonne, France) et sa faune de Vertèbres de l'Éocène supérieur. Palaeontographica 205, 69–102.

Tamura, K., Stecher, G., Peterson, D., Filipski, A., Kumar, S., 2013. MEGA6: Molecular Evolutionary Genetics Analysis Version 6.0. Mol. Biol. Evol. 30, 2725–2729.

Teeling, E.C., Springer, M.S., Madsen, O., Bates, P., O'Brien, S.J., Murphy, W.J., 2005. A molecular phylogeny for bats Illuminates biogeography and the fossil record. Science 307, 580-584.

Thompson, J.D., Gibson, T.J., Plewniak, F., Jeanmougin, F., Higgins, D.G., 1997. The CLUSTAL X windows interface: flexible strategies for multiple sequence alignment aided by quality analysis tools. Nucleic Acids Res. 25(24), 4876–4882.

Thong, V.D., Puechmaille, S.J., Denzinger, A., Bates, P.J.J., Dietz, C., Csorba, G., Soisook, P., Teeling, E.C., Matsumura, S., Furey, N.M., Schnitzler, H.U., 2012. Systematics of the *Hipposideros turpis* complex and a description of a new subspecies from Vietnam. Mammal Review 42, 166–192.

Vaughan, T.A., 1977. Foraging behaviour of the giant leaf-nosed bat (*Hipposideros commersoni*). East Afr. Wildl. J. 15, 237–249.

Vences, M., Wollenberg, K.C., Vieites, D.R., Lees, D.C., 2009. Madagascar as a model region of species diversification. Trends Ecol. Evol. 24, 456–465.

Wesselman, H.B., 1984. The Omo Micromammals: Systematics and Paleoecology of Early Man Sites from Ethiopia. Karger, New York.

Weyeneth, N., Goodman, S.M., Ruedi, M., 2011. Do diversification models of Madagascar's biota explain the population structure of the endemic bat *Myotis goudoti* (Chiroptera: Vespertilionidae)? J, Biogeogr. 38, 44–54. doi: 10.1111/j.1365-2699.2010.02393.x

Wilkinson, G.S., Chapman, A.M., 1991. Length and sequence variation in evening bat d-loop mtDNA. Genetics 128, 607–617.

Wilmé, L., Goodman, S.M., Ganzhorn, J.U., 2006. Biogeographic evolution of Madagascar's microendemic biota. Science 312, 1063–1065.

Xu, L., He, F., Shen, C., Jiang, T., Shi, L., Sun, K., Berquist, S.W., Feng, J., 2010. Phylogeography and population genetic structure of the great leaf-nosed bat (*Hipposideros armiger*) in China. J. Hered. 101 (5), 562-572.

Yoder, A.D., Nowak, M.D., 2006. Has vicariance or dispersal been the predominant force in Madagascar? Only time will tell. Annu. Rev. Ecol. System. 37, 405–431.

Zwickl, D.J., 2006. Genetic algorithm approaches for the phylogenetic analysis of large biological sequence datasets under the maximum likelihood criterion. Ph.D. dissertation, The University of Texas.

Supplementary Table S1:

S1 Table: List of specimens and associatedGenbank accession numbers for the mtDNA control region (CR) and cytochrome b (Cyt b) sequences used in the present study. PN = Parc National, RS = Réserve Spéciale, SF = Station Forestière. Collection numbers are the catalogue numbers of the respective museum: FMNH - Field Museum of Natural History, AMNH -American Museum of Natural History, and UADBA - Université d'Antananarivo, Département de Biologie Animale.

Species	Specimen number	Province/Locality	GenBank numbers	
			CR	*Cyt b*
H. commersoni	FMNH 183978	Antsiranana/Lac Sahaka, Foret d'Analabe	KU302200	KT896149
H. commersoni	FMNH 183979	Antsiranana/Lac Sahaka, Foret d'Analabe	KU302201	KT896150
H. commersoni	FMNH 183980	Antsiranana/Montagne de Français, Foret d'Ampitiliantsambo	KT371766	KT5838013
H. commersoni	FMNH 183981	Antsiranana/Montagne de Français, Foret d'Ampitiliantsambo	KU302208	KT896157
H. commersoni	FMNH 188574	Antsiranana/Nosy Be, Centre National de Recherches Océanographiques, 1.5 km E Hell-ville	KU302190	KT896139
H. commersoni	UADBA 32987	Antsiranana/PN d'Ankarana, 2.6 km E Andrafiabe, in forest near Andrafiabe Cave	KT371768	KT5838014
H. commersoni	UADBA 32988	Antsiranana/PN d'Ankarana, 2.6 km E Andrafiabe, in forest near Andrafiabe Cave	KU302234	KT896183
H. commersoni	UADBA 32989	Antsiranana/PN d'Ankarana, 2.6 km E Andrafiabe, in forest near Andrafiabe Cave	KU302235	KT896184
H. commersoni	FMNH 221307	Antsiranana/PN d'Ankarana, 2.6 km E Andrafiabe, in forest near Andrafiabe Cave	KU302236	KT896185
H. commersoni	FMNH 221308	Antsiranana/PN d'Ankarana, 2.6 km E Andrafiabe, in forest near Andrafiabe Cave	KT371769	KT5838029
H. commersoni	FMNH 169722	Antsiranana/PN d'Ankarana, 2.6 km E Andrafiabe, near Andrafiabe Cave	KU302124	KT896073
H. commersoni	FMNH 169707	Antsiranana/PN d'Ankarana, 2.6 km E Andrafiabe, near Andrafiabe Cave	KT371750	KT5838022
H. commersoni	FMNH 169708	Antsiranana/PN d'Ankarana, 2.6 km E Andrafiabe, near Andrafiabe Cave	KU302130	KT896079

H. commersoni	FMNH 213588	Antsiranana/PN d'Ankarana, 2.6 km E Andrafiabe, near Andrafiabe Cave	KU302196	KT896145
H. commersoni	FMNH 177385	Antsiranana/PN d'Ankarana, 3.5 km ESE Andrafiabe, Grotte d'Andrafiabe	KU302197	KT896146
H. commersoni	FMNH 177386	Antsiranana/PN d'Ankarana, 3.5 km ESE Andrafiabe, Grotte d'Andrafiabe	KU302198	KT896147
H. commersoni	FMNH 177387	Antsiranana/PN d'Ankarana, 3.5 km ESE Andrafiabe, Grotte d'Andrafiabe	KU302199	KT896148
H. commersoni	FMNH 176277	Antsiranana/PN d'Ankarana, 3.5 km SE Andrafiabe (village)	KU302163	KT896112
H. commersoni	FMNH 156340	Antsiranana/PN de la Montagne d'Ambre, Grande Lac, 12 km SW Joffreville	KU302123	KT896072
H. commersoni	FMNH 154601	Antsiranana/PN de la Montagne d'Ambre, 5.5 km SW Joffreville	KU302129	KT896078
H. commersoni	FMNH 178803	Antsiranana/RS d'Analamerana, Grotte de Bazaribe, 3.6 km SE Menagisy	KU302165	KT896114
H. commersoni	FMNH 178804	Antsiranana/RS d'Analamerana, Grotte de Bazaribe, 3.6 km SE Menagisy	KU302166	KT896115
H. commersoni	FMNH 178805	Antsiranana/RS d'Analamerana, Grotte de Bazaribe, 3.6 km SE Menagisy	KU302167	KT896116
H. commersoni	FMNH 178806	Antsiranana/RS d'Analamerana, Grotte de Bazaribe, 3.6 km SE Menagisy	KT371755	KT5838016
H. commersoni	FMNH 178807	Antsiranana/RS d'Analamerana, Grotte de Bazaribe, 3.6 km SE Menagisy	KU302168	KT896117
H. commersoni	FMNH 178808	Antsiranana/RS d'Analamerana, Grotte de Bazaribe, 3.6 km SE Menagisy	KT371756	KT5838017
H. commersoni	FMNH 178809	Antsiranana/RS d'Analamerana, Grotte de Bazaribe, 3.6 km SE Menagisy	KT371757	KT5838018
H. commersoni	FMNH 178810	Antsiranana/RS d'Analamerana, Grotte de Bazaribe, 3.6 km SE Menagisy	KT371758	KT5838019
H. commersoni	FMNH 178811	Antsiranana/RS d'Analamerana, Grotte de Bazaribe, 3.6 km SE Menagisy	KT371759	KT5838020

H. commersoni	FMNH 178812	Antsiranana/RS d'Analamerana, Grotte de Bazaribe, 3.6 km SE Menagisy	KU302169	KT896118
H. commersoni	FMNH 178813	Antsiranana/RS d'Analamerana, Grotte de Bazaribe, 3.6 km SE Menagisy	KU302170	KT896119
H. commersoni	FMNH 178814	Antsiranana/RS d'Analamerana, Grotte de Bazaribe, 3.6 km SE Menagisy	KU302171	KT896120
H. commersoni	FMNH 178815	Antsiranana/RS d'Analamerana, Grotte de Bazaribe, 3.6 km SE Menagisy	KT371760	KT5838021
H. commersoni	FMNH 151706	Fianarantsoa/Ambalavao, 43 km S, Andringitra Reserve	KU302128	KT896077
H. commersoni	FMNH 175962	Fianarantsoa/just outside PN de l'Isalo, along Menamaty River, 8 km N Ranohira (RN7)	KU302144	KT896093
H. commersoni	FMNH 175963	Fianarantsoa/just outside PN de l'Isalo, along Menamaty River, 8 km N Ranohira (RN7)	KU302145	KT896094
H. commersoni	FMNH 175964	Fianarantsoa/just outside PN de l'Isalo, along Menamaty River, 8 km N Ranohira (RN7)	KU302146	KT896095
H. commersoni	FMNH 175965	Fianarantsoa/just outside PN de l'Isalo, along Menamaty River, 8 km N Ranohira (RN7)	KU302147	KT896096
H. commersoni	FMNH 175966	Fianarantsoa/just outside PN de l'Isalo, along Menamaty River, 8 km N Ranohira (RN7)	KT371751	KT5838023
H. commersoni	FMNH 175967	Fianarantsoa/just outside PN de l'Isalo, along Menamaty River, 8 km N Ranohira (RN7)	KU302148	KT896097
H. commersoni	FMNH 217940	Fianarantsoa/PN de l'Isalo, 10,5 km SW Ranohira, Hotel Jardin du Roi	KT371767	KT5838031

H. commersoni	UADBA 50267	Fianarantsoa/PN de l'Isalo, 3,8 km NW Ranohira along Namaza River	KU302221	KT896170
H. commersoni	FMNH 218012	Fianarantsoa/PN de l'Isalo, 3,8 km NW Ranohira along Namaza River	KU302222	KT896171
H. commersoni	UADBA 50268	Fianarantsoa/PN de l'Isalo, 3,8 km NW Ranohira along Namaza River	KU302223	KT896172
H. commersoni	FMNH 175968	Fianarantsoa/PN de l'Isalo, along Sahanafa River, 28 km SE Berenty-Betsileo	KU302149	KT896098
H. commersoni	FMNH 175969	Fianarantsoa/PN de l'Isalo, along Sahanafa River, 28 km SE Berenty-Betsileo	KU302150	KT896099
H. commersoni	FMNH 175971	Fianarantsoa/PN de l'Isalo, along Sahanafa River, 28 km SE Berenty-Betsileo	KU302151	KT896100
H. commersoni	FMNH 175972	Fianarantsoa/PN de l'Isalo, along Sahanafa River, 28 km SE Berenty-Betsileo	KU302152	KT896101
H. commersoni	FMNH 175973	Fianarantsoa/PN de l'Isalo, along Sahanafa River, 28 km SE Berenty-Betsileo	KU302153	KT896102
H. commersoni	FMNH 175974	Fianarantsoa/PN de l'Isalo, along Sahanafa River, 28 km SE Berenty-Betsileo	KU302154	KT896103
H. commersoni	FMNH 175975	Fianarantsoa/PN de l'Isalo, along Sahanafa River, 28 km SE Berenty-Betsileo	KU302155	KT896104
H. commersoni	FMNH 175976	Fianarantsoa/PN de l'Isalo, along Sahanafa River, 28 km SE Berenty-Betsileo	KU302156	KT896105
H. commersoni	FMNH 175977	Fianarantsoa/PN de l'Isalo, along Sahanafa River, 28 km SE Berenty-Betsileo	KU302157	KT896106
H. commersoni	FMNH 175961	Fianarantsoa/PN de l'Isalo, Canyon des Singes (Andranokova), 2 km W Ranohira bas	KU302143	KT896092
H. commersoni	UADBA 50270	Fianarantsoa/PN de l'Isalo, Grotte de Bekapity	KU302224	KT896173
H. commersoni	UADBA 50271	Fianarantsoa/PN de l'Isalo, Grotte de Bekapity	KU302225	KT896174

H. commersoni	UADBA 50272	Fianarantsoa/PN de l'Isalo, Grotte de Bekapity	KU302226	KT896175
H. commersoni	UADBA 50273	Fianarantsoa/PN de l'Isalo, Grotte de Bekapity	KU302227	KT896176
H. commersoni	UADBA 50274	Fianarantsoa/PN de l'Isalo, Grotte de Bekapity	KU302228	KT896177
H. commersoni	FMNH 218016	Fianarantsoa/PN de l'Isalo, Grotte de Bekapity	KU302229	KT896178
H. commersoni	FMNH 218017	Fianarantsoa/PN de l'Isalo, Grotte de Bekapity	KU302230	KT896179
H. commersoni	FMNH 218018	Fianarantsoa/PN de l'Isalo, Grotte de Bekapity	KU302231	KT896180
H. commersoni	FMNH 218019	Fianarantsoa/PN de l'Isalo, Grotte de Bekapity	KU302232	KT896181
H. commersoni	FMNH 218020	Fianarantsoa/PN de l'Isalo, Grotte de Bekapity	KU302233	KT896182
H. commersoni	FMNH 184029	Mahajanga/4.2 km SE Marovaza, in cave	KU302189	KT896138
H. commersoni	FMNH 184030	Mahajanga/Berivotra, village	KT371765	KT5838012
H. commersoni	FMNH 184886	Mahajanga/Berivotra, village	KU302204	KT896153
H. commersoni	FMNH 184887	Mahajanga/Berivotra, village	KU302205	KT896154
H. commersoni	FMNH 187786	Mahajanga/Forêt d'Ampidirabe, 16.3 km N Antsalova	KU302214	KT896163
H. commersoni	FMNH 209236	Mahajanga/Forêt de Beanka, cave along Kimanambolo River	KU302195	KT896144
H. commersoni	FMNH 187784	Mahajanga/Forêt de Mamakibetro, 18.3 km NNE Ansalova	KU302212	KT896161
H. commersoni	FMNH 187785	Mahajanga/Forêt de Mamakibetro, 18.3 km NNE Ansalova	KU302213	KT896162

H. commersoni	FMNH 209108	Mahajanga/Grotte d'Anjohibe, 3.7 km NE Antanamarina	KU302191	KT896140
H. commersoni	FMNH 209109	Mahajanga/Grotte d'Anjohibe, 3.7 km NE Antanamarina	KU302192	KT896141
H. commersoni	FMNH 209110	Mahajanga/Grotte d'Anjohibe, 3.7 km NE Antanamarina	KU302193	KT896142
H. commersoni	FMNH 209111	Mahajanga/Grotte d'Anjohibe, 3.7 km NE Antanamarina	KU302194	KT896143
H. commersoni	UADBA 32916	Mahajanga/Grotte d'Anjohibe, 3.7 km NE Antanamarina	KT371770	KT5838030
H. commersoni	FMNH 184027	Mahajanga/Grotte d'Ankelimahogo, 18.5 km S Anjajavy village	KU302179	KT896128
H. commersoni	FMNH 184028	Mahajanga/Marovaza	KU302188	KT896137
H. commersoni	FMNH 175776	Mahajanga/PN du Tsingy de Namoroka, near source of Mandevy River, 32 km NW Andranomavo	KU302138	KT896087
H. commersoni	FMNH 175777	Mahajanga/PN du Tsingy de Namoroka, near source of Mandevy River, 32 km NW Andranomavo	KT371750	KT5838022
H. commersoni	FMNH 175778	Mahajanga/PN du Tsingy de Namoroka, near source of Mandevy River, 32 km NW Andranomavo	KU302139	KT896088
H. commersoni	FMNH 178558	Mahajanga/PN du Tsingy de Namoroka, Site Andriabe, 2 km SE Namoroka village	KU302164	KT896113
H. commersoni	FMNH 194580	Mahajanga/RS d'Ambohijanahary, Mahajeby Forest, 21.8 km ESE de Beravina	KU302215	KT896164
H. commersoni	FMNH 177299	Mahajanga/SF d'Ampirojoa	KU302160	KT896109

H. commersoni	FMNH 177300	Mahajanga/SF d'Ampirojoa	KU302161	KT896110
H. commersoni	FMNH 177301	Mahajanga/SF d'Ampirojoa	KU302162	KT896111
H. commersoni	FMNH 177302	Mahajanga/SF d'Ampirojoa	KT371754	KT5838025
H. commersoni	FMNH 183982	Toamasina/Foulepointe, Forêt d'Analalava	KU302202	KT896151
H. commersoni	FMNH 183983	Toamasina/Marovaza, in cave	KU302203	KT896152
H. commersoni	FMNH 179200	Toamasina/SF de Tampolo, 10 km NW Fenerive-Est	KU302172	KT896121
H. commersoni	FMNH 179201	Toamasina/SF de Tampolo, 10 km NW Fenerive-Est	KU302173	KT896122
H. commersoni	FMNH 179202	Toamasina/SF de Tampolo, 10 km NW Fenerive-Est	KU302174	KT896123
H. commersoni	FMNH 194633	Toliara/District de Manja, Beronto Forest, 11 km SSE Ankiliabo	KU302216	KT896165
H. commersoni	FMNH 194634	Toliara/District de Manja, Beronto Forest, 11 km SSE Ankiliabo	KU302217	KT896166
H. commersoni	FMNH 176489	Toliara/Fiherenana	KU302206	KT896155
H. commersoni	FMNH 176156	Toliara/Forêt des Mikea, 16 km W Vorehy	KU302209	KT896158
H. commersoni	FMNH 176157	Toliara/Forêt des Mikea, 16 km W Vorehy	KU302210	KT896159
H. commersoni	FMNH 176164	Toliara/Forêt des Mikea, 7.5 km NE Tsifota	KU302158	KT896107
H. commersoni	FMNH 176163	Toliara/Forêt des Mikea, 7.5 km NE Tsifota	KU302159	KT896108
H. commersoni	FMNH 176158	Toliara/Forêt des Mikea, 8.4 km SSE Befandefa	KU302211	KT896160

H. commersoni	FMNH 176155	Toliara/Forêt des Mikea, 9.5 km W Ankiloaka	KT371753	KT5838024
H. commersoni	FMNH 184169	Toliara/Grotte d'Androimpano, 4.2 km NE Itampolo (village), on old road to Ejeda	KU302180	KT896129
H. commersoni	FMNH 184170	Toliara/Grotte d'Androimpano, 4.2 km NE Itampolo (village), on old road to Ejeda	KT371763	KT5838028
H. commersoni	FMNH 184171	Toliara/Grotte d'Androimpano, 4.2 km NE Itampolo (village), on old road to Ejeda	KU302181	KT896130
H. commersoni	FMNH 184172	Toliara/Grotte d'Androimpano, 4.2 km NE Itampolo (village), on old road to Ejeda	KU302182	KT896131
H. commersoni	FMNH 184174	Toliara/Grotte d'Androimpano, 4.2 km NE Itampolo (village), on old road to Ejeda	KU302183	KT896132
H. commersoni	FMNH 184175	Toliara/Grotte d'Androimpano, 4.2 km NE Itampolo (village), on old road to Ejeda	KU302184	KT896133
H. commersoni	FMNH 184176	Toliara/Grotte d'Androimpano, 4.2 km NE Itampolo (village), on old road to Ejeda	KU302185	KT896134
H. commersoni	FMNH 184177	Toliara/Grotte d'Androimpano, 4.2 km NE Itampolo (village), on old road to Ejeda	KU302186	KT896135
H. commersoni	FMNH 184178	Toliara/Grotte d'Androimpano, 4.2 km NE Itampolo (village), on old road to Ejeda	KU302187	KT896136

H. commersoni	UADBA 32378	Toliara/Grotte de Tanambao, 0.75 km E St. Augustin	KU302219	KT896168
H. commersoni	UADBA 32379	Toliara/Grotte de Tanambao, 0.75 km E St. Augustin	KU302220	KT896169
H. commersoni	UADBA 33692	Toliara/Kirindy Forest (CNFEREF)	KU302237	KT896186
H. commersoni	UADBA 33693	Toliara/Kirindy Forest (CNFEREF)	KU302238	KT896187
H. commersoni	UADBA 33694	Toliara/Kirindy Forest (CNFEREF)	KU302239	KT896188
H. commersoni	UADBA 33695	Toliara/Kirindy Forest (CNFEREF)	KU302240	KT896189
H. commersoni	UADBA 33696	Toliara/Kirindy Forest (CNFEREF)	KU302241	KT896190
H. commersoni	UADBA 33697	Toliara/Kirindy Forest (CNFEREF)	KU302242	KT896191
H. commersoni	UADBA 33698	Toliara/Kirindy Forest (CNFEREF)	KU302243	KT896192
H. commersoni	UADBA 33699	Toliara/Kirindy Forest (CNFEREF)	KU302244	KT896193
H. commersoni	UADBA 33700	Toliara/Kirindy Forest (CNFEREF)	KU302245	KT896194
H. commersoni	UADBA 33701	Toliara/Kirindy Forest (CNFEREF)	KU302246	KT896195
H. commersoni	UADBA 33702	Toliara/Kirindy Forest (CNFEREF)	KU302247	KT896196
H. commersoni	FMNH 222747	Toliara/Kirindy Forest (CNFEREF)	KU302248	KT896197
H. commersoni	UADBA 32376	Toliara/Mikea, Grotte de Maki near Hôtel La Mangrove	KU302218	KT896167
H. commersoni	FMNH 176052	Toliara/PN de Kirindy Mite, 0.75 km SW Manahy	KU302140	KT896089

H. commersoni	FMNH 176053	Toliara/PN de Kirindy Mite, 0.75 km SW Manahy	KU302141	KT896090
H. commersoni	FMNH 176054	Toliara/PN de Kirindy Mite, 0.75 km SW Manahy	KU302142	KT896091
H. commersoni	FMNH 173151	Toliara/PN de Tsimanampetsotsa, 6.5 km NE Efoetse, near Mitoho Cave	KU302136	KT896085
H. commersoni	FMNH 173162	Toliara/PN de Tsimanampetsotsa, 6.5 km NE Efoetse, near Mitoho Cave	KU302137	KT896086
H. commersoni	FMNH 183929	Toliara/PN de Tsimanampetsotsa, 6.5 km NE Efoetse, near Mitoho Cave	KU302175	KT896124
H. commersoni	FMNH 183930	Toliara/PN de Tsimanampetsotsa, 6.5 km NE Efoetse, near Mitoho Cave	KU302176	KT896125
H. commersoni	FMNH 183931	Toliara/PN de Tsimanampetsotsa, 6.5 km NE Efoetse, near Mitoho Cave	KU302177	KT896126
H. commersoni	FMNH 183932	Toliara/PN de Tsimanampetsotsa, 6.5 km NE Efoetse, near Mitoho Cave	KT371761	KT583826
H. commersoni	FMNH 183933	Toliara/PN de Tsimanampetsotsa, 6.5 km NE Efoetse, near Mitoho Cave	KU302178	KT896127
H. commersoni	FMNH 183934	Toliara/PN de Tsimanampetsotsa, 6.5 km NE Efoetse, near Mitoho Cave	KT371762	KT5838027
H. commersoni	FMNH 172760	Toliara/PN du Tsingy de Bemaraha, 3.5 km E Bekopaka	KU302135	KT896084
H. commersoni	FMNH 172745	Toliara/PN du Tsingy de Bemaraha, Ankidrodroa, 2.5 km NE Bekopaka	KU302125	KT896074
H. commersoni	FMNH 172747	Toliara/PN du Tsingy de Bemaraha, Ankidrodroa, 2.5 km NE Bekopaka	KU302126	KT896075
H. commersoni	FMNH 172748	Toliara/PN du Tsingy de Bemaraha, Ankidrodroa, 2.5 km NE Bekopaka	KU302127	KT896076
H. commersoni	FMNH 172755	Toliara/PN du Tsingy de Bemaraha, Ankidrodroa, 2.5 km NE Bekopaka	KU302131	KT896080
H. commersoni	FMNH 172756	Toliara/PN du Tsingy de Bemaraha, Ankidrodroa, 2.5 km NE Bekopaka	KU302132	KT896081

H. commersoni	FMNH 172757	Toliara/PN du Tsingy de Bemaraha, Ankidrodroa, 2.5 km NE Bekopaka	KU302133	KT896082
H. commersoni	FMNH 172758	Toliara/PN du Tsingy de Bemaraha, Ankidrodroa, 2.5 km NE Bekopaka	KU302134	KT896083
H. commersoni	FMNH 177371	Toliara/Ranobe	KU302207	KT896156

Supplementary Figure S2:

S2 Fig. Bayesian phylogram based on mtDNA control region (CR) and Cytochrome b (*Cyt b*) data drawn from 146 individual *Hipposideros commersoni*. Nodal support values are represented as Bayesian posterior probability/likelihood bootstrap percent (*=posterior probability values ≥ 0.50 and #= likelihood bootstrap percent ≥ 50).

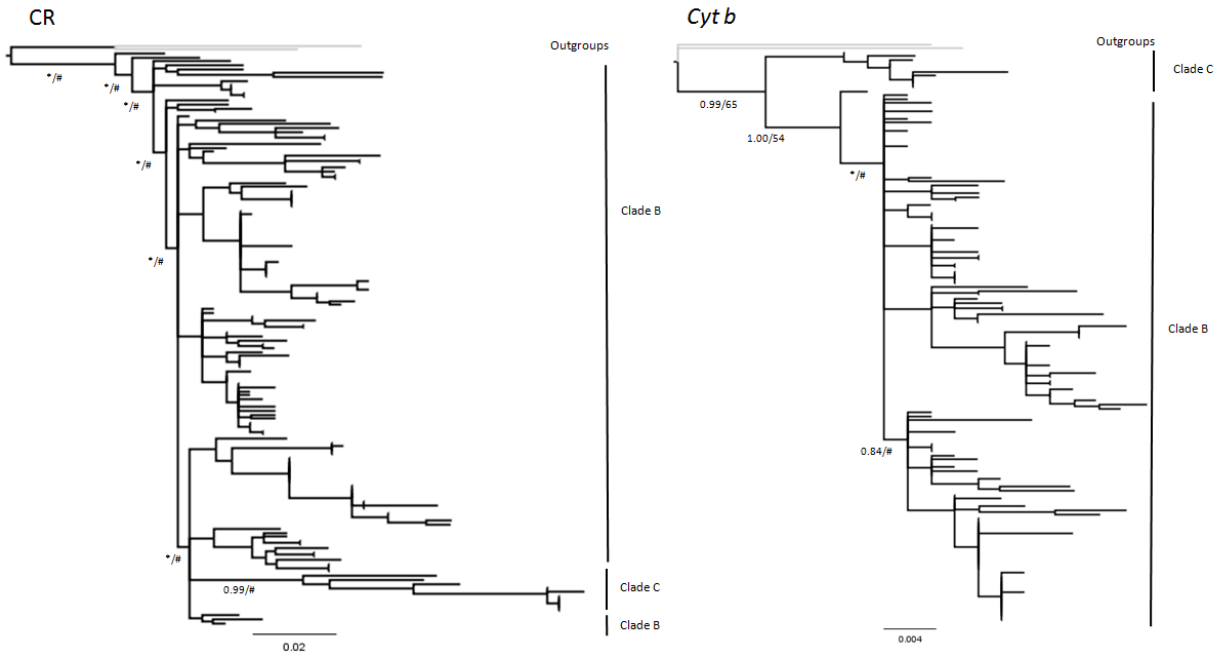

SUMMARY AND SYNTHESIS

The present thesis is composed of three different studies, the results of which are part of original scientific papers. The first paper was published in *BMC Evolutionary Biology*, the second paper is in press in *Zoological Journal of the Linnean Society* with anticipated publication in April 2016, and the third will soon be submitted to *Molecular Phylogenetics and Evolution*.

The focus of this thesis was to study the phylogenetics and the evolutionary history of Malagasy *Hipposideros* using a combination of molecular data (mitochondrial and nuclear) and craniodental morphology. These approaches were used to provide greater insight to the phylogenetics and phylogeography of the *H. commersoni* species complex on Madagascar. The type specimen of this taxon is from Madagascar.

The primary aims of this thesis were to examine:

(i) The phylogenetics and the evolutionary history of the *H. commersoni* species complex on Madagascar, particularly the western portion.
(ii) The taxonomy of Malagasy *Hipposideros*, specifically to examine the possible presence of a cryptic species.
(iii) The phylogeography and population genetics of *H. commersoni* sensu stricto on Madagascar.

Chapter 1 combines evidence from molecular (mtDNA and ncDNA) and morphological characters to provide support for the reciprocal monophyly of several independently evolving lineages within the *H. commersoni* species group occurring in eastern Africa and nearby islands, as well on Madagascar. The primary aim was to investigate the evolutionary history and systematic relationships of Malagasy populations currently assigned to *H. commersoni*, as well as African populations currently placed within the *H. commersoni* species group. Two individuals from southern Madagascar form a well-supported monophyletic group, basal to African *H. vittatus* and *H. gigas*, and separate from the balance of Malagasy *H. commersoni*; a single origin of this species complex on the island is not supported. The long branches separating these clades ranged from 2.6% to 3.2 % (uncorrected sequence divergence), revealing relatively deep divergent evolutionary trajectories of several million years based on molecular clock inferences. The results strongly suggest that previous taxonomic treatments of

the species group underestimated taxonomic diversity of *H. commersoni*, sensu stricto and that a cryptic species appears to be present.

Chapter 2 picks up where Chapter 1 ended and evaluates if a cryptic species of *Hipposideros* exists on Madagascar. The main focus is a molecular analysis of Malagasy and certain African populations of *Hipposideros* belonging to the *commersoni* species group overlaid on morphology. Cytochrome *b* based cladogenesis recovered one well supported clade that was notably divergent from other individuals of Malagasy *H. commersoni*, separated by 9% to 11% average uncorrected sequence divergence. The hypothesized existence of a cryptic *Hipposideros* species on the island was supported by the molecular data. The divergent clade has been described as new to science, *H. cryptovalorona*; known from two sites in the south (within the Parc National de l'Isalo and near Itampolo). It is smaller on average than *H. commersoni* for a few external and craniodental measurements. In order to resolve the taxonomy of this group, it was necessary to name a neotype for *H. commersoni* (Geoffroy St. Hilaire, 1813). Moreover, we evaluated, based on craniodental morphology, if a late Pleistocene taxon, *H. besaoka*, described from subfossils collected in Anjohibe Cave, northwestern Madagascar, is a valid species and the possibility that it is still extant. We conclude that it is a bona fide species and most importantly in the context of our taxonomic revision, morphologically distinct from *H. cryptovalorona.*

In order to examine fine scale patterns of phylogeographic variation in *H. commersoni* sensu stricto, two mitochondrial markers (hypervariable control region and cytochrome *b*) were used, as well as incorporating broader geographical coverage and larger sample size (Chapter 3). Bayesian clustering analysis showed that *H. commersoni* sensu stricto comprised four main lineages: B1, B2, B3 and C. The most recent common ancestor of *H. commersoni* was dated to 3.33 million years ago or the mid-Pliocene. Population expansion events were inferred for groups B1, B2 and B3 from approximately 63,732 (group B1) to 3,396 years BP (group B2). Conflicting results were obtained from Bayesian clustering and AMOVA analyses. BAPS revealed population genetic with a marked split between the northern clade C and the groups of B. On the other hand, AMOVA analyses revealed significant genetic variance found within populations. Sequence data indicated that genetic subdivisions failed to support an isolation-by-distance model. Lineage dispersal, genetic divergence and expansion events of *H. commersoni* are likely to be associated with Plio-Pleistocene climate fluctuations. Our data indicate the northern and the central western regions of Madagascar may have acted as refugia for this species during the Plio-Pleistocene, specifically periods of cooler and drier climate conditions. Hence, based on the mitochondrial markers used herein, the best manner to explain population

genetic structure in this well distributed and apparently broadly dispersing species, is that in the recent geological past populations were isolated and underwent some level of genetic differentiation. Subsequently, these populations expanded and in numerous areas are now overlapping, which in turn has given rise to the modern structure of the clades and groups presented herein.

FUTURE RESEARCH

Our results on the phylogenetics and phylogeography of the *Hipposideroscommersoni* species complex on Madagascar are grounded mainly from maternally inherited mitochondrial data (hypervariable control region and cytochrome *b*). More informative estimation of relationships between lineages is best completed with an analysis of biparentally inherited markers. Our preliminary laboratory studies found notable difficulty in finding a suitable less conservative nuclear intron marker. The use of nuclear markers, such as microsatellites, would help to detect fine scale patterns of phylogeographic variation and gene flow between lineages. Additionally, an integrative study would provide greater insight into additional mechanisms driving the diversification of the *H. commersoni* across its distributional range on Madagascar.

APPENDICES

Appendix 1

Rakotoarivelo, A.R., Willows-Munro, S., Schoeman, M. C., Lamb, J.M., Goodman, S.M., 2015. Cryptic diversity in *Hipposideros commersoni* sensu stricto (Chiroptera: Hipposideridae) in the western portion of Madagascar. BMC Evol. Biol. 15, 235–253.

Appendix 2

Goodman, S.M., Schoeman, M.C., Rakotoarivelo, A., Willows-Munro, S., 2016. How many species of *Hipposideros* have occurred on Madagascar since the Late Pleistocene? Zool. J. Linnean Soc. doi: 10.1111/zoj.12368.